University of Alberta

Development of a Targeted Adenoviral Vector Expressing HSV-TK

for use In Breast Cancer Gene Therapy and

Analysis through Positron Emission Tomography

A Thesis

Submitted to the Faculty of Graduate Studies and Research

in partial fulfillment of the requirements for the degree of

Doctor of Philosophy

in

Experimental Oncology

Department of Oncology

© Alan DeSilva
Fall 2012
Edmonton, Alberta, Canada

ABSTRACT

While adenoviral (Ad) vectors are the most commonly used gene delivery vector for human gene therapy, improvements must be made to increase Ad specificity to tumors if they are to be used for cancer gene therapy. Our goal is to target adenoviral vectors to breast cancer (BrCa) cells to induce cell killing while reducing toxicity to non-tumor cells. We have generated a non-replicating BrCa-targeted adenoviral vector that utilizes a mammary-specific promoter (MPE_2) to drive expression of a therapeutic gene, herpes simplex virus-1 thymidine kinase (HSV-TK). Cells expressing HSV-TK are sensitive to the prodrug ganciclovir (GCV). Thus, AdMPE_2TK can induce BrCa-specific cell death when administered in combination with GCV. The expression of HSV-TK also allows cells to be visualized using positron emission tomography (PET) using radiolabeled PET substrates 3'-[^{18}F]fluoro-3'-deoxythymidine ([^{18}F]FLT) and 9-(4-[^{18}F]fluoro-3-hydroxymethylbutyl)-guanine ([^{18}F]FHBG).

We first characterized the immunocompetent MTHJ murine breast cancer model as having high biological significance to human breast cancer and reveal its ability to uptake standard PET tracers. We then showed the BrCa specificity of the AdMPE_2TK vector to kill BrCa cells *in vitro* in comparison to the non-specific AdCMVTK vector utilizing the cytomegalovirus promoter. Neither vector was shown to induce *in vivo* tumor regression, however the AdCMVTK vector caused liver toxicity in immunocompetent mice. In contrast, the AdMPE_2TK vector did not induce any measurable toxicity, highlighting its specificity and potential for cancer gene therapy. Finally, using MTHJ murine tumor cells, *in vitro* cell uptake experiments revealed the ability of AdTK vectors to induce an increase in accumulation of [^{18}F]FHBG. *In vivo* PET

imaging was then used to evaluate the accumulation of [^{18}F]FLT and [^{18}F]FHBG in established MTHJ tumors injected with AdTK vectors, however no increase in accumulation was observed.

This thesis outlines the first preclinical evaluation of the BrCa-specific MPE_2 promoter to target HSV-TK for cancer gene therapy. We illustrate the ability of AdMPE_2TK to induce a therapeutic effect in combination with GCV. In addition, this project represents the first imaging studies of an adenoviral vector utilizing the MPE_2 promoter. This research outlines the potential of the MPE_2 promoter and illustrates its application in BrCa gene therapy.

ACKNOWLEDGEMENTS

First and foremost I would like to thank my supervisor, Dr. Mary Hitt, for giving me the opportunity to pursue my graduate degree in her laboratory. Your support, encouragement and gentle guidance during my graduate studies was greatly appreciated. I would also like to thank the members of my advisory committee, Dr. John Mercer, Dr. Leonard Wiebe, and Dr. Alan Underhill for their valuable input and assistance during the course of my program. In addition, I must thank Drs. Frank and Melinda Wuest for countless contributions and insights regarding PET imaging.

I must take this opportunity to also thank the past and present members of the Hitt lab for the help, humour, support and suggestions throughout my project. In particular I thank my fellow labmate David Sharon for the endless amount of technical assistance he has provided me and everyone who walks in our lab. To all the faculty and graduate students at the Cross Cancer Institute, I thank you for the support and fun times. We created memories that will never be forgotten. It has been a pleasure working with all of you and I am honoured to have graduated from the Department of Oncology.

Words cannot describe the gratitude I have for my family. I have always felt your love and support despite what has been happening in my life. To my parents, Alex and Celine, for instilling in me the value of education and hard work, I thank you. To my brother, Darryl, for being the perfect older brother, I thank you. To all my inlaws, nieces, nephews, and godchildren, your love, support, and generosity through the years have made more of an impact on my life than you will ever know.

To my children, Gabriel Alexander DeSilva and Anjali Veronica DeSilva, you are and always will be my greatest success. Thank you for your gifts of life, love, and laughter.

Finally, I would like to thank my loving wife, Renee Rose DeSilva. Without you and your encouagement none of this is possible. You are the constant in my ever-evolving life. I will never be able to repay you for your eternal support during my graduate degree, but I will spend my entire life trying.

THANK YOU ALL.

TABLE OF CONTENTS

LIST OF TABLES

LIST OF FIGURES

LIST OF ABBREVIATIONS

Abbreviation	Full Name
5FC	5-fluorocytosine
5FU	5-fluorouracil
Ad	adenovirus
AIDS	acquired immunodeficiency syndrome
ALP	alkaline phosphatase
ALT	alanine transaminase
AST	aspartate transaminase
ATP	adenosine triphosphate
bp	base pairs
BCA	bicinchoninic acid
BrCa	breast cancer
BSA	bovine serum albumin
CAR	coxsackie-adenovirus receptor
CCAC	Canadian Council on Animal Care
CD	cytosine deaminase
CMV	cytomegalovirus
CT	computed tomography
DMEM	Dulbecco's modified Eagle's medium
DNA	deoxyribonucleic acid
DTT	dithiothreitol
EDTA	ethylenediamine-tetraacetic aid
EGF	epidermal growth factor
ER	estrogen receptor
FBS	fetal bovine serum
FDG	2-deoxy-2-[^{18}F]fluoro-D-glucose
FHBG	9-(4-[^{18}F]fluoro-3-hydroxymethylbutyl)-guanine
FLT	3'-deoxy-3'-[^{18}F]fluorothymidine
FG	first generation
FIAU	5-iodo-2'-fluoro-2'-deoxy-1-βD-arabinofuranosyl-5-iodouracil
FIRU	5-iodo-2'-fluoro-2'-deoxyuridine
FMAU	[^{14}C]5-methyl-2'-fluoroarabinouridine
GCV	ganciclovir
GCV-MP	ganciclovir-monophosphate
GCV-TP	ganciclovir-triphosphate
HEPES	4-(2-hydroxyethyl)-1-piperazineethanesulfonic acid
HER2	human epidermal growth factor receptor 2
hFAS	human fatty acid synthase
HIV	human immunodeficiency virus
HSV	herpes simplex virus
hTERT	human telomerase reverse transcriptase
kb	kilobases
MAP	maximum a posteriori
MEM	minimal essential medium

MGB	mammaglobin
MMTV	mouse mammary tumor virus
MOI	multiplicity of infection
MPE_2	minimal mammaglobin promoter with duplicated enhancers
MRI	magnetic resonance imaging
mRNA	messenger ribonucleic acid
MTS	3-(4,5-dimethylthiazol-2-yl)-5-(3-carboxymethoxyphenyl)-2-(4-sulfophenyl)-2H-tetrazolium, inner salt
MTHJ	murine mammary adenocarcinoma cells
MUC1	mucin 1
ori	origin of replication
OSEM	ordered subset expectation maximization
PBS	phosphate buffered saline
PCR	polymerase chain reaction
PET	positron emission tomography
pfu	plaque forming units
PMSF	phenylmethylsulfonyl fluoride
PR	progesterone receptor
PyMT	polyoma virus middle T antigen
RCA	replication competent adenovirus
ROI	region of interest
SCID	severe combined immunodeficiency
SDH	sorbitol dehydrogenase
SDS	sodium dodecyl sulphate
SIV	simian immunodeficiency virus
SPECT	single photon emission computed tomography
SUV	standardized uptake value
TAC	time activity curve
TK	thymidine kinase
wt	wild type

CHAPTER 1:

Introduction

1.1. BREAST CANCER

Breast cancer (BrCa) is the leading malignancy and second leading cause of cancer mortality in women (CancerStats, 2011; Czernin, Benz, and Allen-Auerbach; WHO, 2010). BrCa is rare in men with incidence and mortality rates around 1% (Harlan et al., 2010; Niewoehner and Schorer, 2008). The inherent diversity of transcriptional regulation in human cells extends into human BrCa, which is a heterogenous disease with many biological variations in cellular composition and molecular alterations (Perou et al., 2000). Many parameters are commonly assessed in the clinic to stratify patients for prognostic predictions and treatment selection. Such parameters include clinical factors such as patient age, tumor node status, tumor size, and histological grade, as well as pathological factors such as estrogen receptor (ER), progesterone receptor (PR), and human epidermal growth factor receptor 2 (HER2) statuses. Microarray analysis has allowed characterization of BrCa 'molecular profiles' based on gene expression patterns found in different human tumors.

Five accepted BrCa intrinsic subtypes have been identified: Luminal A, Luminal B, HER2-enriched, Basal-like, and Normal Breast-like (Perou et al., 2000; Prat and Perou, 2011; Sorlie, 2004; Sorlie et al., 2001). Luminal A and B tumor types arise from luminal epithelial cells of the human mammary gland and show similar gene expression patterns such as ER-positive status (Sorlie et al., 2003). The Luminal A subtype is distinguished from the Luminal B subtype by having higher amounts of ER and PR, among other molecular markers (Nakshatri et al., 2009). Patients with Luminal B tumors were also shown to have a poorer prognosis (Sorlie et al., 2001). HER2-enriched tumors have luminal characteristics but are ER-negative and have a high

incidence of p53 mutation. Basal-like tumors are also known as triple negative due to their molecular status as ER-, PR-, and HER2-negative. Patients with basal-like tumors have the poorest prognosis with only an approximately 10% five-year survival rate. Normal breast-like tumors possess similar molecular markers to non-tumor mammary cells and patients with normal breast-like tumors have an approximately 50% five-year survival rate. Recently, another BrCa intrinsic subtype has been identified from tumors in humans, mice (Herschkowitz et al., 2007), and in a panel of BrCa cell lines (Prat et al., 2010). The majority of tumors from this subtype, known as Claudin-low, are poor prognosis triple-negative invasive ductal carcinomas with a high frequency of metaplastic and medullary differentiation (Prat and Perou, 2011). Patients with tumors from each group exhibit differences in tumor incidence (Carey et al., 2006; Millikan et al., 2008), survival (Cheang et al., 2009; Perou et al., 2000; Sorlie et al., 2001), and treatment response (Carey et al., 2007; Hugh et al., 2009; Nielsen et al., 2010; Parker et al., 2009; Prat et al., 2010; Rouzier et al., 2005).

Standard treatment for BrCa can vary, but usually includes one or more of the following: surgery, radiation therapy, chemotherapy, and hormone therapy. Over the last decade developments in early diagnosis and novel treatment approaches have improved the clinical outcome. Despite the advances in screening and treatment methods, BrCa still claims more female lives than all other cancers worldwide (WHO, 2010). The main cause of death among BrCa patients results from distant metastases (Weigelt, Peterse, and van 't Veer, 2005), which are common in patients that develop recurring disease (Gonzalez-Angulo, Morales-Vasquez, and Hortobagyi, 2007). While non-metastatic BrCa has a high survival rate, metastatic disease is more difficult to treat. Metastatic

BrCa is most commonly treated using chemotherapy, but not all BrCa responds to treatment. Patients may benefit from additional forms of treatment analysis to halt or alter non-responsive treatment, thereby preventing unnecessary toxicity (McDermott et al., 2007). To achieve this aim, many preclinical and clinical studies are currently under way to investigate novel BrCa therapeutics.

1.2. GENE THERAPY

Gene therapy refers to the introduction of a transgene to induce a therapeutic effect. The concept of functional exogenous DNA being stably and heritably introduced into cells was initially derived from the Avery, McLeod, and McCarty studies of DNA-mediated transformation of pneumococci (Avery, Macleod, and McCarty, 1944). Later studies began to suggest that tumor viruses could be modified to deliver a payload of genetic information to complement and correct genetic diseases (Friedmann and Roblin, 1972; Jackson, Symons, and Berg, 1972). Retroviral vectors were heavily researched for their application as delivery vectors (Doehmer et al., 1982; Shimotohno and Temin, 1981; Tabin et al., 1982; Wei et al., 1981) and were the first vector to correct human disease *in vitro* (Jolly et al., 1983; Miller et al., 1983; Willis et al., 1984), demonstrating the restoration of adenosine deaminase (ADA) expression in a severe combined immunodeficiency disease (SCID) model (Kantoff et al., 1986). The first gene therapy clinical trial involved ADA-bearing retroviral vectors for treatment of SCID in two children, one of which (famously) exhibited a positive response (Blaese et al., 1995).

1.2.1. Cancer Gene Therapy

Cancer gene therapy takes advantage of differential characteristics of normal and malignant tissue to slow or stop tumor growth, preferably by destroying replicating cancer cells (Ficazzola and Taneja, 1998). This can be achieved through a variety of methods, including addition of a therapeutic gene, functional deletion of a pre-existing gene, or indirectly by enhancing host immune recognition of the tumor. Many variations in gene therapy have been applied to treat cancer in humans. These variations often differ in three main categories: the delivery vector used to deliver the therapeutic gene; the targeting strategy to localize the therapeutic gene specifically to the target cells; and the therapeutic gene itself.

1.2.2. Cancer Gene Therapy Delivery Vectors

All forms of gene therapy require an efficient method for transferring the therapeutic gene(s) to target cells. Gene therapy clinical trials currently employ many vehicles to introduce transgenes. Of all vectors currently used in gene therapy clinical trials about a quarter are based on non-viral methods of gene delivery; about 18.5% of clinical trials have been based on naked plasmid DNA (Wiley, 2012), which is the use of plasmid DNA in aqueous solution, while another 6% are based on lipofection. Versions of these non-viral vectors are generally poorly immunogenic and non-pathogenic, demonstrate low toxicity, are relatively easy to manufacture, and can transport transgenes of nearly unlimited size. The drawbacks of non-viral vectors include relatively low transfection efficiencies, degradation of introduced DNA (both extra- and intracellularly), and low transgene expression (see reviews: Douglas, 2008; Lara and Ramirez, 2012).

The vast majority of vectors used in gene therapy clinical trials involve the use of viral vectors which are highly preferred for cancer gene therapy since they have much higher transfection efficiencies and can induce high levels of transgene expression in infected cells. The most common viruses used in gene therapy are retroviruses (including lentivirus), herpes simplex virus, poxvirus (including vaccinia), and adenovirus (Wiley, 2012).

Lentiviruses constitute a subclass of retroviruses, of which mainly simian immunodeficiency virus (SIV) and human immunodeficiency virus (HIV) have been extensively studied. Lentivirus vectors are advantageous for cancer gene therapy due to the absence of pre-existing anti-vector immunity (Kootstra and Verma, 2003), low induction of anti-vector host immunity (Abordo-Adesida et al., 2005; Blomer et al., 1997), and ability to carry transgenes up to 8 kb in size (Zufferey et al., 1998). Unlike other retroviruses, lentiviruses can also replicate in non-dividing cells (Bukrinsky et al., 1993; Freed and Martin, 1994). However, similar to other retroviruses, lentivirus vectors integrate into the host genome and replicates as part of the host cell's DNA. In addition, this integration can pose the safety risk of insertional mutagenesis (Hacein-Bey-Abina et al., 2003a; Hacein-Bey-Abina et al., 2003b).

Herpes simplex virus (HSV) was one of the first types of virotherapy investigated for cancer gene therapy (Martuza et al., 1991). HSV vectors possess a large genome and have the ability to carry large transgene inserts. Available anti-HSV therapies (such as acyclovir) limit the risk of uncontrolled infections in treated patients. Also, genetically modified HSV vectors have been shown to cause low toxicity in human studies (Hu et al., 2006). These features make HSV attractive for cancer gene therapy.

Vaccinia is the most studied form of poxvirus used in cancer gene therapy, with many oncolytic agents based on it undergoing clinical trials (Liu et al., 2008; Thorne et al., 2007). Vaccinia vectors can carry large transgene inserts (Smith and Moss, 1983), have available antiviral drugs, and are quite genetically stable with a low rate of spontaneous mutagenesis. One of the most important reasons scientists are studying vaccinia vectors for cancer gene therapy is due to its natural selectivity for tumor cells (Thorne et al., 2007) which is an important step in targeting transgenes to tumors.

1.2.2.1. Adenovirus for Cancer Gene Therapy

Adenovirus (Ad) vectors are currently the most frequently used vectors for human gene therapy and cancer therapy (Wiley, 2012). Ads were first isolated in 1953 when scientists attempted to isolate the causative agents of acute respiratory infections (Hilleman and Werner, 1954; Rowe et al., 1953). The term adenovirus refers to their initial isolation from human adenoid tissues (Enders et al., 1956). Ads belong to the *Adenoviridae* family, with numerous identified serotypes infecting a wide range of species (Berk, 2007). Human Ads belong to the *Mastadenovirus* genus and are responsible for a small percentage of acute respiratory morbidity in the general population, an estimated 5 to 10% of respiratory illness in children, and mild and self-limiting infection in most immunocompetent adults (Berk, 2007). Ad infections can also lead to epidemic conjunctivitis and gastroenteritis in children (Mautner, Steinthorsdottir, and Bailey, 1995; O'Brien et al., 2009) Severe and sometimes fatal disease from Ad infections has been noted in immunocompromised patients, such as people with acquired immunodeficiency syndrome or patients who have received organ or bone marrow transplants (Kojaoghlanian, Flomenberg, and Horwitz, 2003; La Rosa et al.,

2001; Leen and Rooney, 2005). While some human Ad serotypes have been observed to be oncogenic in hamsters (Yabe, Trentin, and Taylor, 1962), human Ad serotypes are not normally found to cause cancer in humans (McLaughlin-Drubin and Munger, 2008).

All Ads are non-enveloped double-stranded DNA viruses ranging in size from 26 to 45 kilobases (Davison, Benko, and Harrach, 2003). Viral genomes are contained in icosahedral capsids (Berk, 2005) with fiber proteins projected from the vertices. The capsid itself is composed mainly of hexon proteins, with 720 hexon protein copies per virus grouped into trimers known as hexon capsomers (Grutter and Franklin, 1974). These hexon capsomers subsequently assemble into groups of nine, which make up the faces of the icosahedron capsid. Each apex is occupied by five copies of the penton protein, making a penton capsomer which serves as the base for a trimer of fiber proteins (Berger et al., 1978; Nermut, 1975).

At least 51 human Ad serotypes have been identified (reviewed in Berk, 2007; Ishiko et al., 2008; Jones et al., 2007; Walsh et al., 2009), each distinguished by its resistance to neutralization by antibodies against other known Ad serotypes. Human Ads are separated into at least six groups (A-F) based on their ability to agglutinate erythrocytes, oncogenicity in animals, and genetic homology (Berk, 2007). Ad serotype 5 from Group C represents one of the most extensively studied and utilized (McConnell and Imperiale, 2004; Shenk, 2001; Tatsis and Ertl, 2004).

Ad5 is a 36 kb virus whose genome, like the other Ad serotypes, carries one immediate-early transcription unit (E1A), four early transcription units (E1B, E2, E3, and E4), two delayed early units (IX, and IVa2), one late unit (major late) that is processed to yield five different mRNA families (L1 to L5) and two low molecular weight virus-associated

(VA) RNAs (Evans, 2002; Mathews, 1975; Shenk, 2001) (Figure 1.1). Early viral gene products mediate further viral gene expression and DNA replication, induce cell cycle progression, block apoptosis, and antagonize a variety of host antiviral mechanisms (Shenk, 2001). Late viral gene products mediate host receptor recognition and binding, most notably the penton base and the fiber knob, which is involved in recognition and binding (Nemerow, Cheresh, and Wickham, 1994) to the coxsackie-adenovirus receptor (CAR) (Bergelson et al., 1997).

Ads have emerged as promising vectors for cancer gene therapy due to a number of advantages: Ad vectors are relatively easy to amplify to high concentrations; Ad vectors do not integrate into the host DNA; Ad vectors can harbor large therapeutic gene insertions; Ad vectors have a broad tropism and can infect both dividing and non-dividing cells (Dormond, Perrier, and Kamen, 2009; Hitt and Graham, 2000; Li et al., 1993; Quantin et al., 1992). Initial trials investigating adenovirus for cancer therapy took place in the 1950s where mild cervical cancer regression was observed following wild type (wt) Ad inoculation (1957; Huebner et al., 1956). Since then, first generation (FG) Ad vectors were constructed to block the innate replication ability of wild type Ad in human cells (Berkner, 1988). FGAds have a deletion in the E1 region, rendering these vectors replication deficient. By expressing a transgene in place of the E1 region, researchers can take advantage of the high transduction efficiency of FGAd vectors without concern over uncontrolled virus replication. *In vivo* studies in non-tumor bearing mice have found that injection of Ad directly into the circulation results in 10- to 100-fold less vector transduction in other organs as compared to the liver (Smith et al., 1993).

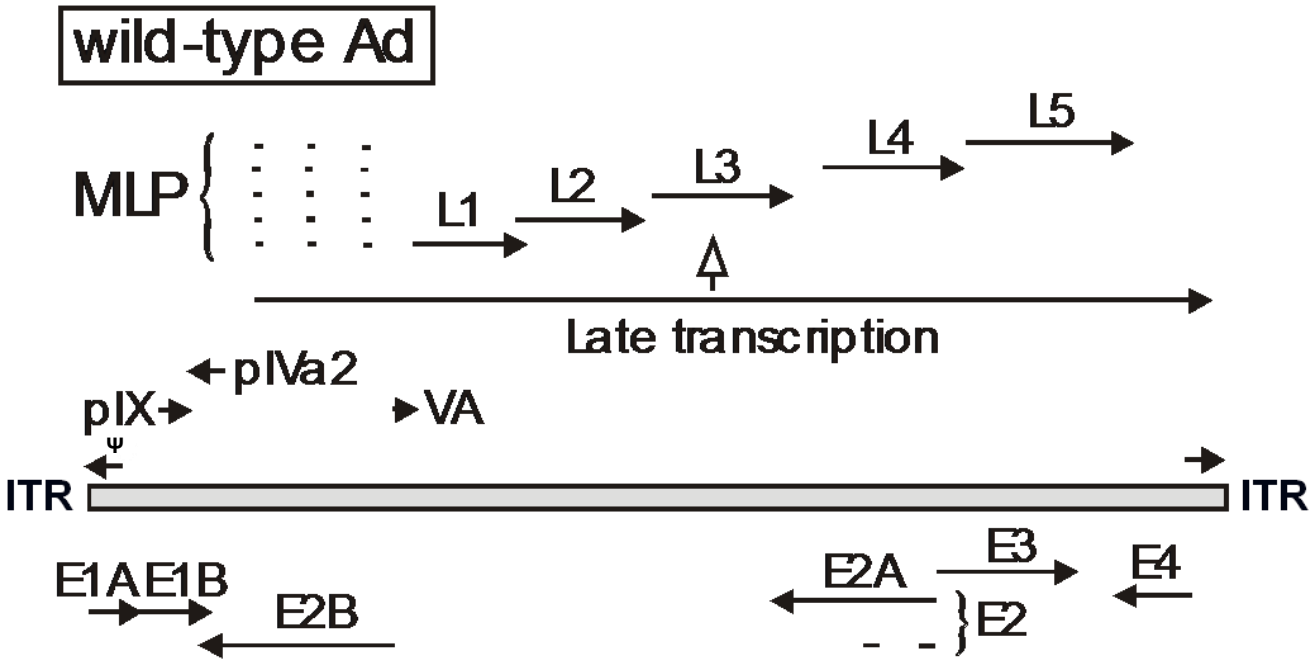

Figure 1.1. Transcription map of wild type adenovirus (Ad) serotype 5.

Arrows at the ends of the linear viral genome (grey bar) indicate the inverted terminal repeats (ITRs). The packaging signal is designated by the symbol Ψ. Early region transcripts (including E1A, E1B, E2A, E2B, E3, and E4) are indicated by solid arrows below the genome map. Intermediate or late transcripts (including pIX, pIVa2 and virus associated [VA] RNAs) are shown above the genome. The primary major late promoter (MLP) transcript is processed to generate 5 families of late transcripts (L1 to L5), each containing the tripartite leader sequences (shown as dashed lines). Reproduced from Sadeghi and Hitt, 2005.

This accumulation and undesirable transgene expression in the liver illustrates the importance of limiting Ad vector expression to their target cell.

1.2.3. Cancer Gene Therapy Transcriptional Targeting

One method of targeting gene expression is through transcriptional targeting, which refers to using cell- or tissue-specific promoters to drive expression of a therapeutic gene. Since many tumors express certain transcripts that are not usually expressed in surrounding cells, the use of the promoters driving the tumor-specific expression of these transcripts may provide a safety measure that can reduce treatment toxicity. In cancer gene therapy, the specific and targeted regulation of therapeutic gene expression is extremely important to limit expression to target cells in order to maximize the killing effect while minimizing toxicity to non-cancer cells. Many strategies using tumor-specific promoters have been employed in adenoviral gene therapy for a variety of human cancers (Sadeghi and Hitt, 2005).

The human telomerase reverse transcriptase (hTERT) promoter is a widely used tumor-specific promoter since it is highly active in many types of cancer, including small cell lung cancer (Hiyama et al., 1995), hepatocellular carcinoma (Tahara et al., 1995), prostate (Sommerfeld et al., 1996), ovarian (Counter et al., 1994), and breast cancer (Hiyama et al., 1996). The hTERT promoter has shown promise as a tumor-specific promoter for a variety of cancer gene therapies (Chen et al., 2011; Murofushi et al., 2006; Riesco-Eizaguirre et al., 2011; Wang et al., 2010; Yu et al., 2011). The prostate-specific antigen (PSA) promoter is another example of a tumor-specific promoter that allows targeted expression in prostate cancer cells (Ast, 2003; Djeha et al., 2001; Latham et al., 2000). In addition to tumor therapy, the PSA promoter has also been

used to drive prostate-specific transgene expression to help visualize tumors using molecular imaging (Pouliot et al., 2011; Sato et al., 2008). Just as with other tissue and tumor types, some promoters have been found to upregulate gene expression specifically in breast cancer. The ErbB2 protein is overexpressed in breast cancer and is correlated with reduced overall patient survival (Lovekin et al., 1991). A Phase I clinical trial showed the safety of breast cancer therapy after administration of a plasmid using the ErbB2 promoter to drive expression of cytosine deaminase (CD), a suicide gene that converts the fluorocytosine (5FC) prodrug into its toxic fluorouracil (5FU) metabolite (Pandha et al., 1999). Another tumor-specific promoter that has been used for breast cancer gene therapy is from the survivin protein, which is found in 70% of breast neoplasms (Tanaka et al., 2000) and whose promoter is preferentially active in tumor cells (Chen et al., 2004). Studies have shown that the survivin promoter may be used to transcriptionally target luciferase expressing Ad vectors to tumor cell lines (Zhu et al., 2004). Other such examples of BrCa-specific promoters studied for application in BrCa gene therapy include PPAR-γ1 (Wang, Southard, and Kilgore, 2004), α-lactalbumin (Li et al., 2005), and L-plastin promoters (Chung et al., 1999).

1.2.3.1. Transcriptional Targeting with the Mammaglobin Promoter

Another promoter shown to be BrCa selective was identified from the *SCGB2A2* gene encoding mammaglobin-1 (MGB). MGB was first identified as showing mRNA overexpression in BrCa from a screen of human breast tumor biopsies and non-tumor (reduction mammoplasty) samples (Watson and Fleming, 1994). The MGB gene encodes a protein of unknown function that is considered to be a member of the secretoglobin family and could possibly be involved in regulating steroid metabolism

and immune function (Carter et al., 2002). MGB maps to the 11q13 region (Watson et al., 1998) which is frequently associated with alterations in breast tumorigenesis (Bieche and Lidereau, 1995; Chuaqui et al., 1997; Courjal et al., 1997; Driouch et al., 1997; Fantl et al., 1990; Kerangueven et al., 1997; Nayar et al., 1997). The gene encodes a 93 amino acid protein with a molecular mass of 10.5 kDa (Watson and Fleming, 1996). In breast tissue, it exists in two forms with molecular masses of 18 and 25 kDa (Watson et al., 1998).

MGB has been shown to possess mammary gland-specific expression and its mRNA was shown to be upregulated 10-fold in tumor biopsies compared to non-tumor cells (Watson and Fleming, 1996). MGB transcripts have been consistently found in tumors from BrCa patients: in healthy patients, patients with hematological malignancies, or patients with solid tumors other than BrCa, MGB transcripts were absent from peripheral blood, bone marrow, or peripheral blood progenitor cells (Silva et al., 2002). The BrCa specificity of MGB indicates its usefulness as a marker of BrCa (Fleming and Watson, 2000). Research has revealed a high level of MGB overexpression in BrCa compared to normal mammary tissue (Leygue et al., 1999; O'Brien et al., 2002; Span et al., 2004; Watson et al., 1999), suggesting its potential applications in the detection of micrometastases in lymph nodes, peripheral blood, and bone marrow, and in identification of metastases originating from the breast (Grunewald et al., 2000; O'Brien et al., 2002). While low levels of MGB transcript expression has been observed in a few other tissues (most notably sweat glands (Sjodin et al., 2003)), human MGB mRNA has been found to be the most specific marker for the hematogenous spread of BrCa cells and is currently being researched and used as a marker for BrCa micrometastases

(Dono et al., 2011; Lacroix, 2006; Li et al., 2011; Marchetti et al., 2001; Wang et al., 2009).

MGB transcripts have been detected in 70-100% of primary and metastatic BrCa samples examined, with levels reaching 10 to 20 times higher in BrCa compared to non-malignant mammary tissue (Fleming and Watson, 2000; Houghton et al., 2001; Ooka et al., 2000). MGB has also been found in a papillary carcinoma of the male breast (Khalbuss et al., 2006), indicating its expression is not confined to females. MGB is believed to be secreted from BrCa cells since MGB protein has been found in the medium of cultured MGB^+ BrCa cells (Bernstein et al., 2005) and in the serum of BrCa patients (Fanger et al., 2002). Recent evidence has shown that MGB may remain associated with the membrane after secretion, which may be useful for BrCa-targeted therapies (Zuo et al., 2009).

Consistent with previous findings, Dr. Hitt's group has also shown BrCa-selective expression from the MGB promoter (Shi et al., 2004). Deletion studies have identified a 344 base pair minimal promoter region and a potential enhancer upstream of the MGB open reading frame. When screened *in silico* potential transcription factor binding locations containing numerous consensus binding sites were indicated in both the minimal promoter and enhancer sequences (Figure 1.2).

Subsequent studies by this group have used different combinations of this minimal promoter and potential enhancers to identify genetic combinations that may drive increased expression of reporter genes in adenoviral vectors (Shi, Graham, and Hitt, 2006). From this study, an optimal version of the MGB promoter has been identified: a

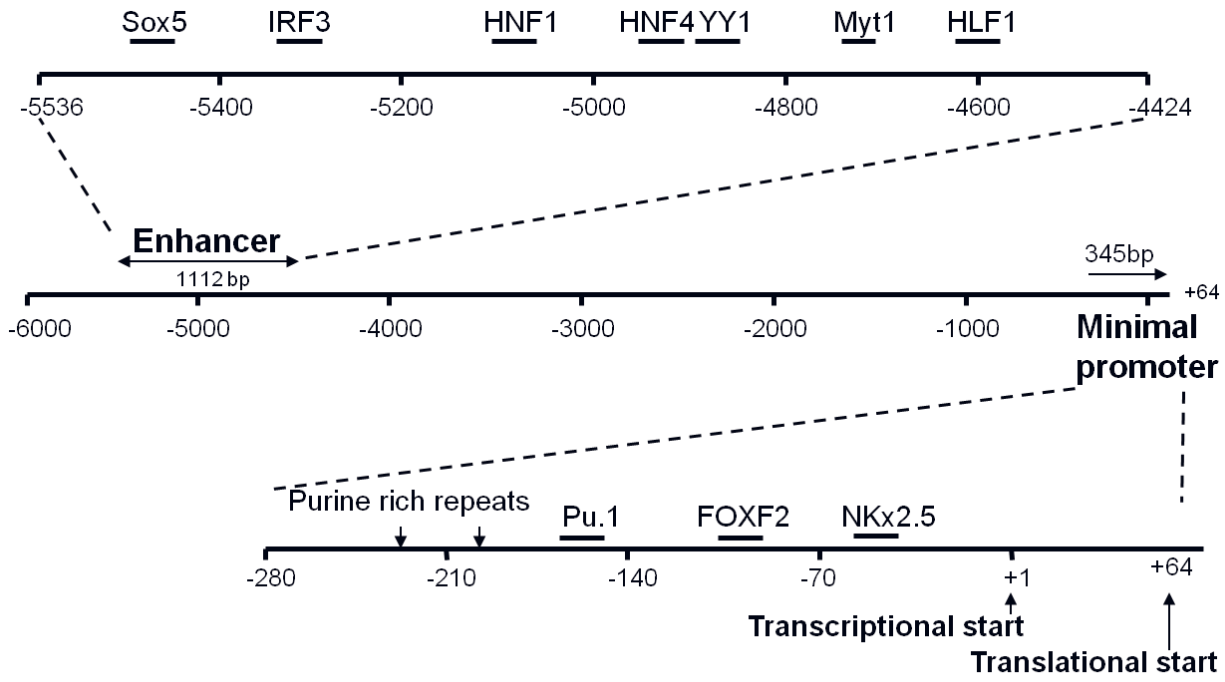

Figure 1.2. Transcription map of minimal mammaglobin promoter and upstream enhancer.

Consensus binding sites for transcription factors are shown. The MPE_2 promoter (~2.5 kb) is composed of the minimal promoter fused to duplicated enhancers. Reproduced from Sadeghi and Hitt, 2005.

duplicated upstream enhancer fused to a minimal mammaglobin promoter (MPE_2; Figure 1.2). This MPE_2 promoter has been shown to achieve high levels of expression in BrCa cells compared to non-tumor cells (Figure 1.3) and thus has potential to be used for targeted gene therapy (Shi, Graham, and Hitt, 2006).

1.2.4. Cancer Gene Therapy Therapeutic Gene: Herpes Simplex Virus Thymidine Kinase

Herpes simplex virus (HSV) thymidine kinase (TK)-1 is an important enzyme for HSV replication. HSV-TK utilizes ATP to phosphorylate deoxythymidine, which is the initial phosphorylation step in the formation of deoxythymidine triphosphate used in viral DNA synthesis (Derse et al., 1981; Elion et al., 1977; Fyfe et al., 1978). The prodrug ganciclovir (GCV) specifically binds to HSV-TK in place of deoxythymidine (Champness et al., 1998) and is phosphorylated into its monophosphate form (Reardon, 1989), which can no longer diffuse out of a cell (Hsieh et al., 2006). Cellular kinases can then further phosphorylate GCV to yield GCV-triphosphate (GCV-TP), a deoxyguanosine triphosphate analogue (Figure 1.4). The incorporation of GCV-TP into an elongating DNA chain can lead to elongation termination, base-pair mismatches, DNA fragmentation, sister chromatid exchange, and lethal genomic instability, all of which can ultimately result in apoptosis (Matthews and Boehme, 1988; Morris et al., 1999; Thust, Schacke, and Wutzler, 1996). GCV was originally developed as an anti-viral agent (see reviews: Buhles, 2011; Whitley, 1988). More recently, GCV has been used in combination with HSV-TK gene therapy since HSV-TK can metabolize GCV into a toxic drug. HSV-TK/GCV gene therapy has also been shown to enhance radiation-induced tumor cell killing and regression of experimental tumors (Niranjan et al., 2000).

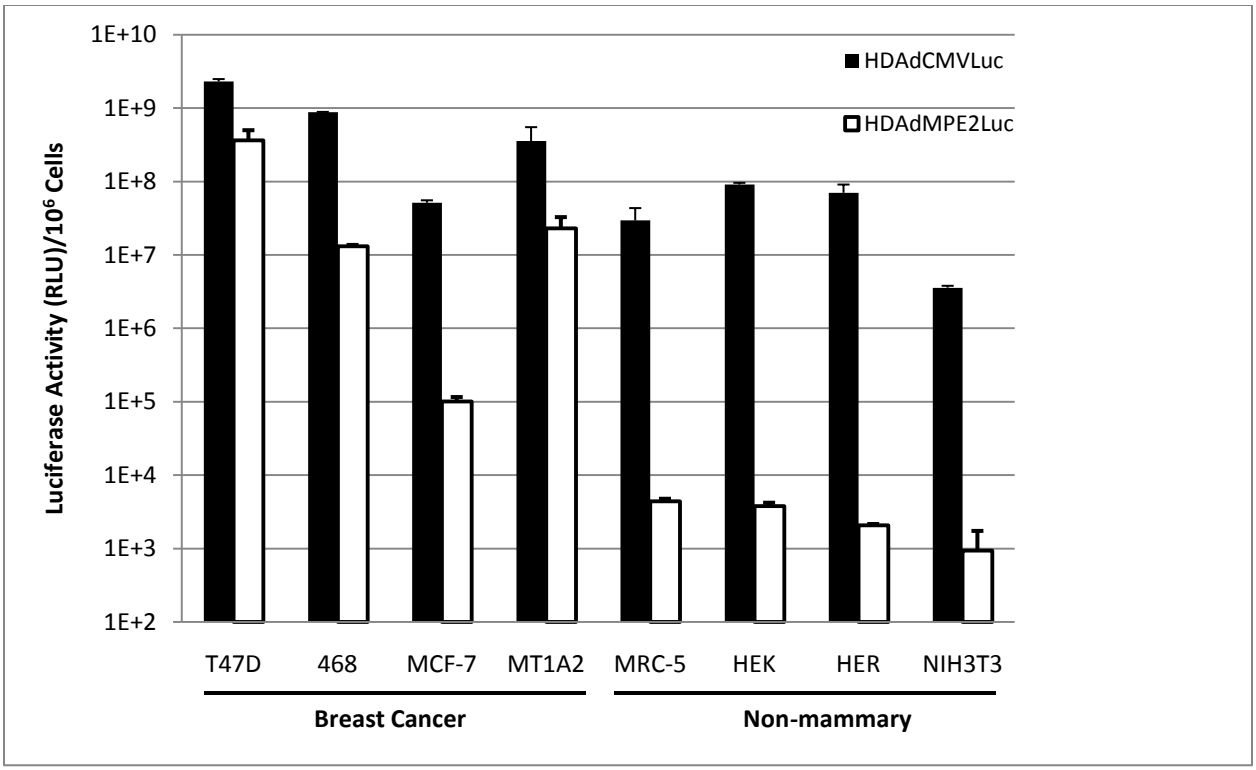

Figure 1.3. Luciferase reporter gene expression induced by the CMV or MPE_2 promoter.

Breast cancer and non-mammary cells were infected with helper-dependent adenovirus encoding the luciferase gene under the control of either the MPE_2 promoter or control mCMV promoter. Expression is shown on log scale in terms of relative light units (RLU) per 10^6 cells. Figure modified from original (Shi et al., 2004).

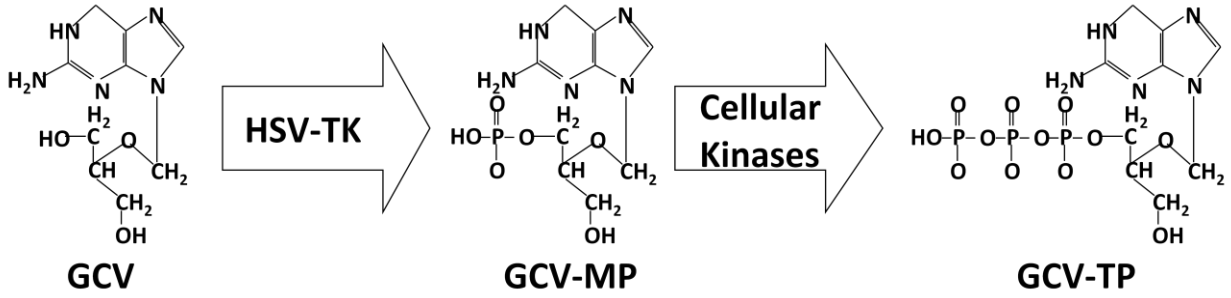

Figure 1.4. Phosphorylation of ganciclovir to ganciclovir-triphosphate.

In the presence of herpes simplex virus thymidine kinase (HSV-TK), the prodrug ganciclovir (GCV) is monophosphorylated to ganciclovir-monophosphate (GCV-MP), which is further phosphorylated by cellular kinases to ganciclovir-triphosphate (GCV-TP).

By targeting cancer cells to express HSV-TK, the administration of GCV can lead to cancer-specific cell death. GCV is selectively cytotoxic to cells expressing HSV-TK since its phosphorylation by HSV-TK is 1000 times more efficient than by mammalian cellular kinases (Aghi, Hochberg, and Breakefield, 2000; Keller et al., 1981). Also, since the prodrug toxicity is due to DNA incorporation in dividing cells during replication, therapeutic effect will mainly occur in rapidly dividing tumor cells and not in non-tumor cells (Matthews and Boehme, 1988).

An important phenomenon involving HSV-TK/GCV gene therapy is referred to as the 'bystander effect'. The bystander effect refers to the death of surrounding nontransduced cells that are not expressing HSV-TK and thus should not be sensitive to GCV treatment (Moolten, 1986). This phenomenon was reported following the observation that even when only 10% of cells in the tumor were transduced with HSV-TK, significant or complete tumor regression was achieved (Culver et al., 1992; Ram et al., 1993; Takamiya et al., 1992). The bystander effect could play a significant role in the elimination of all cancer cells from a patient since it may allow for non-targeted cell death in a heterogenous tumor cell population. Gap junctions are believed to play a role in mediating the bystander effect since toxic derivatives of radiolabeled GCV from HSV-TK-expressing cells have been detected in HSV-TK non-expressing cells (Bi et al., 1993) and phosphorylated nucleotides are known to transfer to adjacent cells through gap junctions (Hooper and Subak-Sharpe, 1981; Subak-Sharpe, Burk, and Pitts, 1969). It is clear that cell-cell communication can play a role since a 1:1 mixture of HSV-TK^+/HSV-TK^- HeLa cells could not induce whole monolayer killing in the absence of a gap junction gene while even a 1:9 mixture could when gap junctions were present

(Mesnil and Yamasaki, 2000). Similar results have been reported *in vivo* where incomplete HSV-TK transduction of gap junction-containing tumors still caused a reduction in tumor growth after GCV administration (Duflot-Dancer et al., 1998). Other transfer mechanisms, including endocytosis of apoptotic vesicles, may also be involved in neighbouring cell death (Agard et al., 2001; Niculescu-Duvaz and Springer, 2004). The bystander effect may also stimulate the host's immune system by attracting dendritic cells and inducing an antitumor inflammatory response (Kianmanesh et al., 1997; Kuriyama et al., 1999). Clearly, the bystander effect provides a tremendous advantage for using HSV-TK/GCV Ad gene therapy since tumor transduction is commonly low in patient *in vivo* trials.

Phase I and II clinical trials using AdHSV-TK vectors have been performed in a variety of tumors, including prostate cancer (Nasu et al., 2007), hepatocellular carcinoma (Li et al., 2007), retinoblastoma (Chevez-Barrios et al., 2005), mesothelioma (Sterman et al., 2005), malignant glioma (Germano et al., 2003), and ovarian cancer (Alvarez et al., 2000). These studies have illustrated the safety of AdTK for use in cancer gene therapy. Phase III clinical trials for patients with prostate cancer (Nasu et al., 2007) and malignant glioma (King et al., 2005) have been carried out, but no significant improvement in survival was observed. All of these trials mentioned used adenoviral vectors expressing HSV-TK driven by the Rous sarcoma virus long terminal repeat (RSV-LTR) promoter, which is not known to be tumor-specific (Zheng and Baum, 2005). The ability to selectively express HSV-TK within cancer cells could enhance the efficacy of HSV-TK/GCV therapy by allowing for a higher treatment dose with less risk of toxicity.

Ad vectors expressing HSV-TK under the control of the hTERT promoter have been used for tumor-selective gene therapy in combination with ganciclovir and induced less toxicity compared to non-selective, ubiquitously expressing promoters like the cytomegalovirus (CMV) promoter (Majumdar et al., 2001). Ad vectors expressing HSV-TK under the control of the PSA promoter have shown growth inhibition of prostate cancer xenografts after treatment with GCV (Blackburn et al., 1998; Cheon et al., 2000; Eastham et al., 1996; Thompson, 1999). A recent clinical trial has shown the safety of using a nonreplicating Ad-HSV-TK vector with GCV treatment on patients with hormone-refractory prostate cancer (Nasu et al., 2007).

Here we describe the investigation of an Ad vector expressing HSV-TK under the control of the MPE_2 promoter for use in breast cancer gene therapy.

1.3. MOUSE MODELS

An important tool in the testing of cancer therapies is a relevant *in vivo* mouse model. The first transgenic mouse model of breast cancer involved mice expressing the Myc oncogene (amplified in 15% of human breast cancers (Deming et al., 2000)) under the control of the mouse mammary tumor virus (MMTV) promoter/enhancer (Stewart, Pattengale, and Leder, 1984). Since then, other oncogenes have been placed under the control of the MMTV promoter to yield different types of mammary tumors. Many of these transgenic mice induce tumors that have a distinct pathology dependent on the initiating oncogene (Cardiff et al., 1991).

Some mouse models provide excellent environments for examining the progression of cancer and can even mimic metastasis. The 4T1 mouse model is a metastatic breast

cancer model utilizing 4T1 cells derived from a mammary tumor that arose spontaneously in a wild-type BALB/c mouse (Aslakson and Miller, 1992). Cells from the 4T1 line are able to complete all steps of metastasis and form visible metastatic nodules in lungs. This model is useful in studying the metastatic progression of breast cancer, the effect of therapies on metastatic mammary tumors, as well as the role of the immune system on cancer progression and therapy (Brin et al., 2006). The EMT6 mouse mammary tumor model is another model that can be used to study treatment effects on tumor growth and metastasis. The EMT6 cell line is a tissue culture clonal isolate derived from a tumor line that arose in a BALB/cCRGL mouse after implantation of a hyperplastic mammary alveolar nodule (Rockwell, Kallman, and Fajardo, 1972).

Other mouse models have been generated that produce more varied tumor morphological patterns which are more analogous to the heterogeneity observed in human breast cancer (Andrechek and Nevins, 2010). One such example is the transgenic mouse model expressing the polyoma virus middle T antigen (PyMT) under the control of the MMTV promoter (Guy, Cardiff, and Muller, 1992) which mimics the progression of ductal carcinoma *in situ*, a precursor of human breast cancer (Maglione et al., 2004). PyMT activates the phosphatidylinositol 3-kinase signaling pathway (Serunian et al., 1990; Talmage et al., 1989; Ulug et al., 1990), whose expression and activity levels are frequently upregulated in human breast cancer tissues (Gershtein et al., 2007). PyMT activates many pathways that are also activated by erbB2 (Her2/*neu*), which has been shown to be overexpressed in up to 30% of human breast cancers (Slamon et al., 1987). Transplantation of cells derived from these transgenic mice has generated important models for studying ductal carcinoma *in situ*, as well as for

preclinical testing (Namba et al., 2005; Varticovski et al., 2007). Another important feature of this model is that immunocompetent FVB mice can be recipients of tumor cells transplanted from this model (Addison et al., 1995; Guy, Cardiff, and Muller, 1992) which were characterized as described in Chapter 3.

An ideal mouse tumor model will exhibit many similaries with its corresponding human tumor. While the standard practice of xenografting tumors into immunocompromised mice can often possess the benefit of convenience, these models may not be ideal for preclinical testing of cancer therapeutics. In fact, these models have been shown to have only moderate predictive value when the same drugs are tested in phase II clinical trials (Johnson et al., 2001; Kelland, 2004; Kerbel, 2003; Voskoglou-Nomikos, Pater, and Seymour, 2003). The use of immunocompromised mice for preclinical testing also makes it difficult to predict the role of the immune system in response to a particular therapy. Here we characterize a unique immunocompetent mouse model for breast cancer and illustrate its potential for use in testing preclinical adenoviral gene therapy and cancer imaging.

1.4. CANCER IMAGING

Another important tool for the detection and monitoring of cancer, as well as evaluating cancer gene therapy, involves cancer imaging. Early detection of cancer can increase the probability of survival. This is especially true for breast cancer, as mammography screening is highly emphasized by the World Health Organization, American Cancer Society, and Canadian Cancer Society. A mammogram, which involves X-rays to image breast density, is the primary imaging modality for breast cancer screening and

diagnosis due to its low cost and widespread availability. Unfortunately, the sensitivity of mammography is low in women with dense breast tissue (Kerlikowske, 1997) and women who carry BRCA mutations (Brekelmans et al., 2001; Kuhl et al., 2005; Lakhani et al., 1998). Magnetic resonance imaging (MRI) has a higher sensitivity than mammography and is not affected by breast density (Sardanelli et al., 2004). In combination with mammography, an MRI can also enhance breast cancer detection and staging (Tofts, Berkowitz, and Schnall, 1995). MRI is a non-invasive procedure that does not use ionizing radiation like X-rays, but rather generates images based on changes in the electric field of hydrogen atoms in the body. Hydrogen nuclei within a patient align like small magnets when placed in the powerful magnetic field of an MRI machine. Radiofrequency pulses are then utilized to create an oscillating magnetic field perpendicular to the main field, from which the nuclei absorb energy and move out of alignment with the static field into a state of excitation. An MRI machine can then translate nuclei returning to the equilibrium state into a diagnostic image. Proton density and relaxation dynamics vary in different tissues, which allows for visualization of different images based on tissue type. Mammography, MRI, and computed tomography (CT), which renders computer-generated 'slices' into three dimensional images, are mainly used for the detection of structural or contrast changes within a tissue (Kwee et al., 2010). These conventional techniques are limited in their ability to measure metabolic changes, which limits their effectiveness for characterizing biological processes and/or molecular responses to therapy within a tumor (Kapty, Murray, and Mercer, 2010; Torigian et al., 2007). Functional imaging modalities have been developed that are able to visualize metabolic or proliferation changes within a tumor.

This ability to image a patient's tumor at a molecular level can play a tremendous role in assisting patients with detection of cancer and monitoring a therapeutic response.

1.4.1. Positron Emission Tomography

Positron emission tomography (PET) is a molecular imaging technology that visualizes the accumulation of positron emitting probes. These radioactive probes are administered intravenously to be distributed throughout the body and can concentrate in specific cells or tissues. When a positron is emitted from a probe, it is annihilated upon contact with a nearby electron and two 511 keV gamma (γ) rays are given off in opposite directions. A PET scanner can detect these gamma rays and localize the source of the annihilation event. The scanner then generates tomographic images of the radioactivity distribution which can be evaluated quantitatively (Phelps, 2000). Advantages of using positron emission tomography are its high sensitivity and the large number of available molecular probes (Papathanassiou et al., 2009) which provides the ability to image various tumor parameters.

1.4.2. [^{18}F] Labeled PET Tracers

PET has been used repeatedly for quantitative noninvasive imaging of transgene expression in animals (Gambhir et al., 1998; MacLaren et al., 1999). Evaluation of glucose metabolism using 2-deoxy-2-[^{18}F]fluoro-D-glucose ([^{18}F]FDG; Figure 1.5A) is the most widely used PET imaging agent due to the increased glucose requirement of cancer cells described as the Warburg effect (Warburg, Wind, and Negelein, 1927). The original theory and model for [^{18}F]FDG is an analog of 2-deoxy-D-glucose, the substrate for hexokinase (Sols and Crane, 1954). The presence of [^{18}F] on position 2 does not impair the ability of [^{18}F]FDG to be used as a hexokinase substrate (Bessell,

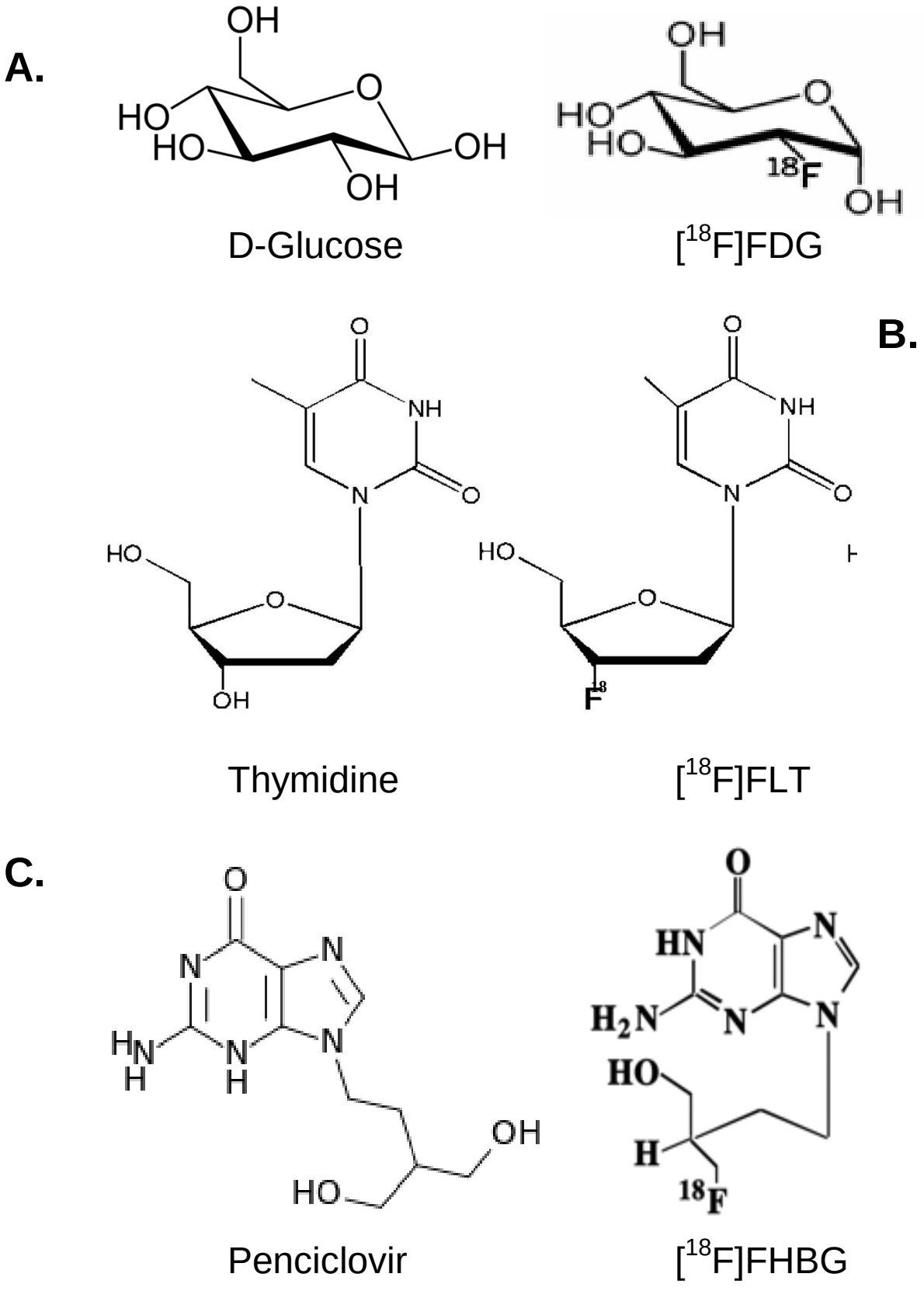

Figure 1.5. D-Glucose, thymidine, penciclovir and their PET analogs

Foster, and Westwood, 1972; Machado de Domenech and Sols, 1980). [^{18}F]FDG was first synthesized in 1977 (Ido et al., 1977). [^{18}F]FDG enters a cell through glucose transporters (mainly GLUT1), which are commonly upregulated in most cancers and are negatively associated with patient prognosis (Medina and Owen, 2002; Smith, 1999). After entering a tumor cell, [^{18}F]FDG is phosphorylated by cellular hexokinase (Bessell, Foster, and Westwood, 1972) to [^{18}F]FDG-6-phosphate, which is a relatively poor substrate for subsequent metabolic steps (Bessell and Thomas, 1973). The enzyme glucose-6-phosphatase, catalyzing the reverse of he hexokinase reaction, has low activity in most tumor cells which leads to the accumulation of [^{18}F]FDG-6-phosphate (Caraco et al., 2000). Thus, [^{18}F]FDG-PET provides information on the expression of glucose transporters and hexokinase activity (Gallagher et al., 1978; Hatanaka, Augl, and Gilden, 1970). The downside of using [^{18}F]FDG for cancer imaging is that it is not cancer specific since this reporter probe may be trapped in any highly metabolically-active sites, such as macrophages (Kubota et al., 1992; Yamada et al., 1998) which invade tumors and are found in inflammatory lesions. The main indication of [^{18}F]FDG-PET in breast cancer is currently for detection of recurrence and metastases (Isasi, Moadel, and Blaufox, 2005; Papathanassiou et al., 2009).

3'-deoxy-3'-[^{18}F]fluorothymidine ([^{18}F]FLT; Figure 1.5B) is a thymidine analog PET reporter which is more specific to cancer since its accumulation is not based on glucose metabolism but rather cellular proliferation, which is known to be high in cancer cells. While earlier studies used [^{11}C]-labeled thymidine as a measure for cell proliferation since it is rapidly incorporated into newly synthesized DNA and imaged with PET (van Eijkeren et al., 1996; Vander Borght et al., 1991), it was not an ideal radiotracer due to

the short half-life of [^{11}C] (20 minutes) and the fact that [^{11}C]thymidine retention declined more rapidly than [^{18}F]FDG (Shields et al., 1998b). [^{18}F]FLT uptake by cells positively correlates with endogenous thymidine kinase 1 (TK1) gene expression (Rasey et al., 2002), which is specifically induced during S-phase at the transcriptional and posttranscriptional level (Sherley and Kelly, 1988; Sutterluety et al., 1998) and leads to intracellular trapping (Kong et al., 1992). The signal measured with [^{18}F]FLT-PET reflects the uptake of [^{18}F]FLT through nucleoside transporters and subsequent monophosphorylation by endogenous TK1 (Shields et al., 2008), correlating with the degree of cellular proliferation (Ellims, Van der Weyden, and Medley, 1981). In cancer imaging, scientists use [^{18}F]FLT uptake as a measure of tumor proliferation (Buck et al., 2002; Grierson and Shields, 2000; Shields et al., 1998a), where tumors can be imaged within 15 to 60 minutes after administration of the radiotracer (Shields et al., 1998a). Many studies have demonstrated the feasibility of [^{18}F]FLT to image early response to anticancer treatments (Apisarnthanarax et al., 2006; Barthel et al., 2003; Graf et al., 2008). Since [^{18}F]FLT is also a substrate for HSV-TK (Buursma et al., 2006), it can be used to measure HSV-TK transgene expression in transduced cells. In addition, due to the 110 minute half life of ^{18}F, imaging using this tracer can be repeated in the same patient over a longitudinal treatment study without interference from an injection on a previous day. While [^{18}F]FLT is more widely used as a response indicator for PET imaging, there are other radiotracers that have been developed.

In fact, early imaging of HSV infection was carried out using autoradiography and [^{14}C]5-methyl-2'-fluoroarabinouridine (FMAU) (Saito et al., 1982; Saito et al., 1984) long before HSV-TK reporter gene activity was ever imaged. These studies demonstrated

trapping of the phosphorylated probe in tissues expressing HSV-TK. A subsequent study used 5-iodo-2'-fluoro-2'-deoxy-1-βD-arabinofuranosyl-5-iodouracil (FIAU) to image HSV-TK-infected cells *in vitro* (Tovell et al., 1988). [^{124}I]FIAU was later used to image HSV-TK gene expression *in vivo* using PET (Tjuvajev, Avril, and Safer, 1997; Tjuvajev et al., 1998). 5-iodo-2'-fluoro-2'-deoxyuridine (FIRU) was then shown to be more selective than FIAU for HSV-TK with higher uptake *in vitro and in vivo* (Wiebe, Knaus, and Morin, 1999).

9-(4-[^{18}F]fluoro-3-hydroxymethylbutyl)-guanine ([^{18}F]FHBG; Figure 1.5C) is another PET reporter probe which acts as a substrate for HSV-TK. Initial *in vitro* studies using [^{18}F]FHBG showed that it does not accumulate in cells that do not express HSV-TK (Alauddin and Conti, 1998), indicating the specificity for the viral kinase over endogenous mammalian TK1. In fact, [^{18}F]FHBG is often considered the most efficient PET tracer for imaging *in vivo* HSV-TK gene expression due to its interaction kinetics with HSV-TK (compared to HSV-TK and thymidine) (Barrio, 2004). Previous research has shown that there is an almost 2-fold accumulation of [^{18}F]FHBG relative to ganciclovir analogs in tissues transduced with HSV-TK (Gambhir et al., 1999a). [^{18}F]FHBG is a useful PET reporter probe when used in combination with AdHSV-TK imaging. *In vitro* and *in vivo* animal studies have shown that the [^{18}F]FHBG signal acquired from PET imaging closely correlates with HSV-TK transgene expression from Ad vectors as determined by mRNA abundance and protein levels (Gambhir et al., 1999b). PET imaging using [^{18}F]FHBG to visualize the HSV-TK transgene has now been established in both animal and human studies (Miletic et al., 2007; Tjuvajev et al., 2002; Yaghoubi et al., 2006). Preclinical studies have been carried out to establish

imaging protocols and dosimetry of [^{18}F]FHBG in healthy human volunteers (Yaghoubi et al., 2001). The application of [^{18}F]FHBG-PET for imaging AdHSV-TK gene expression has been shown in human patients with hepatocellular carcinoma. A FGAd expressing HSV-TK under the control of the ubiquitously active CMV promoter was administered intratumorally and found to induce accumulation of [^{18}F]FHBG in injected tumor nodules (Penuelas et al., 2005). To date, there are relatively few studies that utilize [^{18}F]FHBG-PET for breast cancer. The use of HSV-TK gene therapy for tumor cell killing has been examined, including those administered by Ad vectors, but again very few use [^{18}F]FHBG-PET to monitor therapeutic response. As well, no groups besides ours are currently investigating the MPE_2 modified mammaglobin promoter as a breast cancer-specific promoter. This thesis describes the combination of Ad vector-delivered HSV-TK gene therapy for breast cancer treatment and the application of [^{18}F]FHBG-PET for measuring the tissue biodistribution of HSV-TK expression.

1.5. BREAST CANCER GENE THERAPY AND PET IMAGING OF AdMPE$_2$TK ACTIVITY

Here we illustrate the use of the AdMPE$_2$TK non-replicating Ad vector for breast cancer gene therapy. The MPE_2 promoter can drive breast cancer-selective expression of HSV-TK for therapeutic purposes (in combination with the prodrug GCV) and as a platform to image therapeutic response (in combination with [^{18}F] labeled PET radiotracers). By combining PET imaging with targeted Ad vector HSV-TK gene therapy, it may be possible to visualize vector expression using *in vivo* models, and potentially aid in imaging induced tumor regression.

We hypothesize that the AdMPE$_2$TK vector will induce targeted expression of HSV-TK within BrCa cells due to the specificity of the modified MGB promoter. This BrCa-selective activity should induce tumor regression in therapeutic studies and also allow for tumor-selective accumulation of [^{18}F] labeled PET tracers in imaging studies.

To investigate the potential of the AdMPE$_2$TK vector, we first examined the BrCa selectivity of the MPE$_2$ promoter as well as the therapeutic efficacy of the AdMPE$_2$TK vector to kill tumor cells *in vitro* and regress tumors *in vivo* following GCV. In addition, we also noted minimal toxicity from this vector as compared to the AdCMVTK vector which has been used in clinical trials. We then characterized the immunocompetent MTHJ mouse BrCa model as having high biological significance to human BrCa. Finally, using the MTHJ mouse model, PET imaging was used to evaluate the accumulation of radiolabeled HSV-TK substrates [^{18}F]FLT and [^{18}F]FHBG in cells infected by the AdMPE$_2$TK vector.

1.6. REFERENCES

(1957). VIRUSES in treatment of cancer. *Br Med J* **2**(5059)**,** 1481-2.

Abordo-Adesida, E., Follenzi, A., Barcia, C., Sciascia, S., Castro, M. G., Naldini, L., and Lowenstein, P. R. (2005). Stability of lentiviral vector-mediated transgene expression in the brain in the presence of systemic antivector immune responses. *Hum Gene Ther* **16**(6)**,** 741-51.

Addison, C. L., Braciak, T., Ralston, R., Muller, W. J., Gauldie, J., and Graham, F. L. (1995). Intratumoral injection of an adenovirus expressing interleukin 2 induces regression and immunity in a murine breast cancer model. *Proc Natl Acad Sci U S A* **92**(18)**,** 8522-6.

Agard, C., Ligeza, C., Dupas, B., Izembart, A., El Kouri, C., Moullier, P., and Ferry, N. (2001). Immune-dependent distant bystander effect after adenovirus-mediated suicide gene transfer in a rat model of liver colorectal metastasis. *Cancer Gene Ther* **8**(2)**,** 128-36.

Aghi, M., Hochberg, F., and Breakefield, X. O. (2000). Prodrug activation enzymes in cancer gene therapy. *J Gene Med* **2**(3)**,** 148-64.

Alauddin, M. M., and Conti, P. S. (1998). Synthesis and preliminary evaluation of 9-(4-[18F]-fluoro-3-hydroxymethylbutyl)guanine ([18F]FHBG): a new potential imaging agent for viral infection and gene therapy using PET. *Nucl Med Biol* **25**(3)**,** 175-80.

Alvarez, R. D., Gomez-Navarro, J., Wang, M., Barnes, M. N., Strong, T. V., Arani, R. B., Arafat, W., Hughes, J. V., Siegal, G. P., and Curiel, D. T. (2000). Adenoviral-mediated suicide gene therapy for ovarian cancer. *Mol Ther* **2**(5)**,** 524-30.

Andrechek, E. R., and Nevins, J. R. (2010). Mouse models of cancers: opportunities to address heterogeneity of human cancer and evaluate therapeutic strategies. *J Mol Med (Berl)* **88**(11)**,** 1095-100.

Apisarnthanarax, S., Alauddin, M. M., Mourtada, F., Ariga, H., Raju, U., Mawlawi, O., Han, D., Bornmann, W. G., Ajani, J. A., Milas, L., Gelovani, J. G., and Chao, K. S. (2006). Early detection of chemoradioresponse in esophageal carcinoma by 3'-deoxy-3'-3H-fluorothymidine using preclinical tumor models. *Clin Cancer Res* **12**(15)**,** 4590-7.

Aslakson, C. J., and Miller, F. R. (1992). Selective events in the metastatic process defined by analysis of the sequential dissemination of subpopulations of a mouse mammary tumor. *Cancer Res* **52**(6)**,** 1399-405.

Ast, G. (2003). Drug-targeting strategies for prostate cancer. *Curr Pharm Des* **9**(6)**,** 455-66.

Avery, O. T., Macleod, C. M., and McCarty, M. (1944). Studies on the Chemical Nature of the Substance Inducing Transformation of Pneumococcal Types : Induction of Transformation by a Desoxyribonucleic Acid Fraction Isolated from Pneumococcus Type Iii. *J Exp Med* **79**(2)**,** 137-58.

Barrio, J. R. (2004). The molecular basis of disease. *In* "PET: molecular imaging and its biological applications" (M. E. Phelps, Ed.), pp. 270-320. Springer-Verlag, New York.

Barthel, H., Cleij, M. C., Collingridge, D. R., Hutchinson, O. C., Osman, S., He, Q., Luthra, S. K., Brady, F., Price, P. M., and Aboagye, E. O. (2003). 3'-deoxy-3'-[18F]fluorothymidine as a new marker for monitoring tumor response to antiproliferative therapy in vivo with positron emission tomography. *Cancer Res* **63**(13)**,** 3791-8.

Bergelson, J. M., Cunningham, J. A., Droguett, G., Kurt-Jones, E. A., Krithivas, A., Hong, J. S., Horwitz, M. S., Crowell, R. L., and Finberg, R. W. (1997). Isolation of a common receptor for Coxsackie B viruses and adenoviruses 2 and 5. *Science* **275**(5304)**,** 1320-3.

Berger, J., Burnett, R. M., Franklin, R. M., and Grutter, M. (1978). Small angle x-ray scattering studies on adenovirus type 2 hexon. *Biochim Biophys Acta* **535**(2)**,** 233-40.

Berk, A. J. (2005). Recent lessons in gene expression, cell cycle control, and cell biology from adenovirus. *Oncogene* **24**(52)**,** 7673-85.

Berk, A. J. (2007). Adenoviridae: The viruses and their replication. 5th ed. *In* "Fields Virology" (D. Knipe, Howley, P., Ed.), pp. 2355-2394. Wolters Kluwer Health/Lippincott Williams & Wilkins, Philadelphia.

Berkner, K. L. (1988). Development of adenovirus vectors for the expression of heterologous genes. *Biotechniques* **6**(7)**,** 616-29.

Bernstein, J. L., Godbold, J. H., Raptis, G., Watson, M. A., Levinson, B., Aaronson, S. A., and Fleming, T. P. (2005). Identification of mammaglobin as a novel serum marker for breast cancer. *Clin Cancer Res* **11**(18)**,** 6528-35.

Bessell, E. M., Foster, A. B., and Westwood, J. H. (1972). The use of deoxyfluoro-D-glucopyranoses and related compounds in a study of yeast hexokinase specificity. *Biochem J* **128**(2)**,** 199-204.

Bessell, E. M., and Thomas, P. (1973). The effect of substitution at C-2 of D-glucose 6-phosphate on the rate of dehydrogenation by glucose 6-phosphate dehydrogenase (from yeast and from rat liver). *Biochem J* **131**(1)**,** 83-9.

Bi, W. L., Parysek, L. M., Warnick, R., and Stambrook, P. J. (1993). In vitro evidence that metabolic cooperation is responsible for the bystander effect observed with HSV tk retroviral gene therapy. *Hum Gene Ther* **4**(6)**,** 725-31.

Bieche, I., and Lidereau, R. (1995). Genetic alterations in breast cancer. *Genes Chromosomes Cancer* **14**(4)**,** 227-51.

Blackburn, R. V., Galoforo, S. S., Corry, P. M., and Lee, Y. J. (1998). Adenoviral-mediated transfer of a heat-inducible double suicide gene into prostate carcinoma cells. *Cancer Res* **58**(7)**,** 1358-62.

Blaese, R. M., Culver, K. W., Miller, A. D., Carter, C. S., Fleisher, T., Clerici, M., Shearer, G., Chang, L., Chiang, Y., Tolstoshev, P., Greenblatt, J. J., Rosenberg, S. A., Klein, H., Berger, M., Mullen, C. A., Ramsey, W. J., Muul, L., Morgan, R. A., and Anderson, W. F. (1995). T lymphocyte-directed gene therapy for ADA- SCID: initial trial results after 4 years. *Science* **270**(5235)**,** 475-80.

Blomer, U., Naldini, L., Kafri, T., Trono, D., Verma, I. M., and Gage, F. H. (1997). Highly efficient and sustained gene transfer in adult neurons with a lentivirus vector. *J Virol* **71**(9)**,** 6641-9.

Brekelmans, C. T., Seynaeve, C., Bartels, C. C., Tilanus-Linthorst, M. M., Meijers-Heijboer, E. J., Crepin, C. M., van Geel, A. A., Menke, M., Verhoog, L. C., van den Ouweland, A., Obdeijn, I. M., and Klijn, J. G. (2001). Effectiveness of breast cancer surveillance in BRCA1/2 gene mutation carriers and women with high familial risk. *J Clin Oncol* **19**(4)**,** 924-30.

Brin, E., Atencio, I., Helmich, B. K., Maneval, D., and Laface, D. (2006). Adenovirus delivery provides extended interferon-alpha exposure and augments treatment of metastatic carcinoma. *Cancer Gene Ther* **13**(7)**,** 664-75.

Buck, A. K., Schirrmeister, H., Hetzel, M., Von Der Heide, M., Halter, G., Glatting, G., Mattfeldt, T., Liewald, F., Reske, S. N., and Neumaier, B. (2002). 3-deoxy-3-[(18)F]fluorothymidine-positron emission tomography for noninvasive assessment of proliferation in pulmonary nodules. *Cancer Res* **62**(12)**,** 3331-4.

Buhles, W. C. (2011). Compassionate use: a story of ethics and science in the development of a new drug. *Perspect Biol Med* **54**(3)**,** 304-15.

Bukrinsky, M. I., Haggerty, S., Dempsey, M. P., Sharova, N., Adzhubel, A., Spitz, L., Lewis, P., Goldfarb, D., Emerman, M., and Stevenson, M. (1993). A nuclear localization signal within HIV-1 matrix protein that governs infection of non-dividing cells. *Nature* **365**(6447)**,** 666-9.

Buursma, A. R., Rutgers, V., Hospers, G., Mulder, N., Vaalburg, W., and de Vries, E. (2006). ^{18}F-FEAU as a radiotracer for herpes simplex virus thymidine kinase gene expression: in-vitro comparison with oher PET tracers. *Nucl Med Commun* **27**(1), 25-30.

Canadian Cancer Society (2011). Canadian Cancer Statistics 2011. CancerStats. 2011.

Caraco, C., Aloj, L., Chen, L. Y., Chou, J. Y., and Eckelman, W. C. (2000). Cellular release of [18F]2-fluoro-2-deoxyglucose as a function of the glucose-6-phosphatase enzyme system. *J Biol Chem* **275**(24)**,** 18489-94.

Cardiff, R. D., Sinn, E., Muller, W., and Leder, P. (1991). Transgenic oncogene mice. Tumor phenotype predicts genotype. *Am J Pathol* **139**(3)**,** 495-501.

Carey, L. A., Dees, E. C., Sawyer, L., Gatti, L., Moore, D. T., Collichio, F., Ollila, D. W., Sartor, C. I., Graham, M. L., and Perou, C. M. (2007). The triple negative paradox: primary tumor chemosensitivity of breast cancer subtypes. *Clin Cancer Res* **13**(8)**,** 2329-34.

Carey, L. A., Perou, C. M., Livasy, C. A., Dressler, L. G., Cowan, D., Conway, K., Karaca, G., Troester, M. A., Tse, C. K., Edmiston, S., Deming, S. L., Geradts, J., Cheang, M. C., Nielsen, T. O., Moorman, P. G., Earp, H. S., and Millikan, R. C. (2006). Race, breast cancer subtypes, and survival in the Carolina Breast Cancer Study. *JAMA* **295**(21)**,** 2492-502.

Carter, D., Douglass, J. F., Cornellison, C. D., Retter, M. W., Johnson, J. C., Bennington, A. A., Fleming, T. P., Reed, S. G., Houghton, R. L., Diamond, D. L., and Vedvick, T. S. (2002). Purification and characterization of the mammaglobin/lipophilin B complex, a promising diagnostic marker for breast cancer. *Biochemistry* **41**(21)**,** 6714-22.

Champness, J. N., Bennett, M. S., Wien, F., Visse, R., Summers, W. C., Herdewijn, P., de Clerq, E., Ostrowski, T., Jarvest, R. L., and Sanderson, M. R. (1998). Exploring the active site of herpes simplex virus type-1 thymidine kinase by X-ray crystallography of complexes with aciclovir and other ligands. *Proteins* **32**(3)**,** 350-61.

Cheang, M. C., Chia, S. K., Voduc, D., Gao, D., Leung, S., Snider, J., Watson, M., Davies, S., Bernard, P. S., Parker, J. S., Perou, C. M., Ellis, M. J., and Nielsen, T. O. (2009). Ki67 index, HER2 status, and prognosis of patients with luminal B breast cancer. *J Natl Cancer Inst* **101**(10)**,** 736-50.

Chen, J. S., Liu, J. C., Shen, L., Rau, K. M., Kuo, H. P., Li, Y. M., Shi, D., Lee, Y. C., Chang, K. J., and Hung, M. C. (2004). Cancer-specific activation of the survivin promoter and its potential use in gene therapy. *Cancer Gene Ther* **11**(11)**,** 740-7.

Chen, L., Zheng, J., Zhang, Y., Yang, L., Wang, J., Ni, J., Cui, D., Yu, C., and Cai, Z. (2011). Tumor-specific expression of microRNA-26a suppresses human hepatocellular carcinoma growth via cyclin-dependent and -independent pathways. *Mol Ther* **19**(8)**,** 1521-8.

Cheon, J., Kim, H. K., Moon, D. G., Yoon, D. K., Cho, J. H., and Koh, S. K. (2000). Adenovirus-mediated suicide-gene therapy using the herpes simplex virus thymidine kinase gene in cell and animal models of human prostate cancer: changes in tumour cell proliferative activity. *BJU Int* **85**(6)**,** 759-66.

Chevez-Barrios, P., Chintagumpala, M., Mieler, W., Paysse, E., Boniuk, M., Kozinetz, C., Hurwitz, M. Y., and Hurwitz, R. L. (2005). Response of retinoblastoma with vitreous tumor seeding to adenovirus-mediated delivery of thymidine kinase followed by ganciclovir. *J Clin Oncol* **23**(31)**,** 7927-35.

Chuaqui, R. F., Zhuang, Z., Emmert-Buck, M. R., Liotta, L. A., and Merino, M. J. (1997). Analysis of loss of heterozygosity on chromosome 11q13 in atypical ductal hyperplasia and in situ carcinoma of the breast. *Am J Pathol* **150**(1)**,** 297-303.

Chung, I., Schwartz, P. E., Crystal, R. G., Pizzorno, G., Leavitt, J., and Deisseroth, A. B. (1999). Use of L-plastin promoter to develop an adenoviral system that confers transgene expression in ovarian cancer cells but not in normal mesothelial cells. *Cancer Gene Ther* **6**(2)**,** 99-106.

Counter, C. M., Hirte, H. W., Bacchetti, S., and Harley, C. B. (1994). Telomerase activity in human ovarian carcinoma. *Proc Natl Acad Sci U S A* **91**(8)**,** 2900-4.

Courjal, F., Cuny, M., Simony-Lafontaine, J., Louason, G., Speiser, P., Zeillinger, R., Rodriguez, C., and Theillet, C. (1997). Mapping of DNA amplifications at 15 chromosomal localizations in 1875 breast tumors: definition of phenotypic groups. *Cancer Res* **57**(19)**,** 4360-7.

Culver, K. W., Ram, Z., Wallbridge, S., Ishii, H., Oldfield, E. H., and Blaese, R. M. (1992). In vivo gene transfer with retroviral vector-producer cells for treatment of experimental brain tumors. *Science* **256**(5063)**,** 1550-2.

Czernin, J., Benz, M. R., and Allen-Auerbach, M. S. Breast cancer. *Methods Mol Biol* **727,** 141-70.

Davison, A. J., Benko, M., and Harrach, B. (2003). Genetic content and evolution of adenoviruses. *J Gen Virol* **84**(Pt 11)**,** 2895-908.

Deming, S. L., Nass, S. J., Dickson, R. B., and Trock, B. J. (2000). C-myc amplification in breast cancer: a meta-analysis of its occurrence and prognostic relevance. *Br J Cancer* **83**(12)**,** 1688-95.

Derse, D., Cheng, Y. C., Furman, P. A., St Clair, M. H., and Elion, G. B. (1981). Inhibition of purified human and herpes simplex virus-induced DNA polymerases by 9-(2-hydroxyethoxymethyl)guanine triphosphate. Effects on primer-template function. *J Biol Chem* **256**(22)**,** 11447-51.

Djeha, A. H., Thomson, T. A., Leung, H., Searle, P. F., Young, L. S., Kerr, D. J., Harris, P. A., Mountain, A., and Wrighton, C. J. (2001). Combined adenovirus-mediated nitroreductase gene delivery and CB1954 treatment: a well-tolerated therapy for established solid tumors. *Mol Ther* **3**(2)**,** 233-40.

Doehmer, J., Barinaga, M., Vale, W., Rosenfeld, M. G., Verma, I. M., and Evans, R. M. (1982). Introduction of rat growth hormone gene into mouse fibroblasts via a retroviral DNA vector: expression and regulation. *Proc Natl Acad Sci U S A* **79**(7)**,** 2268-72.

Dono, M., Ferro, P., Franceschini, M. C., Dessanti, P., Bacigalupo, B., Cibei, E., Capellini, C., Amoroso, D., Camerini, A., Fedeli, F., and Roncella, S. (2011). Human mammaglobin transcript amplification for differential diagnosis in a breast cancer metastatic to dura mater. *Anticancer Res* **31**(3)**,** 1061-4.

Dormond, E., Perrier, M., and Kamen, A. (2009). From the first to the third generation adenoviral vector: what parameters are governing the production yield? *Biotechnol Adv* **27**(2)**,** 133-44.

Douglas, K. L. (2008). Toward development of artificial viruses for gene therapy: a comparative evaluation of viral and non-viral transfection. *Biotechnol Prog* **24**(4)**,** 871-83.
Driouch, K., Champeme, M. H., Beuzelin, M., Bieche, I., and Lidereau, R. (1997). Classical gene amplifications in human breast cancer are not associated with distant solid metastases. *Br J Cancer* **76**(6)**,** 784-7.
Duflot-Dancer, A., Piccoli, C., Rolland, A., Yamasaki, H., and Mesnil, M. (1998). Long-term connexin-mediated bystander effect in highly tumorigenic human cells in vivo in herpes simplex virus thymidine kinase/ganciclovir gene therapy. *Gene Ther* **5**(10)**,** 1372-8.
Eastham, J. A., Chen, S. H., Sehgal, I., Yang, G., Timme, T. L., Hall, S. J., Woo, S. L., and Thompson, T. C. (1996). Prostate cancer gene therapy: herpes simplex virus thymidine kinase gene transduction followed by ganciclovir in mouse and human prostate cancer models. *Hum Gene Ther* **7**(4)**,** 515-23.
Elion, G. B., Furman, P. A., Fyfe, J. A., de Miranda, P., Beauchamp, L., and Schaeffer, H. J. (1977). Selectivity of action of an antiherpetic agent, 9-(2-hydroxyethoxymethyl) guanine. *Proc Natl Acad Sci U S A* **74**(12)**,** 5716-20.
Ellims, P. H., Van der Weyden, M. B., and Medley, G. (1981). Thymidine kinase isoenzymes in human malignant lymphoma. *Cancer Res* **41**(2)**,** 691-5.
Enders, J. F., Bell, J. A., Dingle, J. H., Francis, T., Jr., Hilleman, M. R., Huebner, R. J., and Payne, A. M. (1956). Adenoviruses: group name proposed for new respiratory-tract viruses. *Science* **124**(3212)**,** 119-20.
Evans, J. D. a. H., P. (2002). Adenovirus Replication. *In* "Adenoviral Vectors for Gene Therapy" (D. T. Curiel, and Douglas, J.T., Ed.), pp. 39-70. Academic Press, San Diego, CA.
Fanger, G. R., Houghton, R. L., Retter, M. W., Hendrickson, R. C., Babcook, J., Dillon, D. C., Durham, M. D., Reynolds, L. D., Johnson, J. C., Carter, D., Fleming, T. P., Roche, P. C., Persing, D. H., and Reed, S. G. (2002). Detection of mammaglobin in the sera of patients with breast cancer. *Tumour Biol* **23**(4)**,** 212-21.
Fantl, V., Richards, M. A., Smith, R., Lammie, G. A., Johnstone, G., Allen, D., Gregory, W., Peters, G., Dickson, C., and Barnes, D. M. (1990). Gene amplification on chromosome band 11q13 and oestrogen receptor status in breast cancer. *Eur J Cancer* **26**(4)**,** 423-9.
Ficazzola, M. A., and Taneja, S. S. (1998). Prospects for gene therapy in human prostate cancer. *Mol Med Today* **4**(11)**,** 494-504.
Fleming, T. P., and Watson, M. A. (2000). Mammaglobin, a breast-specific gene, and its utility as a marker for breast cancer. *Ann N Y Acad Sci* **923,** 78-89.
Freed, E. O., and Martin, M. A. (1994). HIV-1 infection of non-dividing cells. *Nature* **369**(6476)**,** 107-8.
Friedmann, T., and Roblin, R. (1972). Gene therapy for human genetic disease? *Science* **175**(4025)**,** 949-55.
Fyfe, J. A., Keller, P. M., Furman, P. A., Miller, R. L., and Elion, G. B. (1978). Thymidine kinase from herpes simplex virus phosphorylates the new antiviral compound, 9-(2-hydroxyethoxymethyl)guanine. *J Biol Chem* **253**(24)**,** 8721-7.
Gallagher, B. M., Fowler, J. S., Gutterson, N. I., MacGregor, R. R., Wan, C. N., and Wolf, A. P. (1978). Metabolic trapping as a principle of oradiopharmaceutical design: some factors resposible for the biodistribution of [18F] 2-deoxy-2-fluoro-D-glucose. *J Nucl Med* **19**(10)**,** 1154-61.
Gambhir, S. S., Barrio, J. R., Herschman, H. R., and Phelps, M. E. (1999a). Assays for noninvasive imaging of reporter gene expression. *Nucl Med Biol* **26**(5)**,** 481-90.

Gambhir, S. S., Barrio, J. R., Phelps, M. E., Iyer, M., Namavari, M., Satyamurthy, N., Wu, L., Green, L. A., Bauer, E., MacLaren, D. C., Nguyen, K., Berk, A. J., Cherry, S. R., and Herschman, H. R. (1999b). Imaging adenoviral-directed reporter gene expression in living animals with positron emission tomography. *Proc Natl Acad Sci U S A* **96**(5)**,** 2333-8.

Gambhir, S. S., Barrio, J. R., Wu, L., Iyer, M., Namavari, M., Satyamurthy, N., Bauer, E., Parrish, C., MacLaren, D. C., Borghei, A. R., Green, L. A., Sharfstein, S., Berk, A. J., Cherry, S. R., Phelps, M. E., and Herschman, H. R. (1998). Imaging of adenoviral-directed herpes simplex virus type 1 thymidine kinase reporter gene expression in mice with radiolabeled ganciclovir. *J Nucl Med* **39**(11)**,** 2003-11.

Germano, I. M., Fable, J., Gultekin, S. H., and Silvers, A. (2003). Adenovirus/herpes simplex-thymidine kinase/ganciclovir complex: preliminary results of a phase I trial in patients with recurrent malignant gliomas. *J Neurooncol* **65**(3)**,** 279-89.

Gershtein, E. S., Scherbakov, A. M., Shatskaya, V. A., Kushlinsky, N. E., and Krasil'nikov, M. A. (2007). Phosphatidylinositol 3-kinase/AKT signalling pathway components in human breast cancer: clinicopathological correlations. *Anticancer Res* **27**(4A)**,** 1777-82.

Gonzalez-Angulo, A. M., Morales-Vasquez, F., and Hortobagyi, G. N. (2007). Overview of resistance to systemic therapy in patients with breast cancer. *Adv Exp Med Biol* **608,** 1-22.

Graf, N., Herrmann, K., den Hollander, J., Fend, F., Schuster, T., Wester, H. J., Senekowitsch-Schmidtke, R., zum Buschenfelde, C. M., Peschel, C., Schwaiger, M., Dechow, T., and Buck, A. K. (2008). Imaging proliferation to monitor early response of lymphoma to cytotoxic treatment. *Mol Imaging Biol* **10**(6)**,** 349-55.

Grierson, J. R., and Shields, A. F. (2000). Radiosynthesis of 3'-deoxy-3'-[(18)F]fluorothymidine: [(18)F]FLT for imaging of cellular proliferation in vivo. *Nucl Med Biol* **27**(2)**,** 143-56.

Grunewald, K., Haun, M., Urbanek, M., Fiegl, M., Muller-Holzner, E., Gunsilius, E., Dunser, M., Marth, C., and Gastl, G. (2000). Mammaglobin gene expression: a superior marker of breast cancer cells in peripheral blood in comparison to epidermal-growth-factor receptor and cytokeratin-19. *Lab Invest* **80**(7)**,** 1071-7.

Grutter, M., and Franklin, R. M. (1974). Studies on the molecular weight of the adenovirus type 2 hexon and its subunit. *J Mol Biol* **89**(1)**,** 163-78.

Guy, C. T., Cardiff, R. D., and Muller, W. J. (1992). Induction of mammary tumors by expression of polyomavirus middle T oncogene: a transgenic mouse model for metastatic disease. *Mol Cell Biol* **12**(3)**,** 954-61.

Hacein-Bey-Abina, S., von Kalle, C., Schmidt, M., Le Deist, F., Wulffraat, N., McIntyre, E., Radford, I., Villeval, J. L., Fraser, C. C., Cavazzana-Calvo, M., and Fischer, A. (2003a). A serious adverse event after successful gene therapy for X-linked severe combined immunodeficiency. *N Engl J Med* **348**(3)**,** 255-6.

Hacein-Bey-Abina, S., Von Kalle, C., Schmidt, M., McCormack, M. P., Wulffraat, N., Leboulch, P., Lim, A., Osborne, C. S., Pawliuk, R., Morillon, E., Sorensen, R., Forster, A., Fraser, P., Cohen, J. I., de Saint Basile, G., Alexander, I., Wintergerst, U., Frebourg, T., Aurias, A., Stoppa-Lyonnet, D., Romana, S., Radford-Weiss, I., Gross, F., Valensi, F., Delabesse, E., Macintyre, E., Sigaux, F., Soulier, J., Leiva, L. E., Wissler, M., Prinz, C., Rabbitts, T. H., Le Deist, F., Fischer, A., and Cavazzana-Calvo, M. (2003b). LMO2-associated clonal T cell proliferation in two patients after gene therapy for SCID-X1. *Science* **302**(5644)**,** 415-9.

Harlan, L. C., Zujewski, J. A., Goodman, M. T., and Stevens, J. L. (2010). Breast cancer in men in the United States: a population-based study of diagnosis, treatment, and survival. *Cancer* **116**(15)**,** 3558-68.

Hatanaka, M., Augl, C., and Gilden, R. V. (1970). Evidence for a functional change in the plasma membrane of murine sarcoma virus-infected mouse embryo cells. Transport and transport-associated phosphorylation of 14C-2-deoxy-D-glucose. *J Biol Chem* **245**(4)**,** 714-7.

Herschkowitz, J. I., Simin, K., Weigman, V. J., Mikaelian, I., Usary, J., Hu, Z., Rasmussen, K. E., Jones, L. P., Assefnia, S., Chandrasekharan, S., Backlund, M. G., Yin, Y., Khramtsov, A. I., Bastein, R., Quackenbush, J., Glazer, R. I., Brown, P. H., Green, J. E., Kopelovich, L., Furth, P. A., Palazzo, J. P., Olopade, O. I., Bernard, P. S., Churchill, G. A., Van Dyke, T., and Perou, C. M. (2007). Identification of conserved gene expression features between murine mammary carcinoma models and human breast tumors. *Genome Biol* **8**(5)**,** R76.

Hilleman, M. R., and Werner, J. H. (1954). Recovery of new agent from patients with acute respiratory illness. *Proc Soc Exp Biol Med* **85**(1)**,** 183-8.

Hitt, M. M., and Graham, F. L. (2000). Adenovirus vectors for human gene therapy. *Adv Virus Res* **55,** 479-505.

Hiyama, E., Gollahon, L., Kataoka, T., Kuroi, K., Yokoyama, T., Gazdar, A. F., Hiyama, K., Piatyszek, M. A., and Shay, J. W. (1996). Telomerase activity in human breast tumors. *J Natl Cancer Inst* **88**(2)**,** 116-22.

Hiyama, K., Hiyama, E., Ishioka, S., Yamakido, M., Inai, K., Gazdar, A. F., Piatyszek, M. A., and Shay, J. W. (1995). Telomerase activity in small-cell and non-small-cell lung cancers. *J Natl Cancer Inst* **87**(12)**,** 895-902.

Hooper, M. L., and Subak-Sharpe, J. H. (1981). Metabolic cooperation between cells. *Int Rev Cytol* **69,** 45-104.

Houghton, R. L., Dillon, D. C., Molesh, D. A., Zehentner, B. K., Xu, J., Jiang, J., Schmidt, C., Frudakis, A., Repasky, E., Maltez Filho, A., Nolasco, M., Badaro, R., Zhang, X., Roche, P. C., Persing, D. H., and Reed, S. G. (2001). Transcriptional complementarity in breast cancer: application to detection of circulating tumor cells. *Mol Diagn* **6**(2)**,** 79-91.

Hsieh, C. H., Liu, R. S., Wang, H. E., Hwang, J. J., Deng, W. P., Chen, J. C., and Chen, F. D. (2006). In vitro evaluation of herpes simplex virus type 1 thymidine kinase reporter system in dynamic studies of transcriptional gene regulation. *Nucl Med Biol* **33**(5)**,** 653-60.

Hu, J. C., Coffin, R. S., Davis, C. J., Graham, N. J., Groves, N., Guest, P. J., Harrington, K. J., James, N. D., Love, C. A., McNeish, I., Medley, L. C., Michael, A., Nutting, C. M., Pandha, H. S., Shorrock, C. A., Simpson, J., Steiner, J., Steven, N. M., Wright, D., and Coombes, R. C. (2006). A phase I study of OncoVEXGM-CSF, a second-generation oncolytic herpes simplex virus expressing granulocyte macrophage colony-stimulating factor. *Clin Cancer Res* **12**(22)**,** 6737-47.

Huebner, R. J., Rowe, W. P., Schatten, W. E., Smith, R. R., and Thomas, L. B. (1956). Studies on the use of viruses in the treatment of carcinoma of the cervix. *Cancer* **9**(6)**,** 1211-8.

Hugh, J., Hanson, J., Cheang, M. C., Nielsen, T. O., Perou, C. M., Dumontet, C., Reed, J., Krajewska, M., Treilleux, I., Rupin, M., Magherini, E., Mackey, J., Martin, M., and Vogel, C. (2009). Breast cancer subtypes and response to docetaxel in node-positive

breast cancer: use of an immunohistochemical definition in the BCIRG 001 trial. *J Clin Oncol* **27**(8)**,** 1168-76.

Ido, T., Wan, C. N., Fowler, A. J., and Wolf, A. (1977). Fluorination with F2. A convenient synthesis of 2-Deoxy-2-fluoro-D-glucose. *J Org Chem* **42,** 2341-2342.

Isasi, C. R., Moadel, R. M., and Blaufox, M. D. (2005). A meta-analysis of FDG-PET for the evaluation of breast cancer recurrence and metastases. *Breast Cancer Res Treat* **90**(2)**,** 105-12.

Ishiko, H., Shimada, Y., Konno, T., Hayashi, A., Ohguchi, T., Tagawa, Y., Aoki, K., Ohno, S., and Yamazaki, S. (2008). Novel human adenovirus causing nosocomial epidemic keratoconjunctivitis. *J Clin Microbiol* **46**(6)**,** 2002-8.

Jackson, D. A., Symons, R. H., and Berg, P. (1972). Biochemical method for inserting new genetic information into DNA of Simian Virus 40: circular SV40 DNA molecules containing lambda phage genes and the galactose operon of Escherichia coli. *Proc Natl Acad Sci U S A* **69**(10)**,** 2904-9.

Johnson, J. I., Decker, S., Zaharevitz, D., Rubinstein, L. V., Venditti, J. M., Schepartz, S., Kalyandrug, S., Christian, M., Arbuck, S., Hollingshead, M., and Sausville, E. A. (2001). Relationships between drug activity in NCI preclinical in vitro and in vivo models and early clinical trials. *Br J Cancer* **84**(10)**,** 1424-31.

Jolly, D. J., Okayama, H., Berg, P., Esty, A. C., Filpula, D., Bohlen, P., Johnson, G. G., Shively, J. E., Hunkapillar, T., and Friedmann, T. (1983). Isolation and characterization of a full-length expressible cDNA for human hypoxanthine phosphoribosyl transferase. *Proc Natl Acad Sci U S A* **80**(2)**,** 477-81.

Jones, M. S., 2nd, Harrach, B., Ganac, R. D., Gozum, M. M., Dela Cruz, W. P., Riedel, B., Pan, C., Delwart, E. L., and Schnurr, D. P. (2007). New adenovirus species found in a patient presenting with gastroenteritis. *J Virol* **81**(11)**,** 5978-84.

Kantoff, P. W., Kohn, D. B., Mitsuya, H., Armentano, D., Sieberg, M., Zwiebel, J. A., Eglitis, M. A., McLachlin, J. R., Wiginton, D. A., Hutton, J. J., and et al. (1986). Correction of adenosine deaminase deficiency in cultured human T and B cells by retrovirus-mediated gene transfer. *Proc Natl Acad Sci U S A* **83**(17)**,** 6563-7.

Kapty, J., Murray, D., and Mercer, J. (2010). Radiotracers for noninvasive molecular imaging of tumor cell death. *Cancer Biother Radiopharm* **25(**6)**,** 615-28.

Kelland, L. R. (2004). Of mice and men: values and liabilities of the athymic nude mouse model in anticancer drug development. *Eur J Cancer* **40**(6)**,** 827-36.

Keller, P. M., Fyfe, J. A., Beauchamp, L., Lubbers, C. M., Furman, P. A., Schaeffer, H. J., and Elion, G. B. (1981). Enzymatic phosphorylation of acyclic nucleoside analogs and correlations with antiherpetic activities. *Biochem Pharmacol* **30**(22)**,** 3071-7.

Kerangueven, F., Noguchi, T., Coulier, F., Allione, F., Wargniez, V., Simony-Lafontaine, J., Longy, M., Jacquemier, J., Sobol, H., Eisinger, F., and Birnbaum, D. (1997). Genome-wide search for loss of heterozygosity shows extensive genetic diversity of human breast carcinomas. *Cancer Res* **57**(24)**,** 5469-74.

Kerbel, R. S. (2003). Human tumor xenografts as predictive preclinical models for anticancer drug activity in humans: better than commonly perceived-but they can be improved. *Cancer Biol Ther* **2**(4 Suppl 1)**,** S134-9.

Kerlikowske, K. (1997). Efficacy of screening mammography among women aged 40 to 49 years and 50 to 69 years: comparison of relative and absolute benefit. *J Natl Cancer Inst Monogr*(22)**,** 79-86.

Khalbuss, W. E., Ambaye, A., Goodison, S., Loya, A., and Masood, S. (2006). Papillary carcinoma of the breast in a male patient with a treated prostatic carcinoma diagnosed by fine-needle aspiration biopsy: a case report and review of the literature. *Diagn Cytopathol* **34**(3)**,** 214-7.

Kianmanesh, A. R., Perrin, H., Panis, Y., Fabre, M., Nagy, H. J., Houssin, D., and Klatzmann, D. (1997). A "distant" bystander effect of suicide gene therapy: regression of nontransduced tumors together with a distant transduced tumor. *Hum Gene Ther* **8**(15)**,** 1807-14.

King, G. D., Curtin, J. F., Candolfi, M., Kroeger, K., Lowenstein, P. R., and Castro, M. G. (2005). Gene therapy and targeted toxins for glioma. *Curr Gene Ther* **5**(6)**,** 535-57.

Kojaoghlanian, T., Flomenberg, P., and Horwitz, M. S. (2003). The impact of adenovirus infection on the immunocompromised host. *Rev Med Virol* **13**(3)**,** 155-71.

Kong, X. B., Zhu, Q. Y., Vidal, P. M., Watanabe, K. A., Polsky, B., Armstrong, D., Ostrander, M., Lang, S. A., Jr., Muchmore, E., and Chou, T. C. (1992). Comparisons of anti-human immunodeficiency virus activities, cellular transport, and plasma and intracellular pharmacokinetics of 3'-fluoro-3'-deoxythymidine and 3'-azido-3'-deoxythymidine. *Antimicrob Agents Chemother* **36**(4)**,** 808-18.

Kootstra, N. A., and Verma, I. M. (2003). Gene therapy with viral vectors. *Annu Rev Pharmacol Toxicol* **43,** 413-39.

Kubota, R., Yamada, S., Kubota, K., Ishiwata, K., Tamahashi, N., and Ido, T. (1992). Intratumoral distribution of fluorine-18-fluorodeoxyglucose in vivo: high accumulation in macrophages and granulation tissues studied by microautoradiography. *J Nucl Med* **33**(11)**,** 1972-80.

Kuhl, C. K., Schrading, S., Leutner, C. C., Morakkabati-Spitz, N., Wardelmann, E., Fimmers, R., Kuhn, W., and Schild, H. H. (2005). Mammography, breast ultrasound, and magnetic resonance imaging for surveillance of women at high familial risk for breast cancer. *J Clin Oncol* **23**(33)**,** 8469-76.

Kuriyama, S., Kikukawa, M., Masui, K., Okuda, H., Nakatani, T., Akahane, T., Mitoro, A., Tominaga, K., Tsujinoue, H., Yoshiji, H., Okamoto, S., Fukui, H., and Ikenaka, K. (1999). Cancer gene therapy with HSV-tk/GCV system depends on T-cell-mediated immune responses and causes apoptotic death of tumor cells in vivo. *Int J Cancer* **83**(3)**,** 374-80.

Kwee, T. C., Takahara, T., Klomp, D. W., and Luijten, P. R. (2010). Cancer imaging: novel concepts in clinical magnetic resonance imaging. *J Intern Med* **268**(2)**,** 120-32.

La Rosa, A. M., Champlin, R. E., Mirza, N., Gajewski, J., Giralt, S., Rolston, K. V., Raad, I., Jacobson, K., Kontoyiannis, D., Elting, L., and Whimbey, E. (2001). Adenovirus infections in adult recipients of blood and marrow transplants. *Clin Infect Dis* **32**(6)**,** 871-6.

Lacroix, M. (2006). Significance, detection and markers of disseminated breast cancer cells. *Endocr Relat Cancer* **13**(4)**,** 1033-67.

Lakhani, S. R., Jacquemier, J., Sloane, J. P., Gusterson, B. A., Anderson, T. J., van de Vijver, M. J., Farid, L. M., Venter, D., Antoniou, A., Storfer-Isser, A., Smyth, E., Steel, C. M., Haites, N., Scott, R. J., Goldgar, D., Neuhausen, S., Daly, P. A., Ormiston, W., McManus, R., Scherneck, S., Ponder, B. A., Ford, D., Peto, J., Stoppa-Lyonnet, D., Bignon, Y. J., Struewing, J. P., Spurr, N. K., Bishop, D. T., Klijn, J. G., Devilee, P., Cornelisse, C. J., Lasset, C., Lenoir, G., Barkardottir, R. B., Egilsson, V., Hamann, U., Chang-Claude, J., Sobol, H., Weber, B., Stratton, M. R., and Easton, D. F. (1998).

Multifactorial analysis of differences between sporadic breast cancers and cancers involving BRCA1 and BRCA2 mutations. *J Natl Cancer Inst* **90**(15)**,** 1138-45.
Lara, A. R., and Ramirez, O. T. (2012). Plasmid DNA production for therapeutic applications. *Methods Mol Biol* **824,** 271-303.
Latham, J. P., Searle, P. F., Mautner, V., and James, N. D. (2000). Prostate-specific antigen promoter/enhancer driven gene therapy for prostate cancer: construction and testing of a tissue-specific adenovirus vector. *Cancer Res* **60**(2)**,** 334-41.
Leen, A. M., and Rooney, C. M. (2005). Adenovirus as an emerging pathogen in immunocompromised patients. *Br J Haematol* **128**(2)**,** 135-44.
Leygue, E., Snell, L., Dotzlaw, H., Hole, K., Troup, S., Hiller-Hitchcock, T., Murphy, L. C., and Watson, P. H. (1999). Mammaglobin, a potential marker of breast cancer nodal metastasis. *J Pathol* **189**(1)**,** 28-33.
Li, G., Zhang, J., Jin, K., He, K., Wang, H., Lu, H., and Teng, L. (2011). Human mammaglobin: a superior marker for reverse-transcriptase PCR in detecting circulating tumor cells in breast cancer patients. *Biomark Med* **5**(2)**,** 249-60.
Li, N., Zhou, J., Weng, D., Zhang, C., Li, L., Wang, B., Song, Y., He, Q., Lin, D., Chen, D., Chen, G., Gao, Q., Wang, S., Xu, G., Meng, L., Lu, Y., and Ma, D. (2007). Adjuvant adenovirus-mediated delivery of herpes simplex virus thymidine kinase administration improves outcome of liver transplantation in patients with advanced hepatocellular carcinoma. *Clin Cancer Res* **13**(19)**,** 5847-54.
Li, Q., Kay, M. A., Finegold, M., Stratford-Perricaudet, L. D., and Woo, S. L. (1993). Assessment of recombinant adenoviral vectors for hepatic gene therapy. *Hum Gene Ther* **4**(4)**,** 403-9.
Li, X., Zhang, J., Gao, H., Vieth, E., Bae, K. H., Zhang, Y. P., Lee, S. J., Raikwar, S., Gardner, T. A., Hutchins, G. D., VanderPutten, D., Kao, C., and Jeng, M. H. (2005). Transcriptional targeting modalities in breast cancer gene therapy using adenovirus vectors controlled by alpha-lactalbumin promoter. *Mol Cancer Ther* **4**(12)**,** 1850-9.
Liu, T. C., Hwang, T., Park, B. H., Bell, J., and Kirn, D. H. (2008). The targeted oncolytic poxvirus JX-594 demonstrates antitumoral, antivascular, and anti-HBV activities in patients with hepatocellular carcinoma. *Mol Ther* **16**(9)**,** 1637-42.
Lovekin, C., Ellis, I. O., Locker, A., Robertson, J. F., Bell, J., Nicholson, R., Gullick, W. J., Elston, C. W., and Blamey, R. W. (1991). c-erbB-2 oncoprotein expression in primary and advanced breast cancer. *Br J Cancer* **63**(3)**,** 439-43.
Machado de Domenech, E. E., and Sols, A. (1980). Specificity of hexokinases towards some uncommon substrates and inhibitors. *FEBS Lett* **119**(1)**,** 174-6.
MacLaren, D. C., Gambhir, S. S., Satyamurthy, N., Barrio, J. R., Sharfstein, S., Toyokuni, T., Wu, L., Berk, A. J., Cherry, S. R., Phelps, M. E., and Herschman, H. R. (1999). Repetitive, non-invasive imaging of the dopamine D2 receptor as a reporter gene in living animals. *Gene Ther* **6**(5)**,** 785-91.
Maglione, J. E., McGoldrick, E. T., Young, L. J., Namba, R., Gregg, J. P., Liu, L., Moghanaki, D., Ellies, L. G., Borowsky, A. D., Cardiff, R. D., and MacLeod, C. L. (2004). Polyomavirus middle T-induced mammary intraepithelial neoplasia outgrowths: single origin, divergent evolution, and multiple outcomes. *Mol Cancer Ther* **3**(8)**,** 941-53.
Majumdar, A. S., Hughes, D. E., Lichtsteiner, S. P., Wang, Z., Lebkowski, J. S., and Vasserot, A. P. (2001). The telomerase reverse transcriptase promoter drives efficacious tumor

suicide gene therapy while preventing hepatotoxicity encountered with constitutive promoters. *Gene Ther* **8**(7)**,** 568-78.

Marchetti, A., Buttitta, F., Bertacca, G., Zavaglia, K., Bevilacqua, G., Angelucci, D., Viacava, P., Naccarato, A., Bonadio, A., Barassi, F., Felicioni, L., Salvatore, S., and Mucilli, F. (2001). mRNA markers of breast cancer nodal metastases: comparison between mammaglobin and carcinoembryonic antigen in 248 patients. *J Pathol* **195**(2)**,** 186-90.

Martuza, R. L., Malick, A., Markert, J. M., Ruffner, K. L., and Coen, D. M. (1991). Experimental therapy of human glioma by means of a genetically engineered virus mutant. *Science* **252**(5007)**,** 854-6.

Mathews, M. B. (1975). Genes for VA-RNA in adenovirus 2. *Cell* **6**(2)**,** 223-9.

Matthews, T., and Boehme, R. (1988). Antiviral activity and mechanism of action of ganciclovir. *Rev Infect Dis* **10 Suppl 3,** S490-4.

Mautner, V., Steinthorsdottir, V., and Bailey, A. (1995). Enteric adenoviruses. *Curr Top Microbiol Immunol* **199 (Pt 3),** 229-82.

McConnell, M. J., and Imperiale, M. J. (2004). Biology of adenovirus and its use as a vector for gene therapy. *Hum Gene Ther* **15**(11)**,** 1022-33.

McDermott, G. M., Welch, A., Staff, R. T., Gilbert, F. J., Schweiger, L., Semple, S. I., Smith, T. A., Hutcheon, A. W., Miller, I. D., Smith, I. C., and Heys, S. D. (2007). Monitoring primary breast cancer throughout chemotherapy using FDG-PET. *Breast Cancer Res Treat* **102**(1)**,** 75-84.

McLaughlin-Drubin, M. E., and Munger, K. (2008). Viruses associated with human cancer. *Biochim Biophys Acta* **1782**(3)**,** 127-50.

Medina, R. A., and Owen, G. I. (2002). Glucose transporters: expression, regulation and cancer. *Biol Res* **35**(1)**,** 9-26.

Mesnil, M., and Yamasaki, H. (2000). Bystander effect in herpes simplex virus-thymidine kinase/ganciclovir cancer gene therapy: role of gap-junctional intercellular communication. *Cancer Res* **60**(15)**,** 3989-99.

Miletic, H., Fischer, Y., Litwak, S., Giroglou, T., Waerzeggers, Y., Winkeler, A., Li, H., Himmelreich, U., Lange, C., Stenzel, W., Deckert, M., Neumann, H., Jacobs, A. H., and von Laer, D. (2007). Bystander killing of malignant glioma by bone marrow-derived tumor-infiltrating progenitor cells expressing a suicide gene. *Mol Ther* **15**(7)**,** 1373-81.

Miller, A. D., Jolly, D. J., Friedmann, T., and Verma, I. M. (1983). A transmissible retrovirus expressing human hypoxanthine phosphoribosyltransferase (HPRT): gene transfer into cells obtained from humans deficient in HPRT. *Proc Natl Acad Sci U S A* **80**(15)**,** 4709-13.

Millikan, R. C., Newman, B., Tse, C. K., Moorman, P. G., Conway, K., Dressler, L. G., Smith, L. V., Labbok, M. H., Geradts, J., Bensen, J. T., Jackson, S., Nyante, S., Livasy, C., Carey, L., Earp, H. S., and Perou, C. M. (2008). Epidemiology of basal-like breast cancer. *Breast Cancer Res Treat* **109**(1)**,** 123-39.

Moolten, F. L. (1986). Tumor chemosensitivity conferred by inserted herpes thymidine kinase genes: paradigm for a prospective cancer control strategy. *Cancer Res* **46**(10)**,** 5276-81.

Morris, J. C., Touraine, R., Wildner, O., and Blaese, R. M. (1999). Suicide genes: Gene therapy applications using enzyme/prodrug strategies. *In* "The Development of Human Gene Therapy" (T. Friedmann, Ed.), pp. 477-526. Cold Spring Harbor Laboratory Press, Cold Spring Harbor, NY.

Murofushi, Y., Nagano, S., Kamizono, J., Takahashi, T., Fujiwara, H., Komiya, S., Matsuishi, T., and Kosai, K. (2006). Cell cycle-specific changes in hTERT promoter activity in normal and cancerous cells in adenoviral gene therapy: a promising implication of telomerase-dependent targeted cancer gene therapy. *Int J Oncol* **29**(3)**,** 681-8.

Nakshatri, H., Qi, G., You, J., Kerry, B., Schneider, B., Zon, R., Buck, C., Regnier, F., and Wang, M. (2009). Intrinsic subtype-associated changes in the plasma proteome in breast cancer. *Proteomics Clin Appl* **3**(11)**,** 1305-13.

Namba, R., Young, L. J., Maglione, J. E., McGoldrick, E. T., Liu, S., Wurz, G. T., DeGregorio, M. W., Borowsky, A. D., MacLeod, C. L., Cardiff, R. D., and Gregg, J. P. (2005). Selective estrogen receptor modulators inhibit growth and progression of premalignant lesions in a mouse model of ductal carcinoma in situ. *Breast Cancer Res* **7**(6)**,** R881-9.

Nasu, Y., Saika, T., Ebara, S., Kusaka, N., Kaku, H., Abarzua, F., Manabe, D., Thompson, T. C., and Kumon, H. (2007). Suicide gene therapy with adenoviral delivery of HSV-tK gene for patients with local recurrence of prostate cancer after hormonal therapy. *Mol Ther* **15**(4)**,** 834-40.

Nayar, R., Zhuang, Z., Merino, M. J., and Silverberg, S. G. (1997). Loss of heterozygosity on chromosome 11q13 in lobular lesions of the breast using tissue microdissection and polymerase chain reaction. *Hum Pathol* **28**(3)**,** 277-82.

Nemerow, G. R., Cheresh, D. A., and Wickham, T. J. (1994). Adenovirus entry into host cells: a role for alpha(v) integrins. *Trends Cell Biol* **4**(2)**,** 52-5.

Nermut, M. V. (1975). Fine structure of adenovirus type 5. I. Virus capsid. *Virology* **65**(2)**,** 480-95.

Niculescu-Duvaz, I., and Springer, C. J. (2004). Introduction to the background, principles, and state of the art in suicide gene therapy. *Methods Mol Med* **90,** 1-27.

Nielsen, T. O., Parker, J. S., Leung, S., Voduc, D., Ebbert, M., Vickery, T., Davies, S. R., Snider, J., Stijleman, I. J., Reed, J., Cheang, M. C., Mardis, E. R., Perou, C. M., Bernard, P. S., and Ellis, M. J. (2010). A comparison of PAM50 intrinsic subtyping with immunohistochemistry and clinical prognostic factors in tamoxifen-treated estrogen receptor-positive breast cancer. *Clin Cancer Res* **16**(21)**,** 5222-32.

Niewoehner, C. B., and Schorer, A. E. (2008). Gynaecomastia and breast cancer in men. *BMJ* **336**(7646)**,** 709-13.

Niranjan, A., Moriuchi, S., Lunsford, L. D., Kondziolka, D., Flickinger, J. C., Fellows, W., Rajendiran, S., Tamura, M., Cohen, J. B., and Glorioso, J. C. (2000). Effective treatment of experimental glioblastoma by HSV vector-mediated TNF alpha and HSV-tk gene transfer in combination with radiosurgery and ganciclovir administration. *Mol Ther* **2**(2)**,** 114-20.

O'Brien, N., Maguire, T. M., O'Donovan, N., Lynch, N., Hill, A. D., McDermott, E., O'Higgins, N., and Duffy, M. J. (2002). Mammaglobin a: a promising marker for breast cancer. *Clin Chem* **48**(8)**,** 1362-4.

O'Brien, T. P., Jeng, B. H., McDonald, M., and Raizman, M. B. (2009). Acute conjunctivitis: truth and misconceptions. *Curr Med Res Opin* **25**(8)**,** 1953-61.

Ooka, M., Sakita, I., Fujiwara, Y., Tamaki, Y., Yamamoto, H., Aihara, T., Miyazaki, M., Kadota, M., Masuda, N., Sugita, Y., Iwao, K., and Monden, M. (2000). Selection of mRNA markers for detection of lymph node micrometastases in breast cancer patients. *Oncol Rep* **7**(3)**,** 561-6.

Pandha, H. S., Martin, L. A., Rigg, A., Hurst, H. C., Stamp, G. W., Sikora, K., and Lemoine, N. R. (1999). Genetic prodrug activation therapy for breast cancer: A phase I clinical trial of erbB-2-directed suicide gene expression. *J Clin Oncol* **17**(7)**,** 2180-9.

Papathanassiou, D., Bruna-Muraille, C., Liehn, J. C., Nguyen, T. D., and Cure, H. (2009). Positron Emission Tomography in oncology: present and future of PET and PET/CT. *Crit Rev Oncol Hematol* **72**(3)**,** 239-54.

Parker, J. S., Mullins, M., Cheang, M. C., Leung, S., Voduc, D., Vickery, T., Davies, S., Fauron, C., He, X., Hu, Z., Quackenbush, J. F., Stijleman, I. J., Palazzo, J., Marron, J. S., Nobel, A. B., Mardis, E., Nielsen, T. O., Ellis, M. J., Perou, C. M., and Bernard, P. S. (2009). Supervised risk predictor of breast cancer based on intrinsic subtypes. *J Clin Oncol* **27**(8)**,** 1160-7.

Penuelas, I., Mazzolini, G., Boan, J. F., Sangro, B., Marti-Climent, J., Ruiz, M., Ruiz, J., Satyamurthy, N., Qian, C., Barrio, J. R., Phelps, M. E., Richter, J. A., Gambhir, S. S., and Prieto, J. (2005). Positron emission tomography imaging of adenoviral-mediated transgene expression in liver cancer patients. *Gastroenterology* **128**(7)**,** 1787-95.

Perou, C. M., Sorlie, T., Eisen, M. B., van de Rijn, M., Jeffrey, S. S., Rees, C. A., Pollack, J. R., Ross, D. T., Johnsen, H., Akslen, L. A., Fluge, O., Pergamenschikov, A., Williams, C., Zhu, S. X., Lonning, P. E., Borresen-Dale, A. L., Brown, P. O., and Botstein, D. (2000). Molecular portraits of human breast tumours. *Nature* **406**(6797)**,** 747-52.

Phelps, M. E. (2000). PET: the merging of biology and imaging into molecular imaging. *J Nucl Med* **41**(4)**,** 661-81.

Pouliot, F., Karanikolas, B. D., Johnson, M., Sato, M., Priceman, S. J., Stout, D., Sohn, J., Satyamurthy, N., deKernion, J. B., and Wu, L. (2011). In vivo imaging of intraprostatic-specific gene transcription by PET. *J Nucl Med* **52**(5)**,** 784-91.

Prat, A., Parker, J. S., Karginova, O., Fan, C., Livasy, C., Herschkowitz, J. I., He, X., and Perou, C. M. (2010). Phenotypic and molecular characterization of the claudin-low intrinsic subtype of breast cancer. *Breast Cancer Res* **12**(5)**,** R68.

Prat, A., and Perou, C. M. (2011). Deconstructing the molecular portraits of breast cancer. *Mol Oncol* **5**(1)**,** 5-23.

Quantin, B., Perricaudet, L. D., Tajbakhsh, S., and Mandel, J. L. (1992). Adenovirus as an expression vector in muscle cells in vivo. *Proc Natl Acad Sci U S A* **89**(7)**,** 2581-4.

Ram, Z., Culver, K. W., Walbridge, S., Blaese, R. M., and Oldfield, E. H. (1993). In situ retroviral-mediated gene transfer for the treatment of brain tumors in rats. *Cancer Res* **53**(1)**,** 83-8.

Rasey, J. S., Grierson, J. R., Wiens, L. W., Kolb, P. D., and Schwartz, J. L. (2002). Validation of FLT uptake as a measure of thymidine kinase-1 activity in A549 carcinoma cells. *J Nucl Med* **43**(9)**,** 1210-7.

Reardon, J. E. (1989). Herpes simplex virus type 1 and human DNA polymerase interactions with 2'-deoxyguanosine 5'-triphosphate analogues. Kinetics of incorporation into DNA and induction of inhibition. *J Biol Chem* **264**(32)**,** 19039-44.

Riesco-Eizaguirre, G., De la Vieja, A., Rodriguez, I., Miranda, S., Martin-Duque, P., Vassaux, G., and Santisteban, P. (2011). Telomerase-driven expression of the sodium iodide symporter (NIS) for in vivo radioiodide treatment of cancer: a new broad-spectrum NIS-mediated antitumor approach. *J Clin Endocrinol Metab* **96**(9)**,** E1435-43.

Rockwell, S. C., Kallman, R. F., and Fajardo, L. F. (1972). Characteristics of a serially transplanted mouse mammary tumor and its tissue-culture-adapted derivative. *J Natl Cancer Inst* **49**(3)**,** 735-49.

Rouzier, R., Perou, C. M., Symmans, W. F., Ibrahim, N., Cristofanilli, M., Anderson, K., Hess, K. R., Stec, J., Ayers, M., Wagner, P., Morandi, P., Fan, C., Rabiul, I., Ross, J. S., Hortobagyi, G. N., and Pusztai, L. (2005). Breast cancer molecular subtypes respond differently to preoperative chemotherapy. *Clin Cancer Res* **11**(16)**,** 5678-85.

Rowe, W. P., Huebner, R. J., Gilmore, L. K., Parrott, R. H., and Ward, T. G. (1953). Isolation of a cytopathogenic agent from human adenoids undergoing spontaneous degeneration in tissue culture. *Proc Soc Exp Biol Med* **84**(3)**,** 570-3.

Sadeghi, H., and Hitt, M. M. (2005). Transcriptionally targeted adenovirus vectors. *Curr Gene Ther* **5**(4)**,** 411-27.

Saito, Y., Price, R. W., Rottenberg, D. A., Fox, J. J., Su, T. L., Watanabe, K. A., and Philips, F. S. (1982). Quantitative autoradiographic mapping of herpes simplex virus encephalitis with a radiolabeled antiviral drug. *Science* **217**(4565)**,** 1151-3.

Saito, Y., Rubenstein, R., Price, R. W., Fox, J. J., and Watanabe, K. A. (1984). Diagnostic imaging of herpes simplex virus encephalitis using a radiolabeled antiviral drug: autoradiographic assessment in an animal model. *Ann Neurol* **15**(6)**,** 548-58.

Sardanelli, F., Giuseppetti, G. M., Panizza, P., Bazzocchi, M., Fausto, A., Simonetti, G., Lattanzio, V., and Del Maschio, A. (2004). Sensitivity of MRI versus mammography for detecting foci of multifocal, multicentric breast cancer in Fatty and dense breasts using the whole-breast pathologic examination as a gold standard. *AJR Am J Roentgenol* **183**(4)**,** 1149-57.

Sato, M., Figueiredo, M. L., Burton, J. B., Johnson, M., Chen, M., Powell, R., Gambhir, S. S., Carey, M., and Wu, L. (2008). Configurations of a two-tiered amplified gene expression system in adenoviral vectors designed to improve the specificity of in vivo prostate cancer imaging. *Gene Ther* **15**(8)**,** 583-93.

Serunian, L. A., Auger, K. R., Roberts, T. M., and Cantley, L. C. (1990). Production of novel polyphosphoinositides in vivo is linked to cell transformation by polyomavirus middle T antigen. *J Virol* **64**(10)**,** 4718-25.

Shenk, T. E. (2001). *Adenoviridae*: The Viruses and Their Replication. 4th ed. *In* "Fields Virology" (D. K. a. P. Howley, Ed.), pp. 2265-2300. Lippincott Williams & Wilkins, Philadelphia.

Sherley, J. L., and Kelly, T. J. (1988). Regulation of human thymidine kinase during the cell cycle. *J Biol Chem* **263**(17)**,** 8350-8.

Shi, C. X., Graham, F. L., and Hitt, M. M. (2006). A convenient plasmid system for construction of helper-dependent adenoviral vectors and its application for analysis of the breast-cancer-specific mammaglobin promoter. *J Gene Med* **8**(4)**,** 442-51.

Shi, C. X., Long, M. A., Liu, L., Graham, F. L., Gauldie, J., and Hitt, M. M. (2004). The human SCGB2A2 (mammaglobin-1) promoter/enhancer in a helper-dependent adenovirus vector directs high levels of transgene expression in mammary carcinoma cells but not in normal nonmammary cells. *Mol Ther* **10**(4)**,** 758-67.

Shields, A. F., Grierson, J. R., Dohmen, B. M., Machulla, H. J., Stayanoff, J. C., Lawhorn-Crews, J. M., Obradovich, J. E., Muzik, O., and Mangner, T. J. (1998a). Imaging proliferation in vivo with [F-18]FLT and positron emission tomography. *Nat Med* **4**(11)**,** 1334-6.

Shields, A. F., Lawhorn-Crews, J. M., Briston, D. A., Zalzala, S., Gadgeel, S., Douglas, K. A., Mangner, T. J., Heilbrun, L. K., and Muzik, O. (2008). Analysis and reproducibility of 3'-Deoxy-3'-[18F]fluorothymidine positron emission tomography imaging in patients with non-small cell lung cancer. *Clin Cancer Res* **14**(14)**,** 4463-8.

Shields, A. F., Mankoff, D. A., Link, J. M., Graham, M. M., Eary, J. F., Kozawa, S. M., Zheng, M., Lewellen, B., Lewellen, T. K., Grierson, J. R., and Krohn, K. A. (1998b). Carbon-11-thymidine and FDG to measure therapy response. *J Nucl Med* **39**(10)**,** 1757-62.

Shimotohno, K., and Temin, H. M. (1981). Formation of infectious progeny virus after insertion of herpes simplex thymidine kinase gene into DNA of an avian retrovirus. *Cell* **26**(1 Pt 1)**,** 67-77.

Silva, A. L., Tome, M. J., Correia, A. E., and Passos-Coelho, J. L. (2002). Human mammaglobin RT-PCR assay for detection of occult breast cancer cells in hematopoietic products. *Ann Oncol* **13**(3)**,** 422-9.

Sjodin, A., Guo, D., Hofer, P. A., Henriksson, R., and Hedman, H. (2003). Mammaglobin in normal human sweat glands and human sweat gland tumors. *J Invest Dermatol* **121**(2)**,** 428-9.

Slamon, D. J., Clark, G. M., Wong, S. G., Levin, W. J., Ullrich, A., and McGuire, W. L. (1987). Human breast cancer: correlation of relapse and survival with amplification of the HER-2/neu oncogene. *Science* **235**(4785)**,** 177-82.

Smith, G. L., and Moss, B. (1983). Infectious poxvirus vectors have capacity for at least 25 000 base pairs of foreign DNA. *Gene* **25**(1)**,** 21-8.

Smith, T. A. (1999). Facilitative glucose transporter expression in human cancer tissue. *Br J Biomed Sci* **56**(4)**,** 285-92.

Smith, T. A., Mehaffey, M. G., Kayda, D. B., Saunders, J. M., Yei, S., Trapnell, B. C., McClelland, A., and Kaleko, M. (1993). Adenovirus mediated expression of therapeutic plasma levels of human factor IX in mice. *Nat Genet* **5**(4)**,** 397-402.

Sols, A., and Crane, R. K. (1954). Substrate specificity of brain hexokinase. *J Biol Chem* **210**(2)**,** 581-95.

Sommerfeld, H. J., Meeker, A. K., Piatyszek, M. A., Bova, G. S., Shay, J. W., and Coffey, D. S. (1996). Telomerase activity: a prevalent marker of malignant human prostate tissue. *Cancer Res* **56**(1)**,** 218-22.

Sorlie, T. (2004). Molecular portraits of breast cancer: tumour subtypes as distinct disease entities. *Eur J Cancer* **40**(18)**,** 2667-75.

Sorlie, T., Perou, C. M., Tibshirani, R., Aas, T., Geisler, S., Johnsen, H., Hastie, T., Eisen, M. B., van de Rijn, M., Jeffrey, S. S., Thorsen, T., Quist, H., Matese, J. C., Brown, P. O., Botstein, D., Lonning, P. E., and Borresen-Dale, A. L. (2001). Gene expression patterns of breast carcinomas distinguish tumor subclasses with clinical implications. *Proc Natl Acad Sci U S A* **98**(19)**,** 10869-74.

Sorlie, T., Tibshirani, R., Parker, J., Hastie, T., Marron, J. S., Nobel, A., Deng, S., Johnsen, H., Pesich, R., Geisler, S., Demeter, J., Perou, C. M., Lonning, P. E., Brown, P. O., Borresen-Dale, A. L., and Botstein, D. (2003). Repeated observation of breast tumor subtypes in independent gene expression data sets. *Proc Natl Acad Sci U S A* **100**(14)**,** 8418-23.

Span, P. N., Waanders, E., Manders, P., Heuvel, J. J., Foekens, J. A., Watson, M. A., Beex, L. V., and Sweep, F. C. (2004). Mammaglobin is associated with low-grade, steroid receptor-positive breast tumors from postmenopausal patients, and has independent prognostic value for relapse-free survival time. *J Clin Oncol* **22**(4)**,** 691-8.

Sterman, D. H., Recio, A., Vachani, A., Sun, J., Cheung, L., DeLong, P., Amin, K. M., Litzky, L. A., Wilson, J. M., Kaiser, L. R., and Albelda, S. M. (2005). Long-term follow-up of patients with malignant pleural mesothelioma receiving high-dose adenovirus herpes simplex thymidine kinase/ganciclovir suicide gene therapy. *Clin Cancer Res* **11**(20)**,** 7444-53.

Stewart, T. A., Pattengale, P. K., and Leder, P. (1984). Spontaneous mammary adenocarcinomas in transgenic mice that carry and express MTV/myc fusion genes. *Cell* **38**(3)**,** 627-37.

Subak-Sharpe, H., Burk, R. R., and Pitts, J. D. (1969). Metabolic co-operation between biochemically marked mammalian cells in tissue culture. *J Cell Sci* **4**(2)**,** 353-67.

Sutterluety, H., Bartl, S., Doetzlhofer, A., Khier, H., Wintersberger, E., and Seiser, C. (1998). Growth-regulated antisense transcription of the mouse thymidine kinase gene. *Nucleic Acids Res* **26**(21)**,** 4989-95.

Tabin, C. J., Hoffmann, J. W., Goff, S. P., and Weinberg, R. A. (1982). Adaptation of a retrovirus as a eucaryotic vector transmitting the herpes simplex virus thymidine kinase gene. *Mol Cell Biol* **2**(4)**,** 426-36.

Tahara, H., Nakanishi, T., Kitamoto, M., Nakashio, R., Shay, J. W., Tahara, E., Kajiyama, G., and Ide, T. (1995). Telomerase activity in human liver tissues: comparison between chronic liver disease and hepatocellular carcinomas. *Cancer Res* **55**(13)**,** 2734-6.

Takamiya, Y., Short, M. P., Ezzeddine, Z. D., Moolten, F. L., Breakefield, X. O., and Martuza, R. L. (1992). Gene therapy of malignant brain tumors: a rat glioma line bearing the herpes simplex virus type 1-thymidine kinase gene and wild type retrovirus kills other tumor cells. *J Neurosci Res* **33**(3)**,** 493-503.

Talmage, D. A., Freund, R., Young, A. T., Dahl, J., Dawe, C. J., and Benjamin, T. L. (1989). Phosphorylation of middle T by pp60c-src: a switch for binding of phosphatidylinositol 3-kinase and optimal tumorigenesis. *Cell* **59**(1)**,** 55-65.

Tanaka, K., Iwamoto, S., Gon, G., Nohara, T., Iwamoto, M., and Tanigawa, N. (2000). Expression of survivin and its relationship to loss of apoptosis in breast carcinomas. *Clin Cancer Res* **6**(1)**,** 127-34.

Tatsis, N., and Ertl, H. C. (2004). Adenoviruses as vaccine vectors. *Mol Ther* **10**(4)**,** 616-29.

Thompson, T. C. (1999). In situ gene therapy for prostate cancer. *Oncol Res* **11**(1)**,** 1-8.

Thorne, S. H., Hwang, T. H., O'Gorman, W. E., Bartlett, D. L., Sei, S., Kanji, F., Brown, C., Werier, J., Cho, J. H., Lee, D. E., Wang, Y., Bell, J., and Kirn, D. H. (2007). Rational strain selection and engineering creates a broad-spectrum, systemically effective oncolytic poxvirus, JX-963. *J Clin Invest* **117**(11)**,** 3350-8.

Thust, R., Schacke, M., and Wutzler, P. (1996). Cytogenetic genotoxicity of antiherpes virostatics in Chinese hamster V79-E cells. I. Purine nucleoside analogues. *Antiviral Res* **31**(1-2)**,** 105-13.

Tjuvajev, J., Avril, N., and Safer, M. (1997). Quantitative PET imaging of HSV1-TK gene expression with [I-124]FIAU. *J Nucl Med* **38**(129P).

Tjuvajev, J. G., Avril, N., Oku, T., Sasajima, T., Miyagawa, T., Joshi, R., Safer, M., Beattie, B., DiResta, G., Daghighian, F., Augensen, F., Koutcher, J., Zweit, J., Humm, J., Larson, S. M., Finn, R., and Blasberg, R. (1998). Imaging herpes virus thymidine kinase gene transfer and expression by positron emission tomography. *Cancer Res* **58**(19)**,** 4333-41.

Tjuvajev, J. G., Doubrovin, M., Akhurst, T., Cai, S., Balatoni, J., Alauddin, M. M., Finn, R., Bornmann, W., Thaler, H., Conti, P. S., and Blasberg, R. G. (2002). Comparison of

radiolabeled nucleoside probes (FIAU, FHBG, and FHPG) for PET imaging of HSV1-tk gene expression. *J Nucl Med* **43**(8)**,** 1072-83.

Tofts, P. S., Berkowitz, B., and Schnall, M. D. (1995). Quantitative analysis of dynamic Gd-DTPA enhancement in breast tumors using a permeability model. *Magn Reson Med* **33**(4)**,** 564-8.

Torigian, D. A., Huang, S. S., Houseni, M., and Alavi, A. (2007). Functional imaging of cancer with emphasis on molecular techniques. *CA Cancer J Clin* **57**(4)**,** 206-24.

Tovell, D. R., Samuel, J., Mercer, J. R., Misra, H. K., Xu, L., Wiebe, L. I., Tyrrell, D. L., and Knaus, E. E. (1988). The in vitro evaluation of nucleoside analogues as probes for use in the noninvasive diagnosis of herpes simplex encephalitis. *Drug Des Deliv* **3**(3)**,** 213-21.

Ulug, E. T., Hawkins, P. T., Hanley, M. R., and Courtneidge, S. A. (1990). Phosphatidylinositol metabolism in cells transformed by polyomavirus middle T antigen. *J Virol* **64**(8)**,** 3895-904.

van Eijkeren, M. E., Thierens, H., Seuntjens, J., Goethals, P., Lemahieu, I., and Strijckmans, K. (1996). Kinetics of [methyl-11C]thymidine in patients with squamous cell carcinoma of the head and neck. *Acta Oncol* **35**(6)**,** 737-41.

Vander Borght, T., Labar, D., Pauwels, S., and Lambotte, L. (1991). Production of [2-11C]thymidine for quantification of cellular proliferation with PET. *Int J Rad Appl Instrum A* **42**(1)**,** 103-4.

Varticovski, L., Hollingshead, M. G., Robles, A. I., Wu, X., Cherry, J., Munroe, D. J., Lukes, L., Anver, M. R., Carter, J. P., Borgel, S. D., Stotler, H., Bonomi, C. A., Nunez, N. P., Hursting, S. D., Qiao, W., Deng, C. X., Green, J. E., Hunter, K. W., Merlino, G., Steeg, P. S., Wakefield, L. M., and Barrett, J. C. (2007). Accelerated preclinical testing using transplanted tumors from genetically engineered mouse breast cancer models. *Clin Cancer Res* **13**(7)**,** 2168-77.

Voskoglou-Nomikos, T., Pater, J. L., and Seymour, L. (2003). Clinical predictive value of the in vitro cell line, human xenograft, and mouse allograft preclinical cancer models. *Clin Cancer Res* **9**(11)**,** 4227-39.

Walsh, M. P., Chintakuntlawar, A., Robinson, C. M., Madisch, I., Harrach, B., Hudson, N. R., Schnurr, D., Heim, A., Chodosh, J., Seto, D., and Jones, M. S. (2009). Evidence of molecular evolution driven by recombination events influencing tropism in a novel human adenovirus that causes epidemic keratoconjunctivitis. *PLoS One* **4**(6)**,** e5635.

Wang, W., Jin, B., Li, W., Xu, C. X., Cui, F. A., Liu, B., Yan, Y. F., Liu, X. X., and Wang, X. L. (2010). Targeted antitumor effect induced by hTERT promoter mediated ODC antisense adenovirus. *Mol Biol Rep* **37**(7)**,** 3239-47.

Wang, X., Southard, R. C., and Kilgore, M. W. (2004). The increased expression of peroxisome proliferator-activated receptor-gamma1 in human breast cancer is mediated by selective promoter usage. *Cancer Res* **64**(16)**,** 5592-6.

Wang, Z., Spaulding, B., Sienko, A., Liang, Y., Li, H., Nielsen, G., Yub Gong, G., Ro, J. Y., and Jim Zhai, Q. (2009). Mammaglobin, a valuable diagnostic marker for metastatic breast carcinoma. *Int J Clin Exp Pathol* **2**(4)**,** 384-9.

Warburg, O., Wind, F., and Negelein, E. (1927). The Metabolism of Tumors in the Body. *J Gen Physiol* **8**(6)**,** 519-30.

Watson, M. A., Darrow, C., Zimonjic, D. B., Popescu, N. C., and Fleming, T. P. (1998). Structure and transcriptional regulation of the human mammaglobin gene, a breast cancer

associated member of the uteroglobin gene family localized to chromosome 11q13. *Oncogene* **16**(6)**,** 817-24.
Watson, M. A., Dintzis, S., Darrow, C. M., Voss, L. E., DiPersio, J., Jensen, R., and Fleming, T. P. (1999). Mammaglobin expression in primary, metastatic, and occult breast cancer. *Cancer Res* **59**(13)**,** 3028-31.
Watson, M. A., and Fleming, T. P. (1994). Isolation of differentially expressed sequence tags from human breast cancer. *Cancer Res* **54**(17)**,** 4598-602.
Watson, M. A., and Fleming, T. P. (1996). Mammaglobin, a mammary-specific member of the uteroglobin gene family, is overexpressed in human breast cancer. *Cancer Res* **56**(4)**,** 860-5.
Wei, C. M., Gibson, M., Spear, P. G., and Scolnick, E. M. (1981). Construction and isolation of a transmissible retrovirus containing the src gene of Harvey murine sarcoma virus and the thymidine kinase gene of herpes simplex virus type 1. *J Virol* **39**(3)**,** 935-44.
Weigelt, B., Peterse, J. L., and van 't Veer, L. J. (2005). Breast cancer metastasis: markers and models. *Nat Rev Cancer* **5**(8)**,** 591-602.
Whitley, R. J. (1988). Ganciclovir--have we established clinical value in the treatment of cytomegalovirus infections? *Ann Intern Med* **108**(3)**,** 452-4.
WHO (2010). Breast Cancer: prevention and control.
Wiebe, L. I., Knaus, E. E., and Morin, K. W. (1999). Radiolabelled pyrimidine nucleosides to monitor the expression of HSV-1 thymidine kinase in gene therapy. *Nucleosides Nucleotides* **18**(4-5)**,** 1065-6.
Wiley, J. (2012). Gene Therapy Clinical Trials Worldwide. *In* "Journal of Gene Medicine Clinical Trial Site". John Wiley and Sons Ltd.
Willis, R. C., Jolly, D. J., Miller, A. D., Plent, M. M., Esty, A. C., Anderson, P. J., Chang, H. C., Jones, O. W., Seegmiller, J. E., and Friedmann, T. (1984). Partial phenotypic correction of human Lesch-Nyhan (hypoxanthine-guanine phosphoribosyltransferase-deficient) lymphoblasts with a transmissible retroviral vector. *J Biol Chem* **259**(12)**,** 7842-9.
Yabe, Y., Trentin, J. J., and Taylor, G. (1962). Cancer induction in hamsters by human type 12 adenovirus. Effect of age and of virus dose. *Proc Soc Exp Biol Med* **111,** 343-4.
Yaghoubi, S., Barrio, J. R., Dahlbom, M., Iyer, M., Namavari, M., Satyamurthy, N., Goldman, R., Herschman, H. R., Phelps, M. E., and Gambhir, S. S. (2001). Human pharmacokinetic and dosimetry studies of [(18)F]FHBG: a reporter probe for imaging herpes simplex virus type-1 thymidine kinase reporter gene expression. *J Nucl Med* **42**(8)**,** 1225-34.
Yaghoubi, S. S., Couto, M. A., Chen, C. C., Polavaram, L., Cui, G., Sen, L., and Gambhir, S. S. (2006). Preclinical safety evaluation of 18F-FHBG: a PET reporter probe for imaging herpes simplex virus type 1 thymidine kinase (HSV1-tk) or mutant HSV1-sr39tk's expression. *J Nucl Med* **47**(4)**,** 706-15.
Yamada, Y., Uchida, Y., Tatsumi, K., Yamaguchi, T., Kimura, H., Kitahara, H., and Kuriyama, T. (1998). Fluorine-18-fluorodeoxyglucose and carbon-11-methionine evaluation of lymphadenopathy in sarcoidosis. *J Nucl Med* **39**(7)**,** 1160-6.
Yu, B., Zhang, Y., Zhan, Y., Zha, X., Wu, Y., Zhang, X., Dong, Q., Kong, W., and Yu, X. (2011). Co-expression of herpes simplex virus thymidine kinase and Escherichia coli nitroreductase by an hTERT-driven adenovirus vector in breast cancer cells results in additive anti-tumor effects. *Oncol Rep* **26**(1)**,** 255-64.
Zheng, C., and Baum, B. J. (2005). Evaluation of viral and mammalian promoters for use in gene delivery to salivary glands. *Mol Ther* **12**(3)**,** 528-36.

Zhu, Z. B., Makhija, S. K., Lu, B., Wang, M., Kaliberova, L., Liu, B., Rivera, A. A., Nettelbeck, D. M., Mahasreshti, P. J., Leath, C. A., Barker, S., Yamaoto, M., Li, F., Alvarez, R. D., and Curiel, D. T. (2004). Transcriptional targeting of tumors with a novel tumor-specific survivin promoter. *Cancer Gene Ther* **11**(4)**,** 256-62.

Zufferey, R., Dull, T., Mandel, R. J., Bukovsky, A., Quiroz, D., Naldini, L., and Trono, D. (1998). Self-inactivating lentivirus vector for safe and efficient in vivo gene delivery. *J Virol* **72**(12)**,** 9873-80.

Zuo, L., Li, L., Wang, Q., Fleming, T. P., and You, S. (2009). Mammaglobin as a potential molecular target for breast cancer drug delivery. *Cancer Cell Int* **9,** 8.

CHAPTER 2

Breast cancer selectivity of the MPE_2 promoter

A. DeSilva performed all experiments described in this chapter.
D. Glubrecht performed the sectioning and immunohistochemistry of tumor/tissue sections.

2.1. INTRODUCTION

Breast cancer (BrCa) is the leading malignancy and second leading cause of cancer mortality in women (CancerStats, 2011; Czernin, Benz, and Allen-Auerbach; WHO, 2010). Despite advances in screening and treatment methods, alternative forms of therapy may be necessary to reduce the mortality rate of this disease. Gene therapy, which involves the introduction and expression of a transgene into a cell to induce a therapeutic effect, is currently being studied as an additional treatment option for breast cancer therapy. However, in order to ensure the safety of non-tumor cells, it is advantageous for cancer gene therapy vectors to possess tumor targeting ability. By taking advantage of differences between tumor and non-tumor cells, such as cell surface receptors, genetic mutations, as well as transcription and translation levels of certain genes, there is a high potential to target cancer gene therapy to achieve a maximal therapeutic index.

Suicide gene therapy is the most commonly used cytotoxic approach in cancer gene therapy (Cole et al., 2005; Culver et al., 1992; Moolten and Wells, 1990), and herpes simplex virus (HSV)-1 thymidine kinase (TK) is the gold standard for suicide gene therapy (Sobol, 1996). Inducing HSV-TK expression within a cell renders that cell sensitive to the prodrug ganciclovir (GCV), an otherwise nontoxic compound at low levels (Matthews and Boehme, 1988; Moolten and Wells, 1990). When administered orally to mice, GCV has a median lethal dose (LD_{50}) of 2 g/kg. GCV has been approved by the United States Food and Drug Administration (FDA) at up to 3 g/day to prevent cytomegalovirus (CMV) retinitis

in patients suffering from acquired immunodeficiency syndrome (AIDS) (Baker, 1995). It is also commonly administered to transplant recipients with acceptable tolerability, where dose limiting side effects include neutropenia, thrombocytopenia and anemia (McGavin and Goa, 2001). When used in HSV-TK gene therapy, HSV-TK phosphorylates GCV into its monophosphate form (Reardon, 1989), which can no longer diffuse out of a cell (Hsieh et al., 2006). Cellular kinases can then further phosphorylate GCV to yield GCV-triphosphate (GCV-TP), a deoxyguanosine triphosphate analogue. The incorporation of GCV-TP into an elongating DNA chain can lead to elongation termination, base-pair mismatches, DNA fragmentation, sister chromatid exchange, and lethal genomic instability, all of which can ultimately result in apoptosis (Matthews and Boehme, 1988; Morris et al., 1999; Thust, Schacke, and Wutzler, 1996). By targeting cancer cells to express HSV-TK, the administration of GCV can lead to cancer-specific cell death.

To date, the most commonly used vector for gene therapy is the adenovirus (Ad) vector (Wiley, 2012). Ad vectors possess many advantages over other delivery vectors for gene therapy, such as their ability to be propagated to high titres, their ability to infect both quiescent and proliferating cells, as well as their high transduction efficiency. Our goal is to target an Ad vector to BrCa cells by specifically expressing HSV-TK within the cancer cells.

The use of HSV-TK has been well characterized using Ad gene therapy vectors controlled by breast cancer-associated promoters, including the human telomerase reverse transcriptase (hTERT) (Majumdar et al., 2001), fatty acid

synthase (hFAS) (Yan et al., 2007), mucin 1 (MUC1) (Chen et al., 1995), human alpha-lactalbumin (hALA) (Anderson et al., 1999) and beta-lactogloulin (BLG) (Anderson et al., 1999) promoters. HSV-TK expression from the mammaglobin (MGB) promoter, however, has not been reported to date. MGB has been shown to posses mammary gland-specific expression and was shown to be upregulated 10-fold in tumor biopsies compared to non-tumor cells (Watson and Fleming, 1996). Our lab has also shown BrCa-selective expression from the MGB promoter (Shi et al., 2004), and we have since generated a modified version of this promoter by duplicating an upstream enhancer and fusing both copies to a minimal mammaglobin promoter (MPE_2; Figure 1.2). This MPE_2 promoter has been shown to achieve high levels of expression in BrCa cells compared to non-tumor cells (Figure 1.3) and thus has potential to be used for targeted gene therapy (Shi, Graham, and Hitt, 2006). By placing the MPE_2 promoter upstream of HSV-TK, we expect to generate an Ad vector (AdMPE_2TK) expressing HSV-TK selectively in breast cancer cells.

Tumor specificity is of paramount importance for cancer gene therapy since non-tumor cells must be spared from any toxic effects. By utilizing the novel BrCa-specific MPE_2 promoter, we aim to target an adenoviral vector to selectively express HSV-TK in BrCa cells to induce cell death. This study reveals the breast cancer specificity of the AdMPE_2TK vector *in vitro*, as well as safety when administered *in vivo*.

2.2. MATERIALS & METHODS

2.2.1. Generation of pAD5 (pSJ7-MPE$_2$TK)

All restriction enzymes and DNA modifying enzymes were purchased from New England Biolabs, except where indicated. Plasmid pSJ7 (Figure 2.1) was digested with BamHI to remove the murine cytomegalovirus (mCMV) promoter (Addison et al., 1997), then digested with NcoI. The large fragment was then gel purified and treated with Antarctic phosphatase. The MPE_2 promoter was amplified from pHS04.1 (Figure 2.2) by Polymerase Chain Reaction (PCR) using primers containing NcoI and BamHI sites (Table 2.1). The PCR product was gel purified using Illustra GFX kit (GE Healthcare), digested with BamHI and NcoI and ligated to the BamHI/NcoI-digested pSJ7 fragment using T4 DNA ligase. The ligation mixture was electroporated into $DH5_\alpha$ bacteria. Plasmids isolated from colonies growing on LB-ampicillin plates were screened by restriction enzyme digestion. The correct recombinant, pAD5 (Figure 2.3), was amplified in $DH5_\alpha$ bacteria grown in 200 mL Luria Broth with ampicillin and purified using Qiagen MIDIPREP HiSpeed Plasmid Purification Kit.

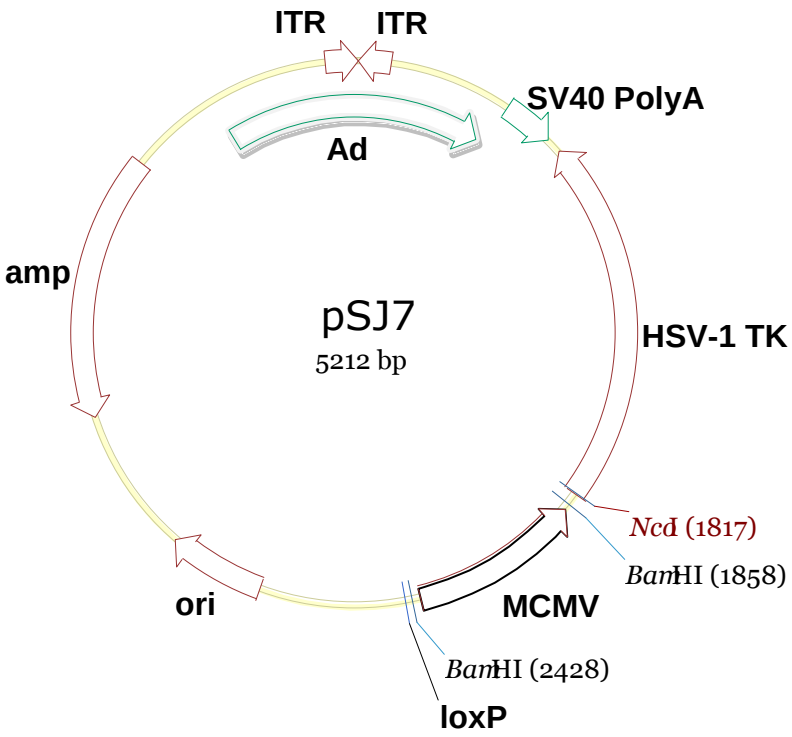

Figure 2.1. pSJ7 plasmid.

The pSJ7 plasmid contains the mCMV promoter driving expression of HSV-TK, as well as other sequences necessary for replication and packaging into adenoviral capsids such as inverted terminal repeats (ITR), and an origin of replication (ori). Other important sequences include an ampicillin resistance gene (amp), a polyadenylation signal downstream of HSV-TK (SV40 PolyA), adenoviral sequences (Ad) and a loxP site for recombination into an Ad vector. Important restriction enzyme locations are also shown.

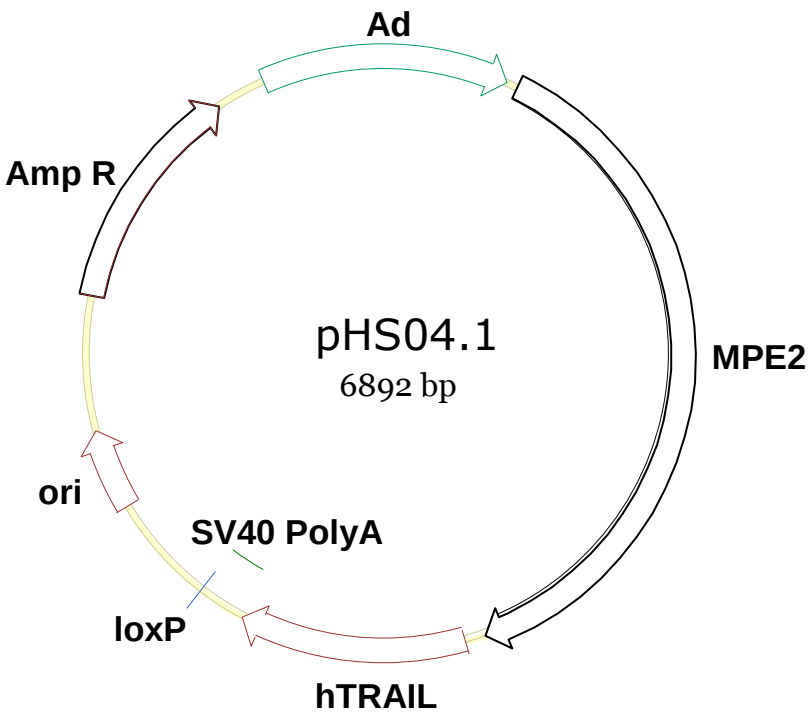

Figure 2.2. pHS04.1 plasmid.

The pHS04.1 plasmid contains the MPE_2 sequence that was amplified by PCR for generation of pAD5.

Primer	Sequence
MPE_2 primer with NcoI	**5'-AACCCATGGTGAGGCTGCTGCTGT-3'**
MPE_2 primer with BamHI	**5'-GATCGGATCCTGAGTCCAGGAATGATCC-3'**

Table 2.1. List of PCR primer sequences used for polymerase chain reaction.

2.2.2. Cell Culture

HEK293 human embryonic kidney cells (gift of Frank Graham) were maintained in Minimum Essential Medium (MEM) supplemented with 10% fetal bovine serum (FBS). This cell line has been transformed with the E1 region of type 5 adenovirus (Graham et al., 1977). NIH3T3 murine embryonic fibroblasts (ATCC #CRL-1658) were maintained in high glucose Dulbecco's Modified Eagle Medium (DMEM) supplemented with 10% FBS. hTERT-HME1 human mammary epithelial cells (ATCC #CRL-4010) were maintained in DMEM/F12 supplemented with 10 mM HEPES, 10 µg/mL insulin, 5 mg/mL BSA, 10 ng/mL Cholera toxin, 10 ng/mL epidermal growth factor (EGF), and 0.5 µg/mL hydrocortisone. MCF-10A human mammary epithelial cells (ATCC #CRL10317) were maintained in modified DMEM/F12 with 5% FBS, 10 µg/mL insulin, 10 ng/mL Cholera toxin, 20 ng/mL EGF, and 0.5 µg/mL hydrocortisone. MTHJ murine mammary adenocarcinoma cells were established as described (Hummel, Safroneeva, and Mossman, 2005) and maintained in high glucose Dulbecco's Modified Eagle Medium (DMEM) supplemented with 10% FBS. ZR-75-1 human breast cancer cells (ATCC #CRL-1500) were cultured in RPMI 1640 supplemented with 10% FBS. All cell lines were supplemented with 2 mM L-glutamine, 0.1 mg/mL penicillin, and 100 U/mL streptomycin, and grown at 37ºC in a humidified atmosphere at 5% CO_2. All media were purchased from Sigma Chemicals and all supplements were purchased from Gibco except for cholera toxin (List Biologicals).

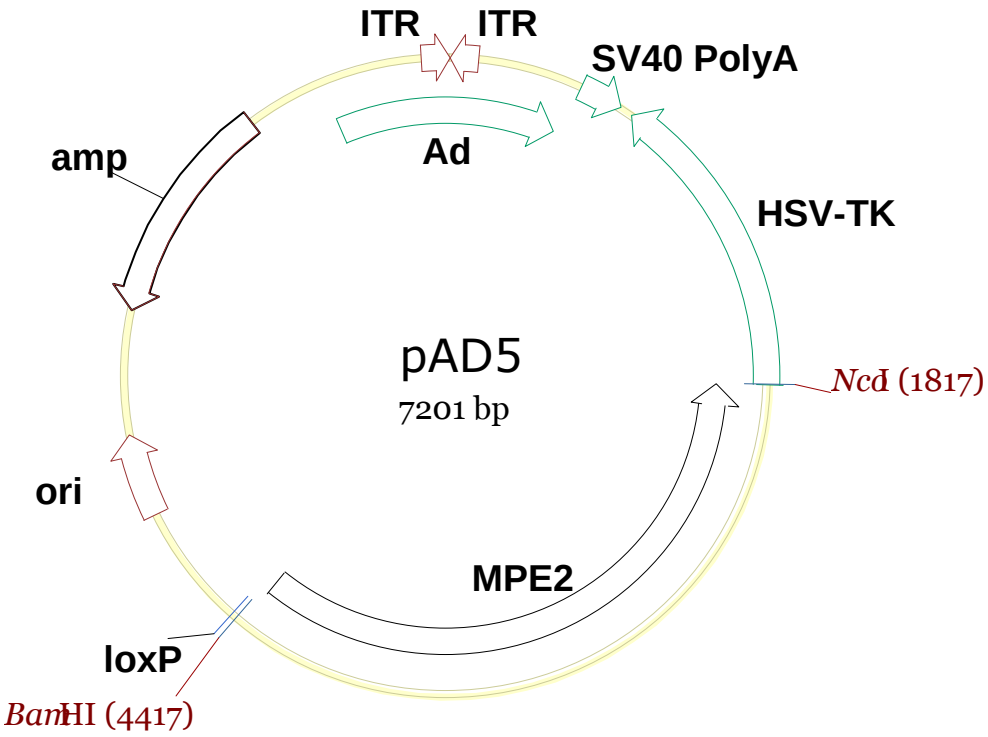

Figure 2.3. pAD5 plasmid.

The pAD5 plasmid contains the MPE_2 promoter upstream of HSV-TK in the same backbone as pSJ7. Other features include sequences necessary for replication and packaging into adenoviral capsids such as inverted terminal repeats (ITR), and an origin of replication (ori). As well, the pAD5 plasmid contains an ampicillin resistance gene (amp), a polyadenylation signal downstream of HSV-TK (SV40 PolyA), adenoviral sequences (Ad) and a loxP site for recombination into an Ad vector. Important restriction enzyme locations are also shown.

2.2.3. Generation of Adenovirus Vectors

FGAdAD5 (FGAdMPE$_2$TK)

The first generation (E1-, E3-deleted) adenoviral vector FGAdAD5 expressing HSV-TK under the control of the MPE$_2$ promoter was generated as previously described (Hitt, 2006). Briefly, 60mm dishes of HEK293 cells were cotransfected with shuttle plasmid pAD5 and viral backbone vector pBHGloxΔE1,E3Cre (Figure 2.4) using calcium phosphate. One day after cotransfection, 60mm plates were overlaid with 0.5% agarose in MEM supplemented with 2 mM L-glutamine, 100 U/mL penicillin, 100 µg/mL streptomycin, 250 ng/mL fungizone, and 10% horse serum (Gibco). Agar plugs (plaque isolates) were suspended in PBS^{++} (PBS, 0.1 g/L $CaCl_2 \cdot 2H_2O$, 0.1 g/L $MgCl_2 \cdot 6H_2O$) + 10% glycerol. Plaque suspensions were used to infect new 60 mm plates of 293 cells. At complete cytopathic effect (4 to 6 days) all cells and media were collected. DNA was extracted using pronase/ethanol precipitation. HindIII restriction enzyme analysis confirmed recombination. Correct recombinant viruses were plaque purified and amplified by infecting forty 150 mm plates of 293 cells. The cell suspension was centrifuged and pellets pooled. Virus was purified using CsCl banding in Tris buffer and dialyzed for 24h in Tris buffer to remove CsCl. Plaque assays were performed on banded virus to quantitate concentration of plaque forming units (pfu). Restriction enzyme analysis confirmed that 6 out of 6 of these plaques were FGAdAD5. Banded virus was tested for the presence of replication competent Ad (RCA), which is a rare outcome of E1-deleted Ad generation in

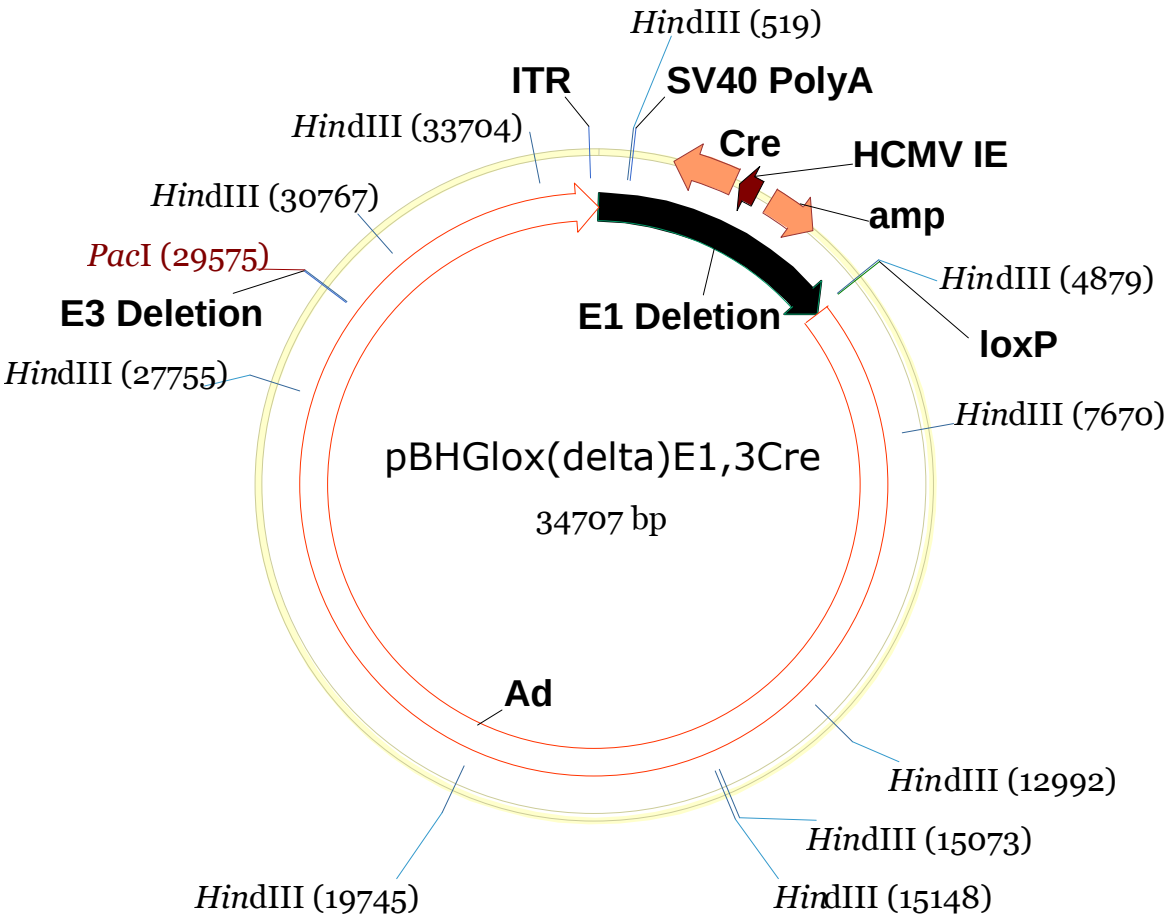

Figure 2.4. pBHGloxΔE1,E3Cre plasmid.

The pBHGloxΔE1,E3Cre plasmid contains mostly Ad5 sequence (including the inverted terminal repeat [ITR]) except for deletions in the E1 and E3 regions. pBHGloxΔE1,E3Cre also contains an ampicillin resistance gene (amp), a Cre recombinase gene (expressed from the human cytomegalovirus immediate early promoter [HCMV IE]) and a loxP site for recombination. Important restriction enzyme sites are also shown.

HEK293 cells (Duigou and Young, 2005). Homologous recombination events during Ad production can possibly lead to E1 transference from the HEK293 genome into the Ad backbone (Hehir et al., 1996; Lochmuller et al., 1994). Infection of A549 human lung carcinoma cells (ATCC #CCL 185) with FGAdAD5 determined that there was <1 RCA per 10^7 infetious FGAdAD5 viral particles.

FGAdSJ7 (FGAdCMVTK)

The first generation adenoviral vector FGAdSJ7 expressing HSV-TK under the control of the murine CMV promoter was previously generated as above using pSJ7 as the shuttle plasmid (Long and Jain, unpublished).

Addl70-3

Addl70-3 negative control virus (Bett et al., 1994) was amplified and purified by CsCl banding (described above). This vector is deleted in E1 and E3 and carries no transgene.

2.2.4. MTS Metabolism Assays

Non-cancer (NIH3T3, hTERT-HME-1, and MCF-10A), and breast cancer (MTHJ and ZR-75-1) cells were grown in 12-well plates until 90% confluent, after which cells were counted and infected with virus at a multiplicity of infection of 50 pfu per cell. Cells were infected with PBS (Mock), control virus (Addl70-3), or a TK-expressing virus under the control of either the MPE_2 promoter ($AdMPE_2TK$), or CMV promoter (AdCMVTK). After 24 hours, cells were seeded into 96-well plates at 10^3 cells/well and incubated at 37˚C with growth medium plus ganciclovir (Sigma) at the indicated concentrations. On day 7, 100 µL MTS reagent (Promega) was added to each well and cells were further incubated at

37˚C for 4 hours. The absorbance of each well on the plate was measured at 490 nm using the FLUOstar Optima plate reader (BMG Labtech). All conditions were carried out in triplicate. 100% cell survival was based on absorbance of infected cells not treated with GCV.

2.2.5. Crystal Violet Staining

Post-MTS assay, the 96-well assay plates of ZR-75-1 cells were rinsed in PBS and incubated in 0.2% crystal violet in 70% methanol + 2% acetic acid at room temperature for 30 minutes. Plates were then washed gently with copious amounts of water then air-dried. Absorbance was read at 584 nm using the FLUOStar Optima plate reader.

2.2.6. ^{3}H-GCV-Phosphate Filter Binding Assays

The indicated cells were grown in 6-well plates and infected with virus at different multiplicities of infection (MOIs). Infected cells were incubated at 37ºC, then washed with PBS after 24 hours and harvested by scraping. Cells were pelleted by centrifugation (1500 rpm), washed in cold PBS, and finally resuspended in extract buffer (50 mM Tris-Cl, pH 7.5; 1 mM EDTA, pH 8; 0.01 vol phenylmethylsulfonyl fluoride [PMSF]; 1 mM dithiothreitol [DTT]). Lysates were freeze/thawed three times, centrifuged (1500 rpm) to clarify, and stored in aliquots at -80ºC.

Filter binding assays were carried out using ^{3}H-GCV as the HSV-TK substrate. 25 µL of lysate was incubated with an equal volume of 2X reaction mix (3 mM $MgCl_2$; 0.1 mg/mL BSA; 50 mM Na phosphate buffer, pH 6.5; 3 mM ATP; 10 µM unlabeled GCV [Sigma]; 0.254 nmol (=1.5 µCi) ^{3}H-GCV [6 Ci/mmol; Moravek] per

reaction) at 37ºC for 30 minutes. Reactions were stopped by placing samples on ice immediately following the 30 minute incubation. Samples were then spotted onto Whatman DE81 filters, which were subsequently washed 3 times batchwise in 500 mL 50% ethanol (20 minutes/wash) with gentle rocking. Filters were dried, transferred to scintillation vials with 5 mL Ready Safe liquid scintillation cocktail (Beckman Coulter), and counted for radioactivity using a LS6500 Scintillation Counter (Beckman). Background was defined as amount of radioactivity on filters spotted with reaction mix without cell lysate.

The amount of ^{3}H-GCV to be used in the filter binding assay was determined through optimization using AdCMVTK-infected ZR-75-1 cell lysates and increasing amounts of ^{3}H-GCV (Figure 2.5). ZR-75-1 cells were treated with PBS or infected with different multiplicities of infection, then harvested 2 days post-infection. Cell lysates prepared as described above. Filter binding assays were carried out by incubating 25 µL of lysate in duplicate with an equal volume of 2X reaction mix as described above, using a constant 10 µM unlabeled GCV but adding increasing amounts of ^{3}H-GCV per reaction. It was determined that 1.5 µCi ^{3}H-GCV per reaction would yield the optimum signal output.

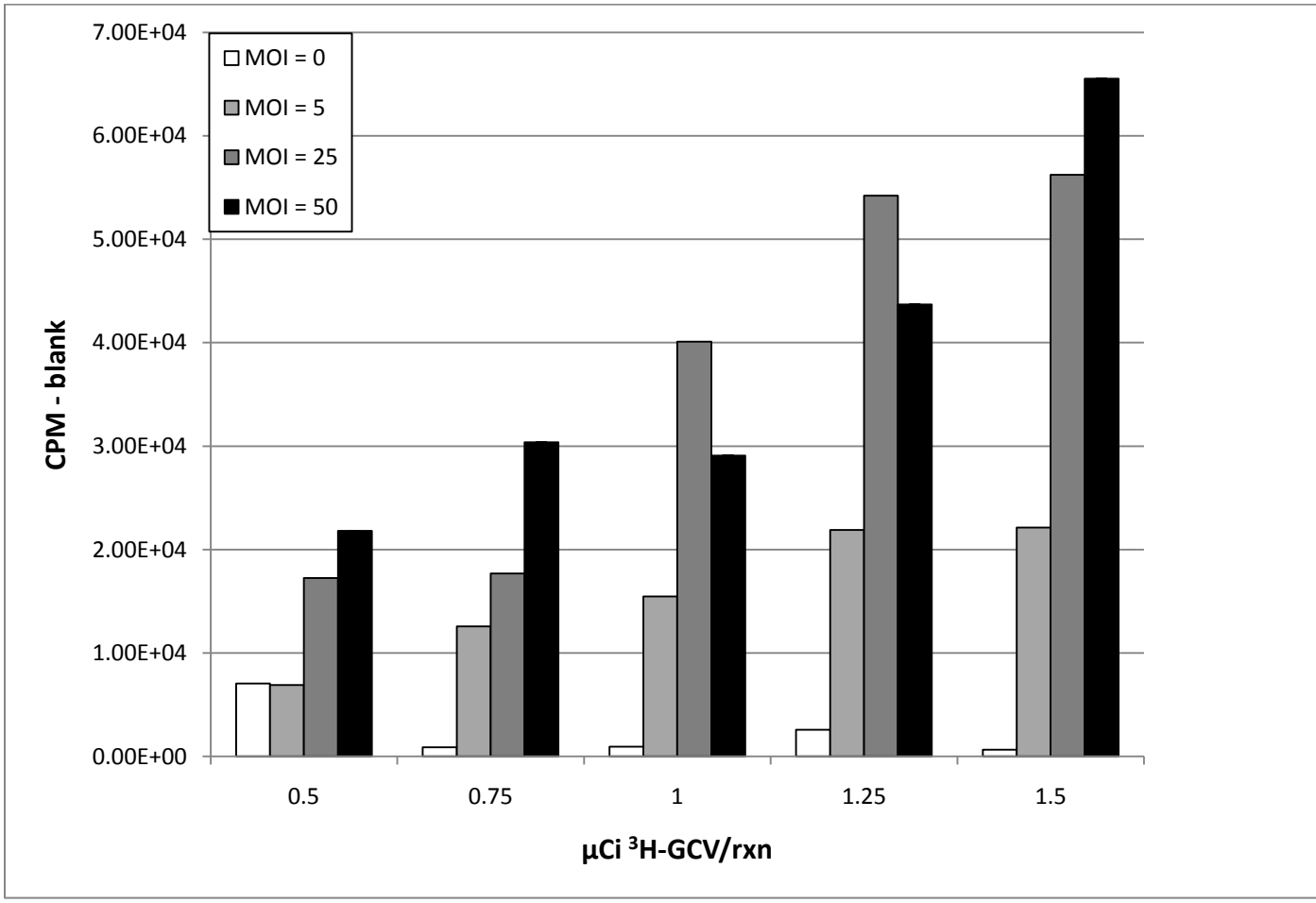

Figure 2.5. Optimum filter binding assay signal output using 1.5 µCi of ^{3}H-GCV/reaction.

ZR-75-1 breast cancer cells were treated in duplicate with PBS (Mock) or infected with AdCMVTK at increasing multiplicity of infection, ranging from 5 to 50 plaque forming units per cell. Cell lysates were harvested 2 days post-infection and incubated with increasing ratios of ^{3}H-GCV:unlabeled GCV to determine conditions required for the optimum signal output. The y-axis shows counts per minute (CPM) – blank (reaction mixture on filter with no cell lysate).

2.2.7. Mouse Model

All animal experiments were carried out in accordance with guidelines of the Canadian Council on Animal Care (CCAC) and were approved by the local animal care committee of the Cross Cancer Institute. Six week old female FVB mice (Charles River, Saint-Constant, Quebec, Canada) were injected subcutaneously in the shoulder with the indicated number of MTHJ cells and monitored for tumor formation. Animals were housed in sterile surroundings with standardized light/dark cycle and access to food and water *ad libitum*. Tumor growth was measured in three dimensions using digital calipers and the size calculated using the formula for the volume of a typical ellipsoid: $T_{vol} = \pi/6$ x width x length x depth (Tomayko and Reynolds, 1989). Tumor-bearing mice were euthanized at the study end point or if tumor burden endpoint was reached (defined as tumor volume ≥ 10% of mouse body weight).

2.2.8. Tumor Regression Studies

Six week old female FVB mice were injected subcutaneously with either $1x10^6$ or $2.5x10^6$ MTHJ cells. After 3 weeks tumor-bearing mice were split into 4 groups of 6 mice/group. Mice from each group were injected with $4x10^8$ plaque forming units (pfu) of either AdCMVTK ($AdCMVTK_{hi}$), $AdMPE_2TK$, or Addl70-3 (control) on day 1. To control for the approximately 10-fold lower expected HSV-TK expression from $AdMPE_2TK$ compared to AdCMVTK, a fourth group of mice was injected with $4x10^7$ pfu AdCMVTK (combined with $3.6x10^8$ pfu Addl70-3 for consistent total viral dose; $AdCMVTK_{lo}$). All intratumoral injections consisted of 50 µL of virus, suspended in PBS, distributed over three injection sites. Viral

injections were repeated on days 4 and 7. Starting on day 2 all mice received 1 mg ganciclovir (Cytovene® Ganciclovir sodium for injection; Roche) diluted in 200 µL PBS intraperitoneally daily for 16 days. Tumor size was measured daily for the duration of the experiment.

2.2.9. Toxicity Study

Six week old female FVB mice were injected subcutaneously with $1x10^6$ MTHJ cells. Upon tumor formation (~4 weeks post-injection of tumor cells) blood samples were taken and sent to IDEXX Laboratories (Edmonton, Alberta, Canada) for baseline liver enzyme analysis. The day of sampling for baseline analysis was defined as day 0. The liver enzyme panel included alanine transaminase (ALT), aspartate transaminase (AST), alkaline phosphatase (ALP), and sorbitol dehydrogenase (SDH), all markers of liver damage when present in serum. One day after baseline blood samples were taken (day 1), all mice from each group were injected intratumorally with $4x10^8$ pfu of either AdCMVTK ($AdCMVTK_{hi}$), $AdMPE_2TK$, Addl70-3 (control), or low dose AdCMVTK + Addl70-3 ($AdCMVTK_{lo}$). Starting on day 2 all mice received 1 mg ganciclovir (Cytovene® Ganciclovir sodium for injection; Roche) intraperitoneally daily for 16 days. Mice were intratumorally injected with virus again on day 4 and 7, with blood samples taken from the tail and sent for liver enzyme analysis on day 5. On day 11 half of the mice from each group were euthanized, with blood samples taken and sent for liver enzyme analysis while tumors, livers, and mammary fat pads were removed, fixed in formalin then paraffin-embedded for immunohistochemistry (see section 2.2.10). On day 19 the remaining mice from each group were

euthanized, with blood samples taken and sent for liver analysis while tumors, livers, and mammary fat pads were removed, fixed in formalin then paraffin-embedded for hematoxylin and eosin staining. Hematoxylin and eosin staining was carried out by Daryl Glubrecht as described (Mita et al., 2007).

2.2.10. HSV-TK Biodistribution

Six week old female FVB mice were injected subcutaneously with $1x10^6$ MTHJ cells. After 4 weeks, mice were split into 4 groups of 2 mice/group. Mice from each group were injected intratumorally with either $4x10^8$ pfu of AdCMVTK, $AdMPE_2TK$, Addl70-3 (control), or low dose AdCMVTK + Addl70-3 (as in toxicity study) on days 1, 4, and 7. No GCV was administered in this experiment. Mice were euthanized two days following the final virus injection, and the tumors and livers were dissected. Tumors and livers were fixed in formalin for 24 hours, paraffin-embedded, and sectioned. HSV-TK staining was carried out by Daryl Glubrecht as described (Mita et al., 2007) with minor modifications. Briefly, sections were dewaxed in xylene and rehydrated in a graded ethanol-water series. Antigen retrieval was performed using citraconic anhydride, pH 7.5, for 13 minutes in a pressure cooker via microwave (750W). Sections were then blocked for 30 minutes in Dako Protein Block and stained for HSV-TK using polyclonal rabbit anti-TK antibody (Dr. William C. Summers, Yale University) at 1/1000 dilution in Dako Antibody Diluent overnight (4ºC). Slides were washed and incubated for 2 hours in DakoCytomation EnvisionPlus anti-rabbit secondary antibody (DakoCytomation, Glostrup, Denmark) at room temperature.

DakoCytomation Liquid DAB$^+$ Substrate Chromagen System was used for immunoreactivity visualization.

2.3. RESULTS

2.3.1. AdMPE$_2$TK Induced Breast Cancer-Selective TK Activity in vitro

To quantitate levels of HSV-TK expression from our AdTK vectors, we used a filter binding assay which measures the amount of ^{3}H-GCV phosphorylated *in vitro* by incubation with infected cell lysates. Enzymatic HSV-TK activity was measured in extracts of infected murine fibroblasts (NIH3T3), human mammary cells transformed with hTERT (hTERT-HME-1), and cancer (MTHJ & ZR-75-1) cell lines (Figure 2.6). We detected high levels of HSV-TK activity in all AdCMVTK-infected cell lines. The high levels of CMV promoter-controlled TK activity in all cell lines indicates efficient infectivity by the adenoviral vectors. AdCMVTK induced 90- and 38-fold higher HSV-TK expression than AdMPE$_2$TK in hTERT-HME-1 and NIH3T3 cells, respectively, while only 6- and 3-fold higher HSV-TK expression in MTHJ and ZR-75-1 cells, respectively. AdMPE$_2$TK infections yielded significantly higher HSV-TK activity in the MTHJ and ZR-75-1 breast cancer cell lines than in the hTERT-HME-1 and NIH3T3 non-cancer cell lines ($p < 0.001$). AdMPE$_2$TK infections in both breast cancer cell lines also yielded significantly higher HSV-TK activity than control mock infections ($p < 0.002$). These findings supported the breast cancer-selective activity of the MPE$_2$ promoter.

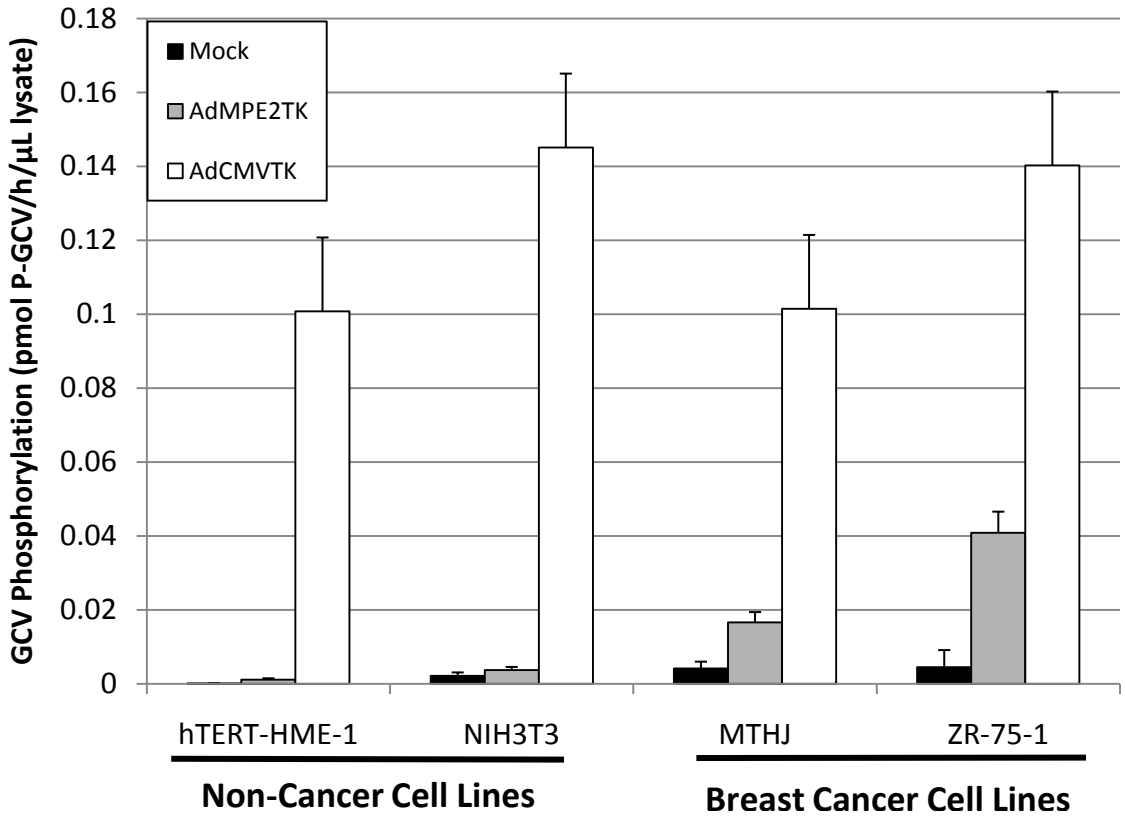

Figure 2.6. ^{3}H-GCV filter binding assay shows BrCa-selective HSV-TK activity after AdMPE$_2$TK vector infection.

Non-cancer (murine NIH3T3 & human hTERT-HME-1) and breast cancer (murine MTHJ & human ZR-75-1) cells were mock infected or infected with a TK-expressing virus under the control of either the MPE$_2$ promoter (AdMPE$_2$TK) or mCMV promoter (AdCMVTK). All infections were at a multiplicity of infection of 50 plaque forming units per cell. Cells were harvested 2 days post-infection and lysates prepared and assayed for TK activity as described in section 2.2.6.

2.3.2. AdMPE$_2$TK with GCV Induced Breast Cancer-Selective Killing in vitro

MTS metabolism assays were performed on a panel of murine and human breast cancer (MTHJ, T47D, SK-BR-3, MDA-MB-468 & ZR-75-1) and non-cancer (hTERT-HME-1, MCF10A & NIH3T3) cell lines to determine if AdMPE$_2$TK can induce breast cancer-selective cell killing in combination with ganciclovir (Figure 2.7). For ZR-75-1 cells, MTS assay results did not reflect actual numbers of cells in each well visualized by microscopy. In some instances, wells containing ZR-75-1 cells infected with the same amount of virus and increasing amount of GCV showed a decrease in absorbance after MTS incubation (indicating an increase in adherent cells) when microscopic observation showed an obvious decrease in adherent cells with increasing [GCV]. This inconsistency between MTS results and microscopic observations did not occur with any other cell line. For this reason crystal violet staining was performed on ZR-75-1 cells and was more representative of observed cell viability.

Mock infections with PBS^{++} and infections with negative control Addl70-3 (no TK) showed little killing below 100 µg/mL GCV in all cell lines except MDA-MB-468. These cells did not grow after Addl70-3 infection, even in the absence of GCV (thus Addl70-3 infection not shown in Figure 2.7A). Not surprisingly, AdCMVTK infection of all cell lines induced a substantial decrease in survival (with increasing ganciclovir concentrations) since AdCMVTK was expected to express high levels of HSV-TK regardless of cell type. This result was consistent with cell viability assays which showed cell death from AdCMVTK infection plus GCV of all cell lines. In combination with GCV, AdMPE$_2$TK infections induced cell death

nearly as well as AdCMVTK in the murine MTHJ, T47D, and SK-BR-3 breast cancer cell lines as well as the human MDA-MB-468 and ZR-75-1 breast cancer cell lines. In contrast, AdMPE$_2$TK did not induce similar cell killing in the hTERT-HME-1 or NIH3T3 non-cancer cell lines. Interestingly, AdMPE$_2$TK also induced killing of MCF-10A cells with increasing GCV concentrations.

2.3.3. AdMPE$_2$TK with GCV Did Not Induce in vivo *Tumor Regression in the Murine MTHJ Tumor Model*

Four tumor regression studies were carried out using MTHJ tumor-bearing mice treated with 3 intratumoral injections of AdCMVTK, AdMPE$_2$TK or Addl70-3 plus GCV (1 mg daily for 17 days). Experiments 1 through 3 were carried out using 1 x 10^6, 2.5 x 10^6, or 5 x 10^6 MTHJ cells per mouse and resulted in a large variation in tumor volume among mice prior to virus treatment (Table 2.2). In the fourth experiment, injection of 10^6 MTHJ cells per mouse resulted in less variation, but tumors still grew quickly (Table 2.2). No tumor regression or increased survival was observed in any of these experiments. Survival of treatment groups in experiment 4 are shown in Figure 2.8. Of note, mice infected with AdCMVTK$_{hi}$ plus GCV did not survive as long as the other treatment groups. Two mice in this group showed signs of toxicity (ruffled fur, lack of response to external stimuli) during week 2 which necessitated euthanization prior to endpoint based on tumor size.

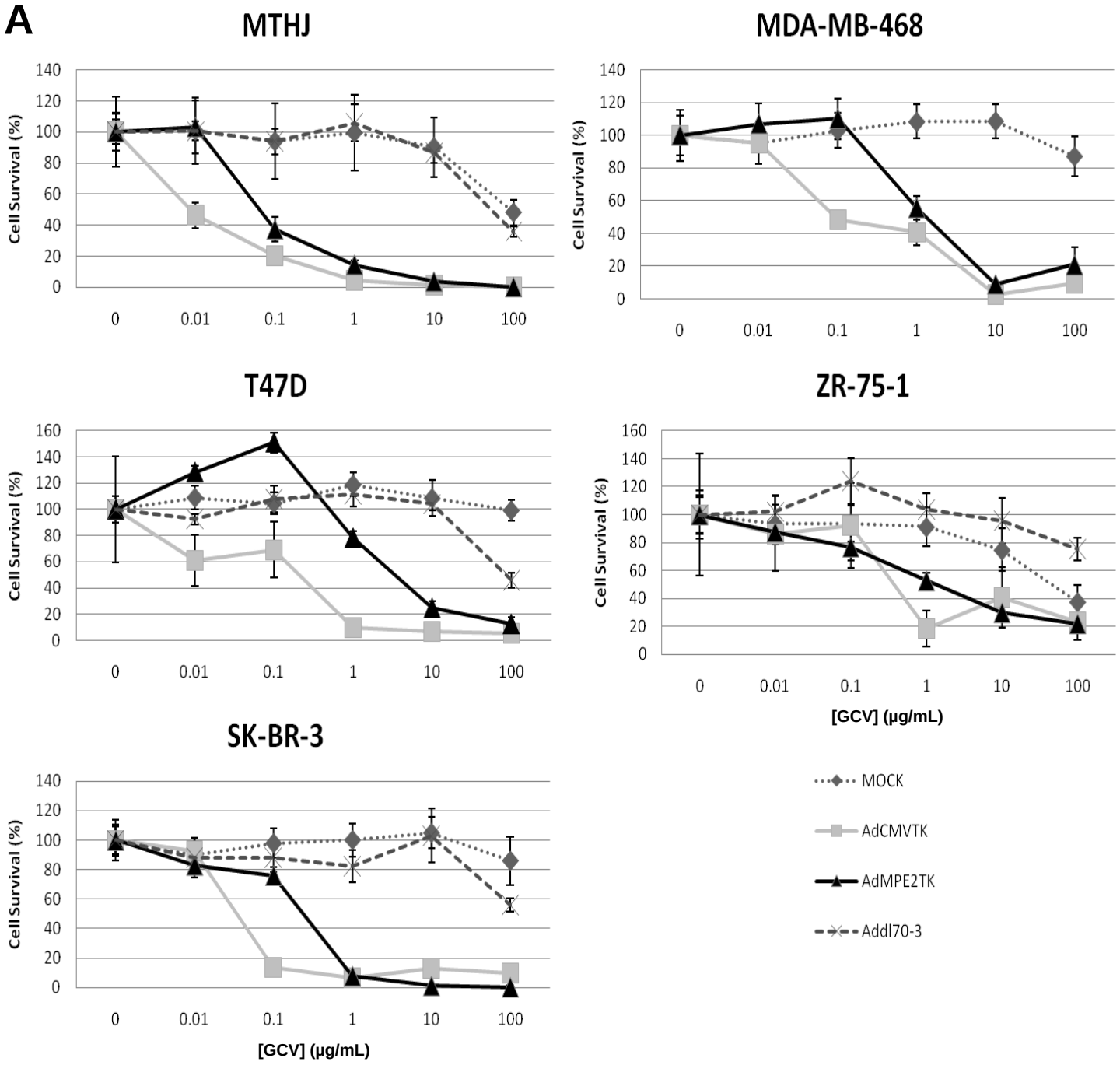
A
MTHJ
MDA-MB-468
T47D
ZR-75-1
SK-BR-3
Cell Survival (%)
[GCV] (µg/mL)
MOCK
AdCMVTK
AdMPE2TK
AddI70-3

B

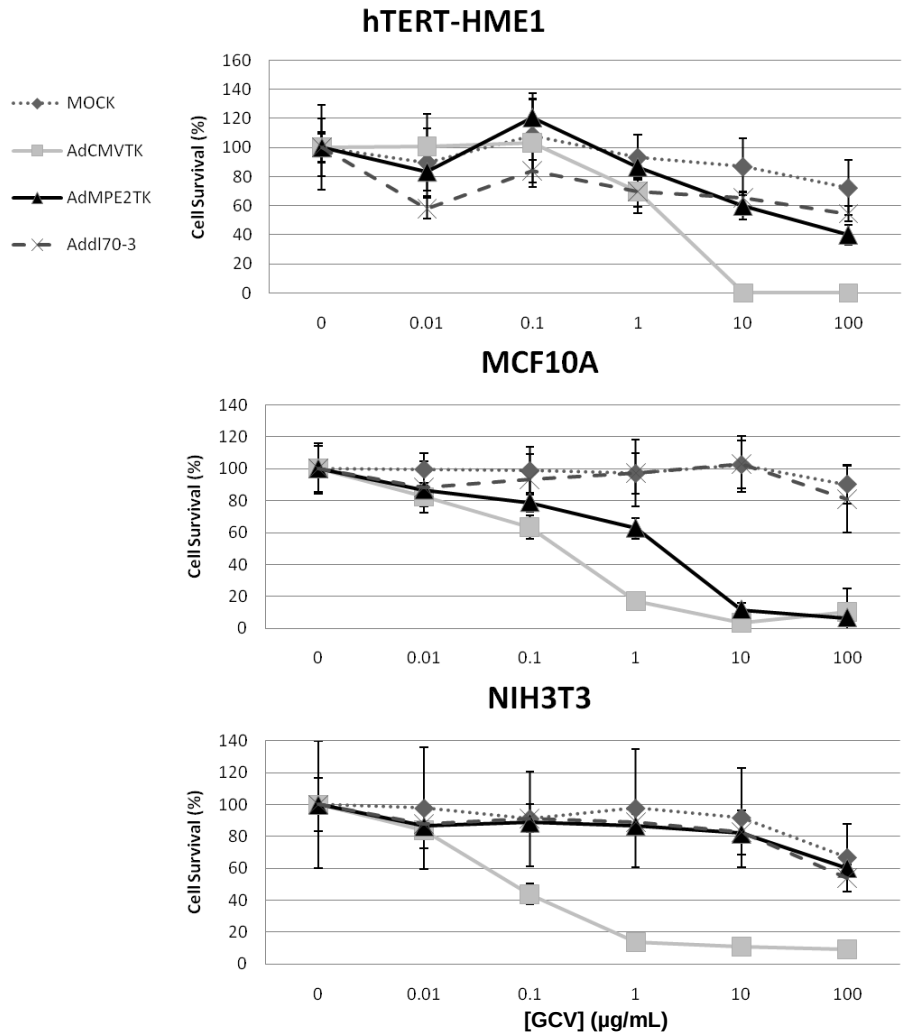

Figure 2.7. Cell viability assays show BrCa-selective decrease in cell survival after AdMPE$_2$TK vector infection.

(A) Breast cancer (MTHJ, T47D, SK-BR-3, MDA-MB-468 & ZR-75-1) and non-cancer (hTERT-HME-1, MCF-10A &NIH3T3) cells were infected with PBS (Mock), AdCMVTK, AdMPE$_2$TK, or a non-TK-expressing control vector Addl70-3. All infections were at a multiplicity of infection of 50 plaque forming units per cell. Infected cells were treated with increasing concentrations of ganciclovir (0 µg/mL to 100 µg/mL) for 7 days. MTS assay was performed on all cell lines except ZR-75-1 cells, which were assayed by crystal violet staining. % Cell survival = 100 x (viability of GCV-treated cells) / (viability of cells incubated without GCV).

Exp #	# Cells Injected	# Mice	Av. Tumor Size at Virus Injection	Range in Tumor Size	# Days to Virus Injection
1	1×10^6	16	78.4 mm^3	14.1 – 223.0 mm^3	39
2	2.5×10^6	20	297.1 mm^3	105.6 – 674.1 mm^3	24
3	5×10^6	24	149.9 mm^3	30.5 – 306.6 mm^3	17
4	1×10^6	24	135.6 mm^3	38.6 – 234.1 mm^3	20

Table 2.2. Tumor size variation from mice injected subcutaneously in th flank with different amounts of MTHJ cells.

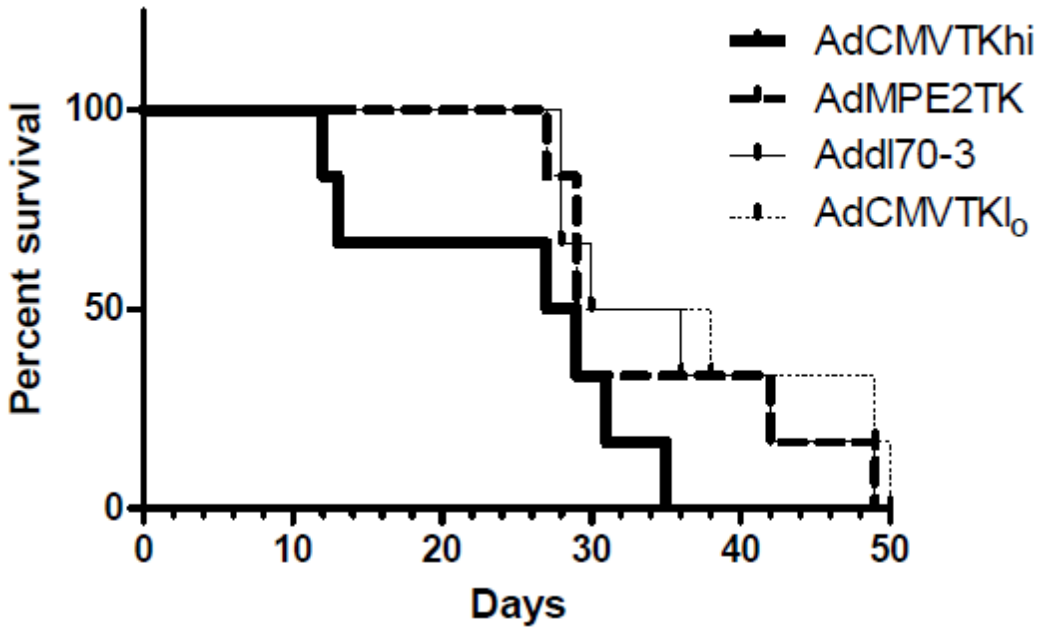

Figure 2.8. Intratumoral injection of AdTK vectors with GCV treatment did not prolong survival.

Six FVB mice per group were injected with 4 x 10^8 pfu virus at day 1, 4, & 7 and treated with ganciclovir 1 mg daily from day 2 to 17. The $AdCMVTK_{lo}$ group was treated with 4x10^7 pfu AdCMVTK combined with 3.6x10^8 pfu Addl70-3 control vector. Two mice from the $AdCMVTK_{hi}$ group were euthanized due to toxicity on day 12 and 13. All other mice were euthanized when tumor volume reached ≥ 10% of mouse body weight.

2.3.4. AdMPE$_2$TK Induces Significantly Less Liver Toxicity than AdCMVTK$_{hi}$ in vivo

To determine the toxicity of AdMPE$_2$TK compared to AdCMVTK (and the control Addl70-3) *in vivo*, we tested blood samples from tumor-bearing immunocompetent mice injected intratumorally with Ad vector and treated with ganciclovir as in the tumor regression studies. Baseline levels of liver enzymes ALT, AST, ALP, and SDH were measured in blood samples of pre-virus-injected mice and compared with blood samples taken at various timepoints: (i) during the course of virus treatment (day 5), where HSV-TK expression levels were expected to be rising; (ii) four days after the last virus dose (day 11), where toxicity from HSV-TK was predicted to be at its highest level; and (iii) twelve days after the last virus dose (day 19), where HSV-TK expression levels were expected to return closer to baseline. Unexpectedly, 3 mice from the AdCMVTK$_{lo}$ group, 2 mice from the Addl70-3 group, and 1 mouse from the AdMPE$_2$TK group died within 24 hours of the first virus injection prior to administration of GCV. No signs of toxicity were observed in these mice before or immediately after virus injection. It seems unlikely that mortality was due to TK expression given the short time interval after injection. On day 5 no elevated liver enzyme concentrations were detected in surviving mice from any group. By day 11, mice injected with AdCMVTK$_{hi}$ showed elevated liver enzyme concentrations for all enzymes measured (8- to 21-fold) at a significance of $P < 0.001$. Mice injected with AdMPE$_2$TK, Addl70-3, or AdCMVTK$_{lo}$ showed no elevation in SDH, AST, or ALP. Although significant ALT elevation ($P < 0.01$) was observed in samples

from day 19 of the AdMPE$_2$TK treatment group, this elevated amount was almost identical (103%) to control treated animals and still less than (84%) the AdCMVTK$_{hi}$ treated group (Figure 2.9).

Hematoxylin and eosin staining of liver sections from these mice support the observations with serum markers for liver damage. Toxicity was confirmed by a pathologist (Dr. P.N. Nation, Animal Pathology Services) in livers of mice injected with AdCMVTK$_{hi}$, but not mice injected with AdMPE$_2$TK, Addl70-3, or AdCMVTK$_{lo}$ (Figure 2.10). No difference in cell damage was observed in stained tumor or mammary fat pad sections from mice receiving different treatments.

2.3.5. AdMPE$_2$TK Induces HSV-TK Expression in Tumor but not in Liver

Immunohistochemistry using anti-HSV-TK antibody revealed HSV-TK expression in tumors injected with AdCMVTKhi, AdCMVTK$_{lo}$, or AdMPE$_2$TK (Figure 2.11), although the regression experiment showed that it was not enough to cause the tumor to shrink in size. Staining was seen in patches, likely corresponding to areas where virus was administered to the tumor. There appeared to be fewer patches in the AdCMVTK$_{lo}^-$ and AdMPE$_2$TK-treated mice.

Supporting our toxicity data, we also observed that HSV-TK expression in the liver was limited to mice injected with AdCMVTK$_{hi}$ or AdCMVTK$_{lo}$, and was not observed in mice treated with AdMPE$_2$TK (Figure 2.12). Expression in the livers was seen as punctate HSV-TK staining throughout the tissue, indicating that AdCMVTK does infect and express in liver cells. Expression correlates with the observed liver toxicity from the AdCMVTK$_{hi}$-treated mice. We expect that the AdMPE$_2$TK vector is able to infect liver cells similarly to AdCMVTK, however it is

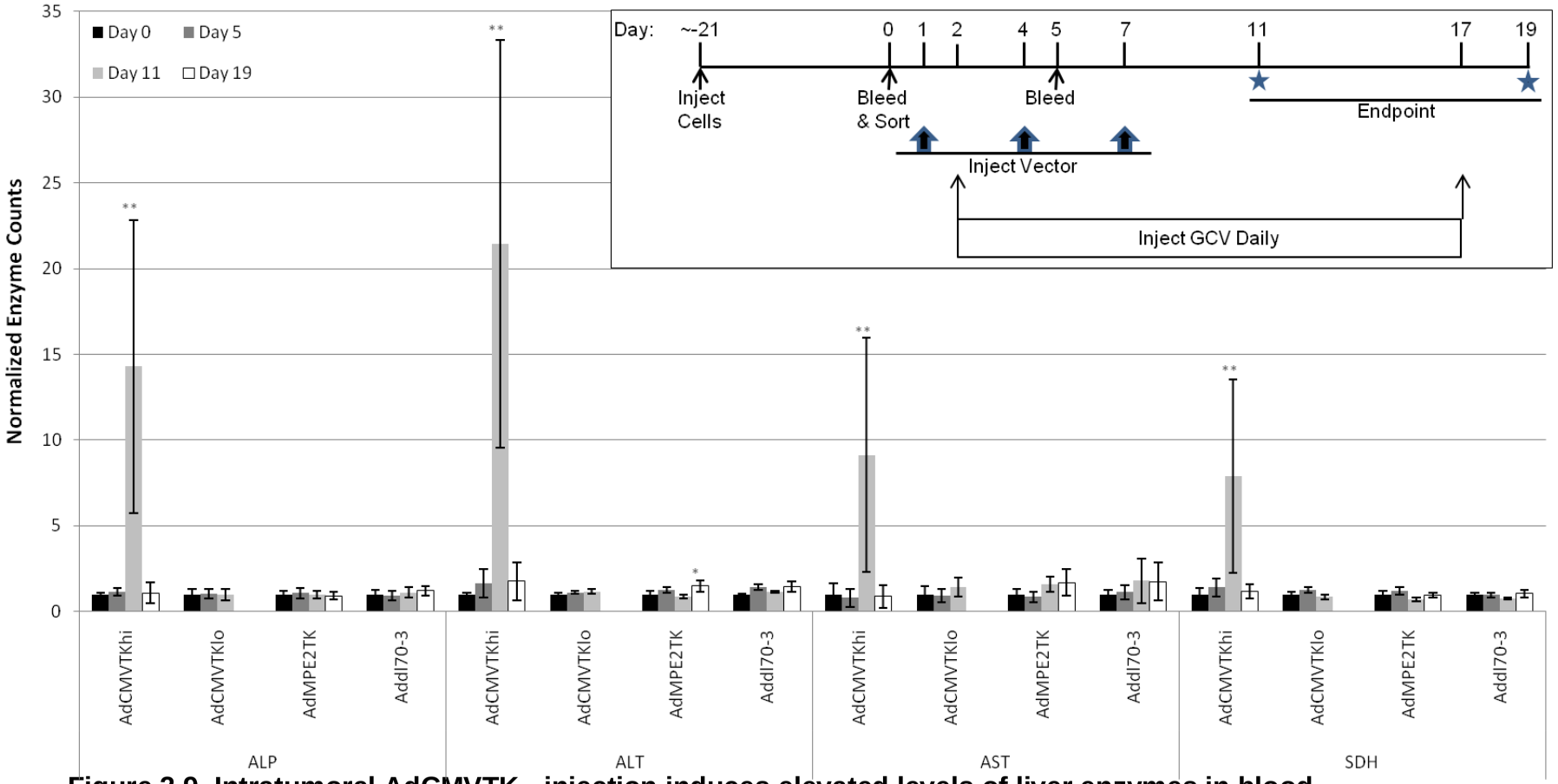

Figure 2.9. Intratumoral AdCMVTK$_{hi}$ injection induces elevated levels of liver enzymes in blood.

Tumor-bearing FVB were injected three times with Ad vectors on day 1, 4, and 7. Blood samples were taken at day 0, 5, 11, and 19. Blood samples were tested for liver enzyme counts of alanine phosphatase (ALP), alanine transaminase (ALT), aspartate transaminase (AST), and sorbitol dehydrogenase (SDH). * above bar represents P<0.01 significance from Day 0 of same virus dose.

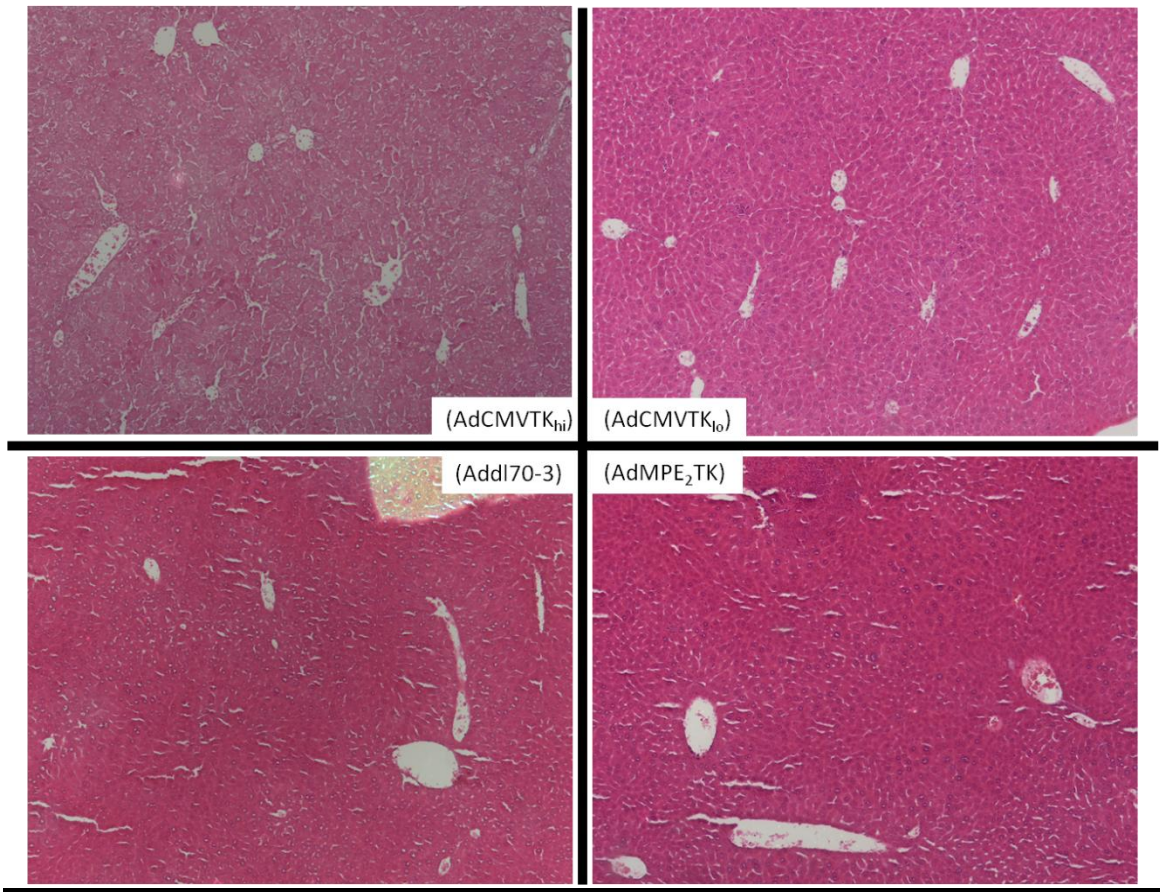

Figure 2.10. Intratumoral injection of AdCMVTK$_{hi}$ induces liver toxicity *in vivo*.

Mice were injected three times intratumorally with Ad vectors ($4x10^8$ pfu per injection) and sacrificed 2 days after the final injection. Liver sections were stained with hematoxylin and eosin and visualized at 10x magnification. The large number of 'cracks' in the AdCMVTK$_{hi}$ liver section were confirmed as a sign of toxicity by a pathologist.

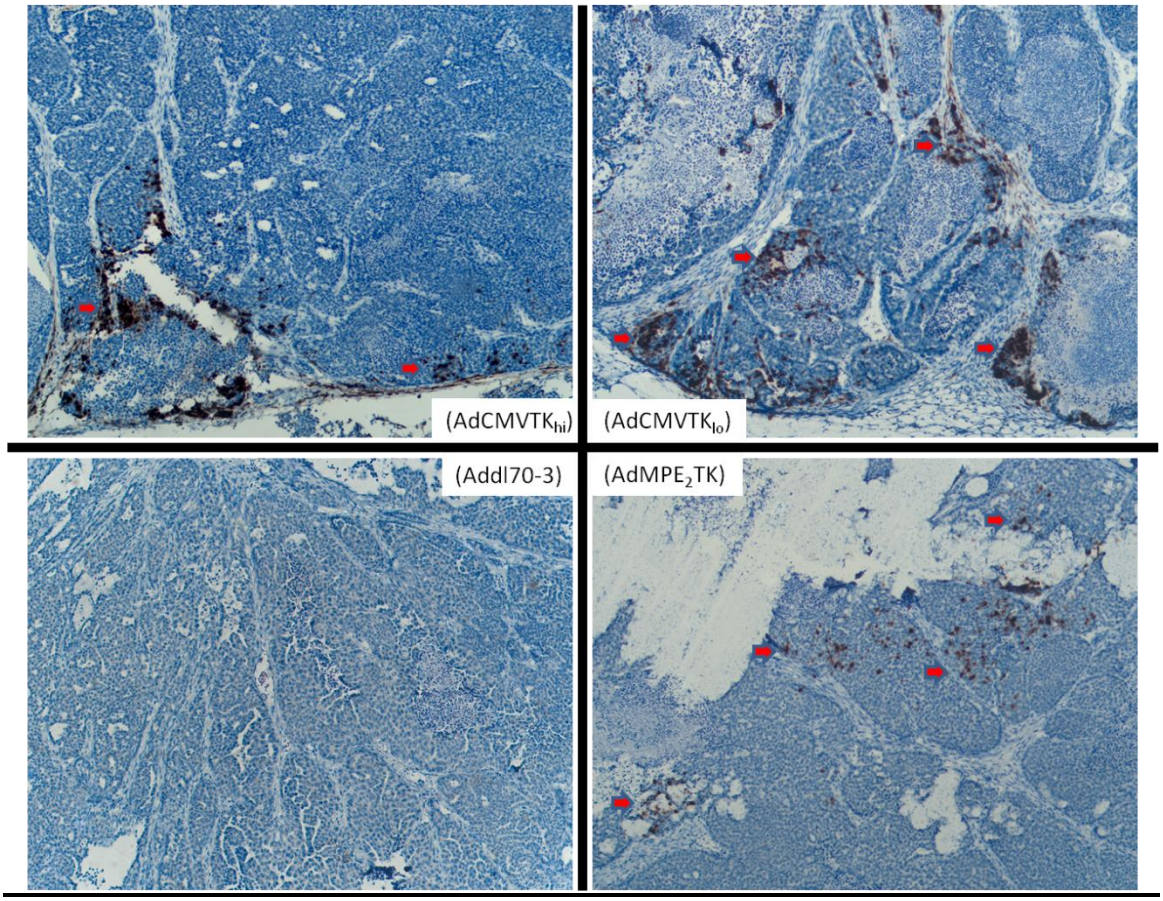

Figure 2.11. HSV-TK expression detected in MTHJ tumors following intratumoral injection of AdCMVTK and AdMPE$_2$TK.

Tumor sections were generated from mice injected three times intratumorally with Ad vectors (4x10^8 pfu per injection) and sacrificed 2 days after the final injection. Sections were stained using anti-HSV-TK antibody and visualized at 10x magnification. Presence of HSV-TK is seen as brown stained cells (indicated with red arrows).

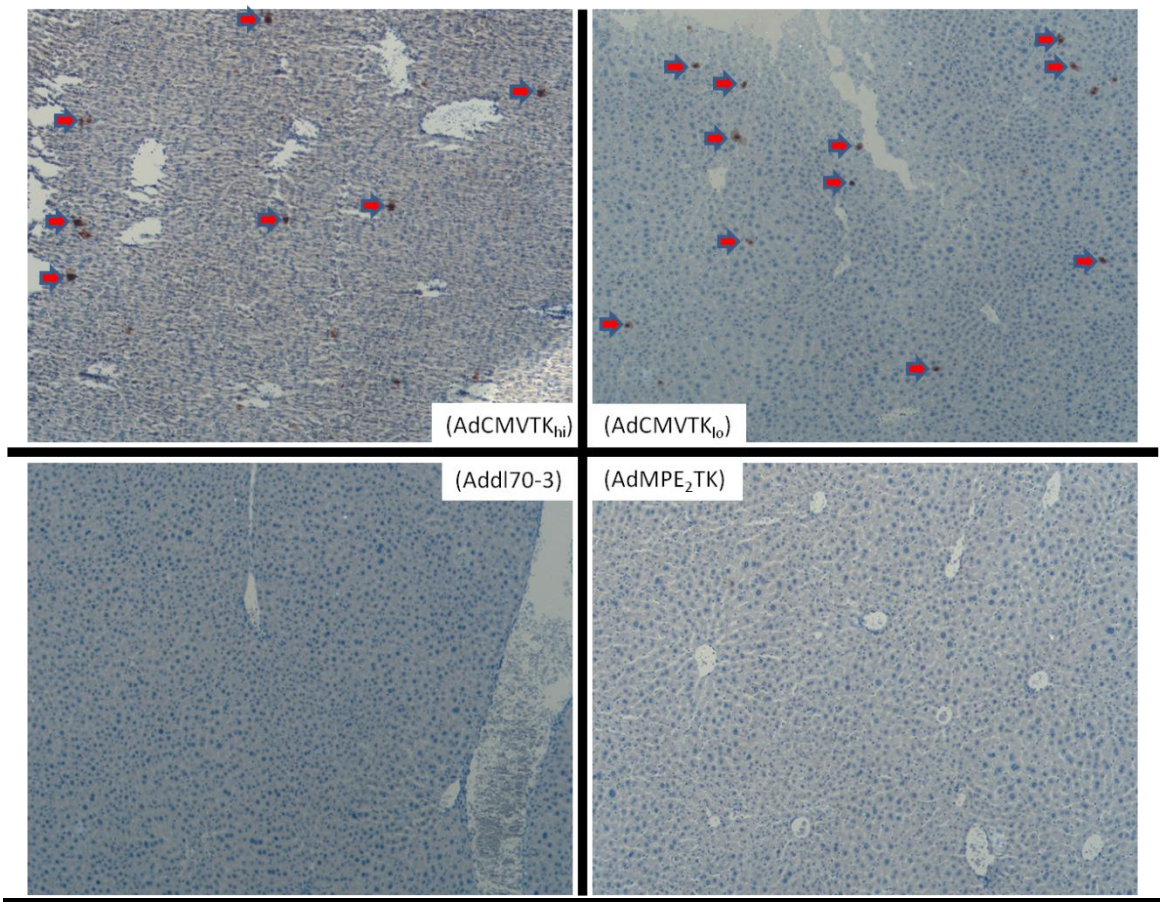

Figure 2.12. HSV-TK expression detected in liver following intratumoral injection of AdCMVTK.

Liver sections were generated from mice injected three times intratumorally with Ad vectors ($4x10^8$ pfu per injection) and sacrificed 2 days after the final injection. Sections were stained using anti-HSV-TK antibody (as described in Section 2.2.10) and visualized at 10x magnification. Presence of HSV-TK is seen as brown stained cells (indicated with red arrows).

clear that expression of HSV-TK from the AdMPE$_2$TK vector is much lower than the AdCMVTK vector since no staining was observed.

2.4 DISCUSSION

Tumor-specific promoters may play a major role in adenoviral cancer gene therapy due to their potential to target gene expression to tumor cells and focus the therapeutic effect away from non-cancer cells. The goal of this project was to determine the utility of using the breast cancer-selective MPE$_2$ promoter for adenoviral cancer gene therapy. While many vectors have been tested in preclinical settings to determine cancer specificity using transcriptional targeting (Casado et al., 2001; Huang et al., 2003; Lanson et al., 2003; Osaki et al., 1994; Peter et al., 2003; Yamamoto et al., 2001), to date no vector using any variation of the mammaglobin promoter has been investigated for a therapeutic effect. The MPE$_2$ promoter has previously been shown to induce luciferase transgene expression at high levels in breast cancer cell lines as opposed to non-cancer lines (Shi, Graham, and Hitt, 2006). Results discussed here reinforce the *in vitro* selectivity of the MPE$_2$ promoter and illustrate the low *in vivo* toxicity of the AdMPE$_2$TK vector when used for HSV-TK/GCV gene therapy.

In vitro assays revealed breast cancer-selective HSV-TK expression in cells infected with AdMPE$_2$TK. The filter binding assay using ^{3}H-GCV detected HSV-TK expression from the AdCMVTK vector in all cell lines tested, which was expected based on the ubiquitous activity of this promoter. AdMPE$_2$TK infection of the hTERT-HME-1 and NIH3T3 non-cancer cell lines resulted in

phosphorylated GCV levels not significantly higher than mock infected cells. However, infections in both the mouse MTHJ and human ZR-75-1 breast cancer cell lines resulted in phosphorylated GCV levels significantly higher than mock infected cells, demonstrating the breast cancer-selective expression from the MPE_2 promoter. Furthermore, AdMPE_2TK expression levels were higher than 10% of AdCMVTK expression levels in breast cancer cell lines, especially in ZR-75-1 cells, which are known to induce high levels of MPE_2 activity (Shi, Graham, and Hitt, 2006).

The cell killing experiments are consistent with enzymatic levels of TK in supporting *in vitro* breast cancer selectivity of the AdMPE_2TK vector. While the AdCMVTK vector induced cell death in all cell lines treated with GCV, the AdMPE_2TK vector induced cell death in combination with GCV only in the breast cancer cell lines (murine MTHJ, T47D & SK-BR-3 and human MDA-MB-468 & ZR-75-1). The only exception was the MCF-10A human non-cancer cell line, which interestingly showed a similar marked decrease in cell survival with AdMPE_2TK infection as with AdCMVTK in combination with GCV.

It is currently unclear why MCF-10A cells would activate the MPE_2 promoter to cause HSV-TK expression. MCF10A cells are widely used as a model for normal human mammary epithelial cells due their anchorage-dependent growth, 3 dimensional growth in collagen, and their lack of tumorigenicity in nude mice (Soule et al., 1990). Despite their usage, however, these immortalized cells are not karyotypically normal (Marella et al., 2009), which could provide a possible explanation as to why they respond to AdMPE_2TK gene therapy with ganciclovir.

The hTERT-HME1 cell line was derived from mammary cells removed from a patient with no history of breast cancer. These cells were immortalized through the stable expression of human telomerase reverse transcriptase, which allows cells to divide indefinitely while maintaining telomere length and retaining normal function, phenotype, and karyotype of normal primary epithelial cells (Seitz et al., 2002). As well, these cells are karyotypically, morphologically, and phenotypically similar to their primary parent cells (ATCC product information). Because of these qualities, the hTERT-HME1 cells may represent a 'closer to normal' mammary cell phenotype. When infected with AdMPE_2TK in the presence of ganciclovir, these cells maintained similar survival to cells infected with the control Addl70-3 virus and mock infected cells, suggesting the low HSV-TK expression levels.

The MTHJ and ZR-75-1 breast cancer cell lines showed a clear decrease in cell viability after infection with AdMPE_2TK and ganciclovir treatment. While the filter binding assay showed low levels of HSV-TK expression from the MPE_2 promoter in MTHJ cells, the cell viability assay revealed a marked decrease in cell survival from AdMPE_2TK-infected MTHJ cells treated with ganciclovir. Taken together, these assays suggest that low levels of HSV-TK are sufficient to induce a killing effect *in vitro*. This finding strengthens the argument for taking the next step toward using AdMPE_2TK in the clinical setting since lower amounts of an AdTK vector targeted to cancer cells may result in less toxicity to a cancer patient while still inducing a therapeutic effect. To test this hypothesis, *in vivo* experiments were carried out using MTHJ tumor-bearing immunocompetent mice.

We chose to use immunocompetent mice because these mice more closely mimic a human cancer patient than immunodeficient mice. Since we are testing the preclinical application of the AdMPE$_2$TK vector, we felt it was important to include a functional immune system to leave open the possibility of inducing an anti-tumor immune response. Also, previous studies have shown that cells transduced by adenoviral vectors *in vivo* can be cleared by the immune system (Hartman, Appledorn, and Amalfitano, 2008; Muruve, 2004; Yang et al., 1994). As well, the MTHJ cell line is derived from tumors of a well-characterized model for human breast cancer (Lin et al., 2003).

While others have used a AdCMVTK vector in combination with GCV to regress tumors in preclinical models (Esandi et al., 1997), including using a T47D breast tumor xenograft model (Anderson et al., 1999), to date no one has shown regression of MTHJ tumors mediated by TK and GCV. Tumor regression studies reported here show that neither AdMPE$_2$TK nor AdCMVTK induced regression of MTHJ tumors following GCV treatment. Implanted tumors did not all grow at the same rate, thus tumor sizes among mice were variable and larger than desired for initial virus injections. We propose that no tumor regression was observed because of low virus transduction of these large tumors, leading to insufficient HSV-TK expression to induce a therapeutic effect. Despite the lack of tumor regression, however, we did observe AdTK/GCV-induced toxicity in a number of mice, specifically those injected with AdCMVTK$_{hi}$.

To determine potential sites of HSV-TK expression in the MTHJ tumor model *in vivo*, liver toxicity and immunohistochemistry studies were carried out. Following

intratumoral administration of Ad vectors into mice, we expected transgene levels to be highest in the tumor and liver (Bramson et al., 1996). The liver is a primary site of Ad infection due to the high transduction efficiency in hepatocytes and Kuppfer cells (Li et al., 1993). Despite the lack of tumor regression in AdCMVTK treated mice, mice injected with three doses of 4 x 10^8 pfu of this vector displayed obvious liver toxicity. Liver toxicity can be measured by serum analysis of elevated levels of liver enzymes such as AST and ALT (Brunetti-Pierri et al., 2004). At day 11 (four days after third dose of vector), these levels were 8 to 21 times higher than pre-treatment levels. Since control vector injection did not induce elevated liver enzyme levels, we suggest that the observed $AdCMVTK_{hi}$ toxicity was caused by HSV-TK expression and subsequent GCV phosphorylation in liver cells. This suggestion was strengthened by pathological examination of liver sections.

$AdMPE_2TK$ and $AdCMVTK_{lo}$ injections did not cause a rise in liver enzyme levels, likely due to the low amount of HSV-TK expressed in the liver. In order to determine whether this low expression was a result of MPE_2 tumor selectivity, immunohistochemistry was performed on tumor and liver sections from vector-injected mice.

HSV-TK immunohistochemistry results correlate with the toxicity data. Tumor sections from mice injected with Ad vectors revealed large regions of positive staining with slightly less overall HSV-TK expression in $AdMPE_2TK$- and $AdCMVTK_{lo}$-injected mice than $AdCMVTK_{hi}$-injected mice. Liver sections from the same mice showed punctate staining throughout in both $AdCMVTK_{hi}$ and

$AdCMVTK_{lo}$-injected mice but no HSV-TK expression seen in sections from mice injected with $AdMPE_2TK$. These data convey the breast cancer- selectivity of the $AdMPE_2TK$ vector.

AdCMVTK has long been known to induce hepatic cell death in combination with GCV treatment (Brand et al., 1997). Other promoters used for tumor selective expression of HSV-TK have shown much lower liver toxicity than the CMV promoter, highlighting the potential for cancer gene therapy. On example includes the hTERT promoter, which has shown tumor selectivity in Ad vectors in combination with HSV-TK/GCV but insufficient anti-tumor activity even *in vitro* (Yu et al., 2011). Ad vectors carrying the hFAS promoter reveal anti-tumor effects both *in vitro* and *in vivo* (Yan et al., 2007), however the investigators have not yet looked at liver toxicitiy from this vector, nor compared it with any other AdHSV-TK vector. Studies involving AdHSV-TK vectors controlled by the MUC1 promoter showed promise for regression of MCF-7 tumors in nude mice (Chen et al., 1995), however further research involving this promoter has not focused on HSV-TK/GCV gene therapy. The $AdMPE_2TK$ vector investigated here compares favorably to other breast cancer selective Ad vectors due to its high selectivity *in vitro* and low liver toxicity *in vivo*.

Tumor-targeted adenoviral vectors hold great potential for cancer-selective expression of therapeutic genes. Many research laboratories are currently investigating methods to effectively enhance the therapeutic effect while increasing safety to non-cancerous cells. Here we report the usefulness of the MPE_2 promoter for targeting expression of HSV-TK to breast cancer cells.

The *in vitro* selectivity and reduced *in vivo* toxicity of the AdMPE_2TK vector suggest a potential use of a MPE_2 promoter-driven HSV-TK vector for use in cancer patients. It has been shown that phosphorylated GCV can damage both nuclear and mitochondrial DNA (Herraiz et al., 2003; van der Eb et al., 2003), thus HSV-TK/GCV gene therapy may cause toxicity in nondividing cells or cells at low proliferation rates. These findings emphasize the importance of inducing tumor selective expression of HSV-TK to ensure protection of nontumor cells. More work must still be done to enhance the HSV-TK expression levels from AdMPE_2TK within tumors to induce a more potent anti-cancer effect. Possibilities include using an oncolytic adenoviral vector that has the ability to replicate within tumor cells, thereby amplifying its therapeutic effect. As well, modifications to the adenoviral capsid to bind other cell surface receptors may increase the infectivity of an Ad vector in breast cancer cells. If HSV-TK expression can be enhanced to induce a strong therapeutic effect, it may be valuable to combine the transcriptional targeting described here with other types of cancer-specific targeting, such as transductional targeting through capsid modifications (Li et al., 2009) and translational targeting through strong 5' untranslated regions (Chu et al., 2007; Stoff-Khalili et al., 2008). Likely, some combination of many different types of targeting methods in the same vector will lead to optimization of a tumor-specific Ad vector for clinical use in cancer gene therapy.

2.5. REFERENCES

Addison, C. L., Hitt, M., Kunsken, D., and Graham, F. L. (1997). Comparison of the human versus murine cytomegalovirus immediate early gene promoters for transgene expression by adenoviral vectors. *J Gen Virol* **78 (Pt 7),** 1653-61.

Anderson, L. M., Swaminathan, S., Zackon, I., Tajuddin, A. K., Thimmapaya, B., and Weitzman, S. A. (1999). Adenovirus-mediated tissue-targeted expression of the HSVtk gene for the treatment of breast cancer. *Gene Ther* **6**(5)**,** 854-64.

Baker (1995). FDA approves oral ganciclovir as first drug to prevent CMV disease. Food and Drug Administration. *Beta* **8**.

Bett, A. J., Haddara, W., Prevec, L., and Graham, F. L. (1994). An efficient and flexible system for construction of adenovirus vectors with insertions or deletions in early regions 1 and 3. *Proc Natl Acad Sci U S A* **91**(19)**,** 8802-6.

Bramson, J. L., Hitt, M., Addison, C. L., Muller, W. J., Gauldie, J., and Graham, F. L. (1996). Direct intratumoral injection of an adenovirus expressing interleukin-12 induces regression and long-lasting immunity that is associated with highly localized expression of interleukin-12. *Hum Gene Ther* **7**(16)**,** 1995-2002.

Brand, K., Arnold, W., Bartels, T., Lieber, A., Kay, M. A., Strauss, M., and Dorken, B. (1997). Liver-associated toxicity of the HSV-tk/GCV approach and adenoviral vectors. *Cancer Gene Ther* **4**(1)**,** 9-16.

Brunetti-Pierri, N., Palmer, D. J., Beaudet, A. L., Carey, K. D., Finegold, M., and Ng, P. (2004). Acute toxicity after high-dose systemic injection of helper-dependent adenoviral vectors into nonhuman primates. *Hum Gene Ther* **15**(1)**,** 35-46.

Canadian Cancer Society (2011). Canadian Cancer Statistics 2011. CancerStats. 2011.

Casado, E., Gomez-Navarro, J., Yamamoto, M., Adachi, Y., Coolidge, C. J., Arafat, W. O., Barker, S. D., Wang, M. H., Mahasreshti, P. J., Hemminki, A., Gonzalez-Baron, M., Barnes, M. N., Pustilnik, T. B., Siegal, G. P., Alvarez, R. D., and Curiel, D. T. (2001). Strategies to accomplish targeted expression of transgenes in ovarian cancer for molecular therapeutic applications. *Clin Cancer Res* **7**(8)**,** 2496-504.

Chen, L., Chen, D., Manome, Y., Dong, Y., Fine, H. A., and Kufe, D. W. (1995). Breast cancer selective gene expression and therapy mediated by recombinant adenoviruses containing the DF3/MUC1 promoter. *J Clin Invest* **96**(6)**,** 2775-82.

Chu, Q. D., Sun, L., Li, J., Byrnes, K., Chervenak, D., DeBenedetti, A., Mathis, J. M., and Li, B. D. (2007). Rat adenocarcinoma cell line infected with an adenovirus carrying a novel herpes-simplex virus-thymidine kinase suicide gene construct dies by apoptosis upon treatment with ganciclovir. *J Surg Res* **143**(1)**,** 189-94.

Cole, C., Qiao, J., Kottke, T., Diaz, R. M., Ahmed, A., Sanchez-Perez, L., Brunn, G., Thompson, J., Chester, J., and Vile, R. G. (2005). Tumor-targeted, systemic delivery of therapeutic viral vectors using hitchhiking on antigen-specific T cells. *Nat Med* **11**(10)**,** 1073-81.

Culver, K. W., Ram, Z., Wallbridge, S., Ishii, H., Oldfield, E. H., and Blaese, R. M. (1992). In vivo gene transfer with retroviral vector-producer cells for treatment of experimental brain tumors. *Science* **256**(5063)**,** 1550-2.

Czernin, J., Benz, M. R., and Allen-Auerbach, M. S. Breast cancer. *Methods Mol Biol* **727,** 141-70.

Duigou, G. J., and Young, C. S. (2005). Replication-competent adenovirus formation in 293 cells: the recombination-based rate is influenced by structure and location of the transgene cassette and not increased by overproduction of HsRad51, Rad51-interacting, or E2F family proteins. *J Virol* **79**(9)**,** 5437-44.

Esandi, M. C., van Someren, G. D., Vincent, A. J., van Bekkum, D. W., Valerio, D., Bout, A., and Noteboom, J. L. (1997). Gene therapy of experimental malignant mesothelioma using adenovirus vectors encoding the HSVtk gene. *Gene Ther* **4**(4)**,** 280-7.

Graham, F. L., Smiley, J., Russell, W. C., and Nairn, R. (1977). Characteristics of a human cell line transformed by DNA from human adenovirus type 5. *J Gen Virol* **36**(1)**,** 59-74.

Hartman, Z. C., Appledorn, D. M., and Amalfitano, A. (2008). Adenovirus vector induced innate immune responses: impact upon efficacy and toxicity in gene therapy and vaccine applications. *Virus Res* **132**(1-2)**,** 1-14.

Hehir, K. M., Armentano, D., Cardoza, L. M., Choquette, T. L., Berthelette, P. B., White, G. A., Couture, L. A., Everton, M. B., Keegan, J., Martin, J. M., Pratt, D. A., Smith, M. P., Smith, A. E., and Wadsworth, S. C. (1996). Molecular characterization of replication-competent variants of adenovirus vectors and genome modifications to prevent their occurrence. *J Virol* **70**(12)**,** 8459-67.

Herraiz, M., Beraza, N., Solano, A., Sangro, B., Montoya, J., Qian, C., Prieto, J., and Bustos, M. (2003). Liver failure caused by herpes simplex virus thymidine kinase plus ganciclovir therapy is associated with mitochondrial dysfunction and mitochondrial DNA depletion. *Hum Gene Ther* **14**(5)**,** 463-72.

Hitt, M., Ng, P., and Graham, F.L. (2006). Construction and propagation of human adenovirus vectors. Third ed. *In* "Cell Biology: A Laboratory Handbook" (J. E. Celis, Ed.), Vol. 1, pp. 465-443. Academic Press, San Diego, CA.

Hsieh, C. H., Liu, R. S., Wang, H. E., Hwang, J. J., Deng, W. P., Chen, J. C., and Chen, F. D. (2006). In vitro evaluation of herpes simplex virus type 1 thymidine kinase reporter system in dynamic studies of transcriptional gene regulation. *Nucl Med Biol* **33**(5)**,** 653-60.

Huang, T. G., Savontaus, M. J., Shinozaki, K., Sauter, B. V., and Woo, S. L. (2003). Telomerase-dependent oncolytic adenovirus for cancer treatment. *Gene Ther* **10**(15)**,** 1241-7.

Hummel, J. L., Safroneeva, E., and Mossman, K. L. (2005). The role of ICP0-Null HSV-1 and interferon signaling defects in the effective treatment of breast adenocarcinoma. *Mol Ther* **12**(6)**,** 1101-10.

Lanson, N. A., Jr., Friedlander, P. L., Schwarzenberger, P., Kolls, J. K., and Wang, G. (2003). Replication of an adenoviral vector controlled by the human telomerase reverse transcriptase promoter causes tumor-selective tumor lysis. *Cancer Res* **63**(22)**,** 7936-41.

Li, H. J., Everts, M., Yamamoto, M., Curiel, D. T., and Herschman, H. R. (2009). Combined transductional untargeting/retargeting and transcriptional restriction enhances adenovirus gene targeting and therapy for hepatic colorectal cancer tumors. *Cancer Res* **69**(2)**,** 554-64.

Li, Q., Kay, M. A., Finegold, M., Stratford-Perricaudet, L. D., and Woo, S. L. (1993). Assessment of recombinant adenoviral vectors for hepatic gene therapy. *Hum Gene Ther* **4**(4)**,** 403-9.

Lin, E. Y., Jones, J. G., Li, P., Zhu, L., Whitney, K. D., Muller, W. J., and Pollard, J. W. (2003). Progression to malignancy in the polyoma middle T oncoprotein mouse breast cancer model provides a reliable model for human diseases. *Am J Pathol* **163**(5)**,** 2113-26.

Lochmuller, H., Jani, A., Huard, J., Prescott, S., Simoneau, M., Massie, B., Karpati, G., and Acsadi, G. (1994). Emergence of early region 1-containing replication-competent adenovirus in stocks of replication-defective adenovirus recombinants (delta E1 + delta E3) during multiple passages in 293 cells. *Hum Gene Ther* **5**(12)**,** 1485-91.

Majumdar, A. S., Hughes, D. E., Lichtsteiner, S. P., Wang, Z., Lebkowski, J. S., and Vasserot, A. P. (2001). The telomerase reverse transcriptase promoter drives efficacious tumor suicide gene therapy while preventing hepatotoxicity encountered with constitutive promoters. *Gene Ther* **8**(7)**,** 568-78.

Marella, N. V., Malyavantham, K. S., Wang, J., Matsui, S., Liang, P., and Berezney, R. (2009). Cytogenetic and cDNA microarray expression analysis of MCF10 human breast cancer progression cell lines. *Cancer Res* **69**(14)**,** 5946-53.

Matthews, T., and Boehme, R. (1988). Antiviral activity and mechanism of action of ganciclovir. *Rev Infect Dis* **10 Suppl 3,** S490-4.

McGavin, J. K., and Goa, K. L. (2001). Ganciclovir: an update of its use in the prevention of cytomegalovirus infection and disease in transplant recipients. *Drugs* **61**(8)**,** 1153-83.

Mita, R., Coles, J. E., Glubrecht, D. D., Sung, R., Sun, X., and Godbout, R. (2007). B-FABP-expressing radial glial cells: the malignant glioma cell of origin? *Neoplasia* **9**(9)**,** 734-44.

Moolten, F. L., and Wells, J. M. (1990). Curability of tumors bearing herpes thymidine kinase genes transferred by retroviral vectors. *J Natl Cancer Inst* **82**(4)**,** 297-300.

Morris, J. C., Touraine, R., Wildner, O., and Blaese, R. M. (1999). Suicide genes: Gene therapy applications using enzyme/prodrug strategies. *In* "The Development of Human Gene Therapy" (T. Friedmann, Ed.), pp. 477-526. Cold Spring Harbor Laboratory Press, Cold Spring Harbor, NY.

Muruve, D. A. (2004). The innate immune response to adenovirus vectors. *Hum Gene Ther* **15**(12)**,** 1157-66.

Osaki, T., Tanio, Y., Tachibana, I., Hosoe, S., Kumagai, T., Kawase, I., Oikawa, S., and Kishimoto, T. (1994). Gene therapy for carcinoembryonic antigen-producing human lung cancer cells by cell type-specific expression of herpes simplex virus thymidine kinase gene. *Cancer Res* **54**(20)**,** 5258-61.

Peter, I., Graf, C., Dummer, R., Schaffner, W., Greber, U. F., and Hemmi, S. (2003). A novel attenuated replication-competent adenovirus for melanoma therapy. *Gene Ther* **10**(7)**,** 530-9.

Reardon, J. E. (1989). Herpes simplex virus type 1 and human DNA polymerase interactions with 2'-deoxyguanosine 5'-triphosphate analogues. Kinetics of incorporation into DNA and induction of inhibition. *J Biol Chem* **264**(32)**,** 19039-44.

Seitz, S., Wassmuth, P., Fischer, J., Nothnagel, A., Jandrig, B., Schlag, P. M., and Scherneck, S. (2002). Mutation analysis and mRNA expression of trail-receptors in human breast cancer. *Int J Cancer* **102**(2)**,** 117-28.

Shi, C. X., Graham, F. L., and Hitt, M. M. (2006). A convenient plasmid system for construction of helper-dependent adenoviral vectors and its application for analysis of the breast-cancer-specific mammaglobin promoter. *J Gene Med* **8**(4)**,** 442-51.

Shi, C. X., Long, M. A., Liu, L., Graham, F. L., Gauldie, J., and Hitt, M. M. (2004). The human SCGB2A2 (mammaglobin-1) promoter/enhancer in a helper-dependent adenovirus vector directs high levels of transgene expression in mammary carcinoma cells but not in normal nonmammary cells. *Mol Ther* **10**(4)**,** 758-67.

Sobol, R., Shawler, D., Dorigo, O., Gold, D., Royston, I., Fakhrai, H. (1996). Immunogene therapy of cancer. *In* "The Internet book of gene therapy" (R. Sobol, Scanlon, KJ, Ed.). Prentice Hall Health, Stamford, Conn.

Soule, H. D., Maloney, T. M., Wolman, S. R., Peterson, W. D., Jr., Brenz, R., McGrath, C. M., Russo, J., Pauley, R. J., Jones, R. F., and Brooks, S. C. (1990). Isolation and characterization of a spontaneously immortalized human breast epithelial cell line, MCF-10. *Cancer Res* **50**(18)**,** 6075-86.

Stoff-Khalili, M. A., Rivera, A. A., Nedeljkovic-Kurepa, A., DeBenedetti, A., Li, X. L., Odaka, Y., Podduturi, J., Sibley, D. A., Siegal, G. P., Stoff, A., Young, S., Zhu, Z. B., Curiel, D. T., and Mathis, J. M. (2008). Cancer-specific targeting of a conditionally replicative adenovirus using mRNA translational control. *Breast Cancer Res Treat* **108**(1)**,** 43-55.

Thust, R., Schacke, M., and Wutzler, P. (1996). Cytogenetic genotoxicity of antiherpes virostatics in Chinese hamster V79-E cells. I. Purine nucleoside analogues. *Antiviral Res* **31**(1-2)**,** 105-13.

Tomayko, M. M., and Reynolds, C. P. (1989). Determination of subcutaneous tumor size in athymic (nude) mice. *Cancer Chemother Pharmacol* **24**(3)**,** 148-54.

van der Eb, M. M., Geutskens, S. B., van Kuilenburg, A. B., van Lenthe, H., van Dierendonck, J. H., Kuppen, P. J., van Ormondt, H., van de Velde, C. J., Wanders, R. J., van Gennip, A. H., and Hoeben, R. C. (2003). Ganciclovir nucleotides accumulate in mitochondria of rat liver cells expressing the herpes simplex virus thymidine kinase gene. *J Gene Med* **5**(12)**,** 1018-27.

Watson, M. A., and Fleming, T. P. (1996). Mammaglobin, a mammary-specific member of the uteroglobin gene family, is overexpressed in human breast cancer. *Cancer Res* **56**(4)**,** 860-5.

WHO (2010). Breast Cancer: prevention and control.

Wiley, J. (2012). Vectors Used in Gene Therapy Clinical Trials. *The Journal of Gene Medicine*.

Yamamoto, M., Alemany, R., Adachi, Y., Grizzle, W. E., and Curiel, D. T. (2001). Characterization of the cyclooxygenase-2 promoter in an adenoviral vector and its application for the mitigation of toxicity in suicide gene therapy of gastrointestinal cancers. *Mol Ther* **3**(3)**,** 385-94.

Yan, C., Wen-Chao, L., Hong-Yan, Q., Rui, Z., Wei-Lin, J., and Hua, H. (2007). A new targeting approach for breast cancer gene therapy using the human fatty acid synthase promoter. *Acta Oncol* **46**(6)**,** 773-81.

Yang, Y., Nunes, F. A., Berencsi, K., Gonczol, E., Engelhardt, J. F., and Wilson, J. M. (1994). Inactivation of E2a in recombinant adenoviruses improves the prospect for gene therapy in cystic fibrosis. *Nat Genet* **7**(3)**,** 362-9.

Yu, B., Zhang, Y., Zhan, Y., Zha, X., Wu, Y., Zhang, X., Dong, Q., Kong, W., and Yu, X. (2011). Co-expression of herpes simplex virus thymidine kinase and Escherichia coli nitroreductase by an hTERT-driven adenovirus vector in breast cancer cells results in additive anti-tumor effects. *Oncol Rep* **26**(1)**,** 255-64.

CHAPTER 3:

Analysis of PET Imaging for Monitoring Tumor Growth and Virus Dissemination in Mouse Breast Cancer Models

Portions of this chapter have been published:

DeSilva A, Wuest M, Wang M, Hummel J, Mossman K, Wuest F, Hitt M. 2012. Comparative functional evaluation of immunocompetent mouse breast cancer models established from PyMT-tumors using small animal PET with [^{18}F]FDG and [^{18}F]FLT. Am J Nucl Med Mol Imaging 2(1):88-98.

A. DeSilva performed all cell culture & in vitro *and* in vivo *virus treatments*
J. Hummel and K. Mossman provided the MTHJ cells used in this chapter
M. Wang performed all in vitro *radiotracer cell uptake studies*
M. Wuest performed radiotracer injection, PET imaging, figure preparation & technical expertise regarding PET
F. Wuest provided the [^{18}F]FHBG radiotracer & technical expertise regarding PET
M. Hitt provided technical expertise regarding in vitro *and* in vivo *virus treatments*

3.1. INTRODUCTION

For patients with breast cancer (BrCa), early detection and accurate discovery of recurrence after therapy is important to aid in treatment outcomes and decrease mortality rates (Murakami et al., 2011). Over the last decade achievements in early diagnosis and novel treatment strategies have improved the clinical outcome. Several imaging methods are currently used for early detection, including morphological mapping such as X-ray mammography, computed tomography (CT), magnetic resonance imaging (MRI) and ultrasound. Functional imaging of BrCa, which can detect changes in cell functions such as metabolism, is performed with nuclear molecular imaging techniques like single photon emission computed tomography (SPECT) and positron emission tomography (PET) (Mankoff, 2008; Tafreshi et al., 2010).

PET is a powerful tool for molecular imaging of cancer *in vivo*, allowing for visualization and analysis of molecular characteristics of the intracellular and extracellular components of both tumor and normal tissue (Tafreshi et al., 2010). PET allows assessment of changes in the metabolic rate of tumors at high sensitivity. In the clinic, enhanced glucose uptake and high aerobic glycolysis in tumor cells (Warburg effect) is used for the detection of primary tumors and metastases, as well as for monitoring tumor metabolism in response to therapy using 2-deoxy-2-[^{18}F]fluoro-D-glucose ([^{18}F]FDG) (Lee, Rosen, and Mankoff, 2009a; Lee, Rosen, and Mankoff, 2009b). [^{18}F]FDG enters the cells through specific glucose transporters, mainly GLUT1, which exhibit altered expression levels during malignant transformation (Flier et al., 1987). [^{18}F]FDG is subsequently phosphorylated by hexokinase, which leads to intracellular trapping (Macheda, Rogers, and Best, 2005). However, [^{18}F]FDG also accumulates in

non-malignant tissues like inflammatory lesions which can lead to false positive results. Moreover, the poor spatial resolution of PET also limits the detection of small tumors (Escalona et al.). Besides [^{18}F]FDG, alternative PET radiotracers targeting different receptors, transporters or enzymes overexpressed in breast cancer cells have been developed (Fleming et al.). A prominent example includes 3'-deoxy-3'-[^{18}F]fluorothymidine ([^{18}F]FLT) as a marker for proliferative activity (Buck et al., 2004; Sundararajan et al., 2007). [^{18}F]FLT is an analog of thymidine, which is phosphorylated by thymidine kinase 1 (TK 1) within the cytosol, but not incorporated into DNA. TK 1 is a cell cycle regulated enzyme with particularly high expression levels during S phase. In many malignant lesions, TK 1 is constitutively up-regulated. [^{18}F]FLT is a selective substrate for TK 1. Intracellular trapping of [^{18}F]FLT is governed by the formation of mono-, di- and triphosphate nucleotides. Phosphorylation of [^{18}F]FLT through TK 1 is dominant to competitive de-phosphorylation processes and subsequent efflux from the cell (Reske and Deisenhofer, 2006). Several clinical studies have reported the usefulness of [^{18}F]FDG-PET and [^{18}F]FLT-PET for monitoring efficacy of therapeutic interventions in breast cancer (Dawson and Sharpe, 2006; Dehdashti et al., 2009; Kurdziel et al., 2007; Pio et al., 2006; Schelling et al., 2000). While gene therapy continues to be studied as a treatment for cancer, it is important to be able to measure the effect of these new therapeutics. In a clinical setting it is essential to define the biodistribution of gene expression within a patient without performing repetitive, invasive procedures (Penuelas et al., 2005). PET imaging allows for non-invasive detection of changes in the metabolic or proliferation rate of a tumor and can provide a quantitative assessment of therapeutic responses that may precede

morphologic changes (Cochet et al., 2011). PET can also provide a direct measurement of *in vivo* gene expression location, which can aid in the progress of molecular medicine and gene therapy (Larson, Tjuvajev, and Blasberg, 1997; Nichol and Kim, 2001; Penuelas et al., 2004). Considering the high incidence and mortality rate for BrCa (Czernin, Benz, and Allen-Auerbach), improvements to cancer detection and treatment imaging methods may allow for a better understanding of patient tumors and lead to enhanced therapies.

Gene therapy provides tremendous opportunities for the parallel introduction of vectors enabling PET imaging. The specific introduction of herpes simplex virus thymidine kinase (HSV-TK) into tumor cells can allow for selective imaging of transduced cells based on the capacity of HSV-TK to phosphorylate certain PET tracers. [^{18}F]FLT can be phosphorylated by either endogenous mammalian TK-1 or HSV-TK, which leads to intracellular trapping and accumulation (Rasey et al., 2002). The exogenous expression of HSV-TK may enhance the accumulation of [^{18}F]FLT due to a higher enzyme concentration increasing total phosphorylation. 9-(4-[^{18}F]fluoro-3-hydroxymethylbutyl)-guanine ([^{18}F]FHBG) is a PET tracer that is poorly phosphorylated by endogenous mammalian thymidine kinase, which leads to selective accumulation in cells expressing HSV-TK (Alauddin et al., 2001). Just as targeted adenoviral vectors are commonly used for cancer-specific delivery of HSV-TK for therapeutic purposes, their cancer-specific HSV-TK expression may be visualized by PET imaging.

Development of novel strategies in cancer therapy requires extensive pre-clinical experiments before translation into clinical application with cancer patients. For the preclinical development of novel anti-cancer therapies the selection, establishment and

characterization of a suitable animal model represents a critical key step (Kim, O'Hare, and Stein, 2004).

The mouse mammary adenocarcinoma cell line MTHJ represents can be used for a specific immunocompetent murine breast cancer model. This cell line was derived by *in vitro* serial passaging of tumor cells explanted from a transgenic mouse carrying the polyoma virus middle T antigen (PyMT) regulated by the mouse mammary tumor virus (MMTV) promoter. These transgenic mice (FVB/N-Tg(MMTV-PyVT)634Mul/J, The Jackson Laboratory) spontaneously develop mammary epithelial adenocarcinoma (Guy, Cardiff, and Muller, 1992). At first, pre-malignant multiple mammary adenocarcinomas develop which are generally fibrotic with dense connective tissue separating individual tumor cell nests. Within a couple weeks palpable mammary tumors involving the entire mammary fat pad are detectable, gradually increasing in cellular proliferation but with no evidence of invasion. Soon these tumors become malignant and invasive through the surrounding stroma. By 10 weeks of age, 50% of virgin female PyMT transgenic mice progress to advanced carcinoma with tumors comprising of solid sheets of epithelial cells and displaying a marked loss of stroma often leading to lung metastases by week 12 (Lin et al., 2003; Qiu et al., 2004; Wang et al., 2009). These features reveal how tumor development in the PyMT tumor closely resembles and represents a well-characterized model for the development and progresssion of human BrCa. The transgenic model covers various stages of tumorigenesis and progression ranging from premalignancy to all neoplastic stages in the primary tumor, including the malignant transition producing a high frequency of distant metastasis, which reflect the development of human breast cancer (Lin et al., 2003). In addition to these

morphological similarities, expression profile of several biomarkers (e.g. loss of estrogen and progesterone receptors during progression into the malignant stage of PyMT-induced tumors) is comparable to that of human BrCa cells (Lin et al., 2003). MTHJ cells derived from a PyMT transgenic mouse breast tumor have been shown to also be tumorigenic, and have been used to analyze anti-tumor immunity induced by oncolytic herpes simplex viruses (Hummel, Safroneeva, and Mossman, 2005). A goal of the present study was the functional characterization of the immunocompetent mouse tumor model MTHJ utilizing PET radiotracers [^{18}F]FDG and [^{18}F]FLT in direct comparison with subcutaneous tumors developed from explants of primary PyMT tumors. The systematic evaluation of both tumor models *in vitro* and *in vivo* by means of PET should provide insights on metabolic and proliferative activity in established vs. primary PyMT tumor cells.

In addition, we aim to illustrate the BrCa-specific expression of the adenoviral (Ad) vector AdMPE_2TK, which is transcriptionally targeted to express HSV-TK controlled by the MPE_2 promoter. We have previously illustrated the ability of this vector to target HSV-TK to breast cancer cells *in vitro* (Chapter 2). Furthermore, immunohistochemistry experiments have shown that AdMPE_2TK and the non-targeted AdCMVTK vector can express HSV-TK *in vivo* in an immunocompetent mouse model bearing subcutaneous MTHJ mammary tumors. Here we investigate if HSV-TK expression levels from AdMPE_2TK are sufficient to enhance [^{18}F]FLT and [^{18}F]FHBG accumulation and visualization in breast cancer cells using PET.

3.2. MATERIALS AND METHODS

3.2.1. Chemicals and Radiotracers

All chemicals used for *in vitro* cell uptake and solutions for the preparation for the injections for the *in vivo* experiments were purchased from Fisher Scientific or Sigma Aldrich. The PET radiotracers [^{18}F]FDG, [^{18}F]FLT and [^{18}F]FHBG were prepared at the Edmonton PET Center of the Cross Cancer Institute. [^{18}F]FDG was synthesized according to Hamacher et al. using a TracerLab MX automated synthesis unit from G.E. Healthcare (Hamacher, Coenen, and Stocklin, 1986; Wilson et al., 2008). Radiosynthesis of [^{18}F]FLT was carried out according to the procedure reported by Machulla (Machulla, 2000). [^{18}F]FHBG was manually prepared by Dr. Frank Wuest according to previously published procedures (Alauddin and Conti, 1998).

3.2.2. Adenoviruses

Both adenoviral vectors (AdCMVTK and AdMPE$_2$TK) were generated as described in Chapter 2 Materials & Methods.

3.2.3. Cell Lines

16-20 week old FVB/N-Tg(MMTV-PyVT)634Mul/J transgenic mice (Guy, Cardiff, and Muller, 1992)bearing spontaneous adenocarcinomas of the mammary epithelium were sacrificed for isolation of primary tumor cells (PyMT) as described (Addison et al., 1995). Tumors from these mice were minced and incubated at 37ºC with gentle stirring in a collagenase/dispase solution, after which large clumps of cells were allowed to settle. The supernatant was then centrifuged and the resulting pellets were resuspended in freeze medium and stored in liquid nitrogen until use. Aliquots of frozen cells were thawed, resuspended in minimal essential medium supplemented with

penicillin, streptomycin, L-glutamine, and fetal bovine serum (FBS), plated in 150 mm tissue culture plates and incubated overnight. Adherent tumor cells were rinsed, supplemented with fresh medium, and incubated for an additional 24 to 72 hours before use in *in vitro* or *in vivo* experiments.

The stable MTHJ cell line was established by continuous culture of a PyMT tumor explant. At early passages, fibroblasts were removed by light trypsinization (Hummel, Safroneeva, and Mossman, 2005). PyMT and MTHJ cells were maintained in high glucose Dulbecco's Modified Eagle Medium (DMEM) supplemented with 10% (FBS), 100 U/mL penicillin, 100 µg/mL streptomycin, 250 ng/mL fungizone and 2 mM L-glutamine. All media were purchased from Sigma-Aldrich Chemicals (USA) and all supplements were purchased from Gibco® (USA).

3.2.4. Tumor growth curves

All animal experiments were carried out in accordance with guidelines of the Canadian Council on Animal Care (CCAC) and were approved by the local animal care committee of the Cross Cancer Institute. Six week old female FVB mice (Charles River) were injected subcutaneously in both flanks with either explanted primary PyMT-expressing murine breast cancer cells ($5x10^5$ or $1x10^6$ cells/flank) or cultured MTHJ cells ($5x10^5$, $2.5x10^6$ or $5x10^6$ cells/flank) and monitored for tumor formation. Animals were housed in sterile surroundings with standardized light/dark cycle and access to food and water *ad libitum*. Tumor growth was measured in three dimensions using digital calipers and the size calculated using the formula for the volume of a typical ellipsoid: $T_{vol} = \pi/6$ x width x length x depth (Tomayko and Reynolds, 1989). Tumor-bearing mice were euthanized at the study end point or sooner if tumor burden endpoint was reached

(defined as tumor volume ≥ 10% of mouse body weight). No spontaneous regression was observed using either the primary cell- or established cell line-based PyMT tumor model.

3.2.5. In vitro *[^{18}F]FDG and [^{18}F]FLT Cell Uptake*

Primary PyMT cells and passaged MTHJ cells were grown to ~80 - 90% confluency in 12-well tissue culture plates in a CO_2 incubator at 37°C, in high glucose DMEM supplemented with FBS, penicillin, streptomycin, fungizone, and L-glutamine as described above, with media renewal every 2-3 days. One hour prior to the experiment, the medium was removed and the cells were washed twice with phosphate-buffered saline solution (PBS). Next, cells were washed with glucose-free Krebs-Ringer solution (120 mM NaCl, 4 mM KCl, 1.2 mM KH_2PO_4, 2.5 mM $MgSO_4$, 25 mM $NaHCO_3$, 70 μM $CaCl_2$, pH 7.4). 300 μL glucose-free Krebs-Ringer solution, with 0.1-0.5 MBq [^{18}F]FDG or [^{18}F]FLT, was added to each well and the plates were incubated at 37°C for specific periods of time (5, 10, 15, 30, 45, 60, 90 and 120 min). After incubation, cells were rinsed twice with ice-cold Krebs-Ringer solution to stop radiotracer uptake and then immediately lysed using 500 μL of 5% trichloracetic acid. Radioactivity in the cell lysate was counted in a γ-counter (Wallac 1480 Wizard-3, Perkin-Elmer). Protein levels were quantified using the BCA protein assay kit (Pierce) according to the manufacturer's recommendations with bovine serum albumin as the protein standard. Tissue culture was performed by Alan DeSilva while cell uptake experiments were performed by Monica Wang. Cell uptake levels are expressed as a percent of input radioactivity normalized to mg lysate protein.

3.2.6. **In vitro *[^{18}F]FLT and [^{18}F]FHBG Cell Uptake after Virus Infection***

MTHJ cells were passaged and grown to ~90% confluency in 150 mm tissue culture plates in a CO_2 incubator at 37°C, in high glucose DMEM supplemented with FBS, penicillin, streptomycin, fungizone, and L-glutamine as described above. When confluent, cells were infected with AdCMVTK or AdMPE$_2$TK at various multiplicities of infection (MOIs) and incubated at 37ºC overnight. Cells were then rinsed with PBS, trypsinized, seeded into 12-well tissue culture plates with fresh medium, and incubated at 37ºC overnight. One hour prior to the experiment, the medium was removed and the cells were washed twice with PBS. Next, cells were washed with glucose-free Krebs-Ringer solution as described above. 300 μL Krebs-Ringer solution, with or without 5 mM glucose and with 0.1-0.5 MBq [^{18}F]FLT or [^{18}F]FHBG, was added to each well and the plates were incubated at 37°C for the same periods of time as described above. After incubation, cells were rinsed and lysed, then radioactivity from the cell lysate was counted in a γ-counter. Tissue culture and virus infection were performed by Alan DeSilva while cell uptake experiments were performed by Monica Wang. Protein levels were quantified using the BCA protein assay kit (Pierce) according to the manufacturer's recommendations with bovine serum albumin as the protein standard. Cell uptake levels are expressed as a percent of input radioactivity normalized to mg lysate protein.

3.2.7. In vivo *Small Animal PET Experiments with Uninfected Mice*

For the PET imaging studies female FVB mice were injected subcutaneously in the lower left flank and the upper right flank close to the shoulder with either 5 x 10^5 primary PyMT cells or 10^6 MTHJ cells in 0.1 mL PBS per injection site. Tumor-bearing mice were used for the PET experiments after 4-5 weeks of tumor growth reaching ~160 mm^3 in size for primary PyMT and ~70 mm^3 for MTHJ tumors. The mice were fasted for 3-4 hours prior to [^{18}F]FDG imaging experiments. The animals were anesthetised through inhalation of isoflurane in 40% oxygen / 60% nitrogen (gas flow, 1 L/min). Mice were positioned and immobilized in the prone position with their medial axis parallel to the axial axis of the scanner in the centre of the field of view of the microPET® R4 scanner (Siemens Preclinical Solutions). A transmission scan for attenuation correction was not acquired. The amount of radioactivity present in the injection solution in a 0.5 ml syringe was determined with a dose calibrator (Atomlab™ 300, Biodex Medical Systems), which was cross calibrated with the scanner. The emission scan of 60 min PET acquisition was started. After a delay of approximately 15 s, 5-8 MBq of either [^{18}F]FDG or [^{18}F]FLT in 100 - 150 μL saline was injected through a needle catheter into the tail vein. Data acquisition continued for 60 min in 3D list mode. The list mode data were sorted into sinograms with 53 time frames (10 x 2 s, 8 x 5 s, 6 x 10 s, 6 x 20 s, 8 x 60 s, 10 x 120 s, 6 x 300 s). The frames were reconstructed using the Ordered Subset Expectation Maximization applied to the 2D sinograms (2D OSEM) and maximum a posteriori (MAP). The pixel size was 0.085 by 0.085 by 0.12 cm and the resolution in the centre field of view was 1.8 mm. No correction for partial volume effects was performed. The image files were further processed using the ROVER v2.0.30 software (ABX GmbH).

Masks for defining 3D regions of interest (ROI) over tumors and the muscle tissue on the contralateral axilla were set and the ROI's were defined after maximum intensity thresholding. ROI time-activity curves (TACs) were generated for subsequent data analysis. Standardized uptake values (SUV = [activity/mL tissue] / [injected activity/body weight]) were calculated for each ROI.

3.2.8. In vivo *Small Animal PET Experiments with Infected Mice*

[^{18}F]FLT PET imaging of tumor-bearing mice was carried out 2 days post-injection of 4 x 10^8 pfu adenoviral vector, when transgene expression was predicted to be maximal (Kovesdi et al., 1997). [^{18}F]FHBG PET imaging was carried out one day later for the same mouse. *In vivo* small animal PET experiments with infected mice were carried out as described for uninfected mice (Section 3.2.7) except for the following points: 10^6 MTHJ cells were injected into the left and right upper flank close to the shoulder; After 3-5 weeks of tumor growth, the right upper flank tumor was injected with 4 x 10^8 pfu Ad vector in 50 µL PBS through three injection sites while the left upper flank tumor was not injected; Mice injected with Ad vector were housed in isolated sterile surroundings with standardized light/dark cycle and access to food and water *ad libitum*; Mice injected with virus were imaged while contained in a fiberglass holder and attenuated signal correction was performed. Dr. Melinda Wuest carried out the PET imaging and analysis. [^{18}F]FLT measurements were carried out over 60 minutes while [^{18}F]FHBG measurements were carried out over 120 minutes. ROI TACs were generated for subsequent data analysis. Standardized uptake values (SUV = [activity/mL tissue] / [injected activity/body weight]) were calculated for each ROI.

*3.2.9. **Biodistribution studies***

Immediately following the *in vivo* PET experiment, mice were euthanized. Both tumors, livers, blood samples, and hind leg muscle were removed, placed into separate scintillation tubes, and weighed. The amount of [^{18}F] radiotracer accumulation in each tissue was measured using a gamma counter (Wallac 1480 Wizard-3, Perkin Elmer, USA). Percentage of injected dose per gram of tissue (%ID/g) was calculated for each tissue.

*3.2.11. **Data analysis***

All data are expressed as means ± S.E.M. from n investigated animals or cell experiments. All tumor growth curves and TACs were constructed using GraphPad Prism® 4.0 (GraphPad Software). Where applicable, statistical differences were tested by Student's t-test and were considered significant for $p < 0.05$.

3.3. RESULTS

3.3.1. Similar Growth Rates for MTHJ and PyMT Tumors in vivo

In total, 24 female FVB mice were injected in both upper flanks with the indicated concentrations of either primary explants of PyMT-derived tumors, or MTHJ cells passaged 20 to 30 times in culture. After 14 days tumors were palpable and were measured twice weekly until 39 days post-injection (Figure 3.1). All groups showed accelerated tumor growth after 24 days, with comparable growth rates observed for all groups except those injected with the highest dose of primary cells, which had tumors twice the size of other groups at the endpoint of this study.

3.3.2. MTHJ Cells Show Higher Cell Uptake of [^{18}F]FLT in vitro

Radiotracer cell uptake into primary PyMT and cultured MTHJ cells was analyzed over a time period of 120 min. While uptake of [^{18}F]FDG continuously increased, the rate of accumulation of [^{18}F]FLT plateaued after 30 min (Figure 3.2). Uptake of [^{18}F]FDG was comparable for primary PyMT and MTHJ cells within the first 60 min. After 90 and 120 min, primary PyMT cells showed higher [^{18}F]FDG uptake reaching an uptake value of 1321 ± 26 % radioactivity / mg protein (n = 3) vs. 1048 ± 48 % radio-activity / mg protein (n = 3; $p < 0.01$) in MTHJ cells (Figure 3.2A). Conversely, [^{18}F]FLT uptake was significantly lower in primary PyMT cells compared to MTHJ cells at all time points during the study reaching uptake values of 99 ± 8 % radioactivity / mg protein (n = 3) in primary cells and 306 ± 21 % radio-activity / mg protein (n = 3; $p < 0.001$) in MTHJ cells, respectively, after 120 min (Figure 3.2B).

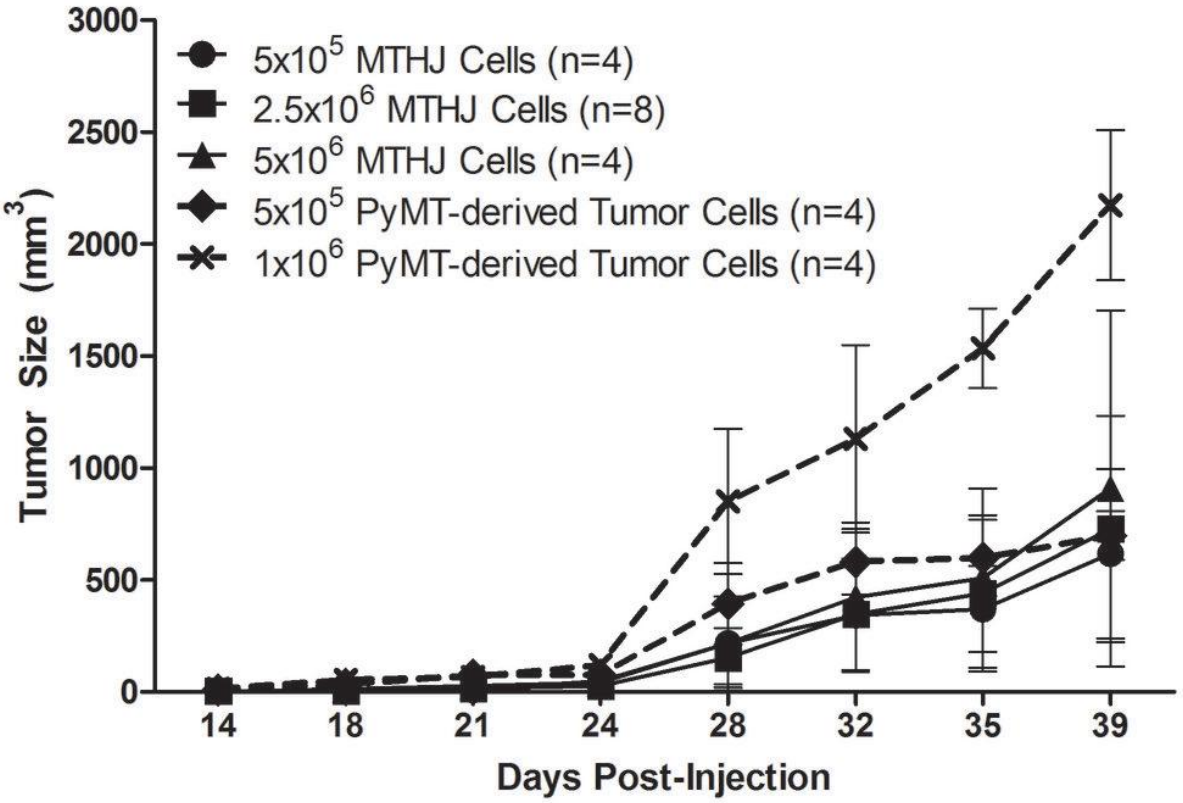

Figure 3.1. MTHJ and PyMT-derived tumor cells grow at comparable rates after *in vivo* subcutaneous injection.

Tumor growth following injection of the indicated numbers of MTHJ or primary PyMT-derived tumor cells subcutaneously into the shoulders of FVB mice (2 sites per mouse). Tumors were measured as described in the Materials and Methods section. The mean tumor volumes ± S.E.M. are shown (at least 4 animals per group).

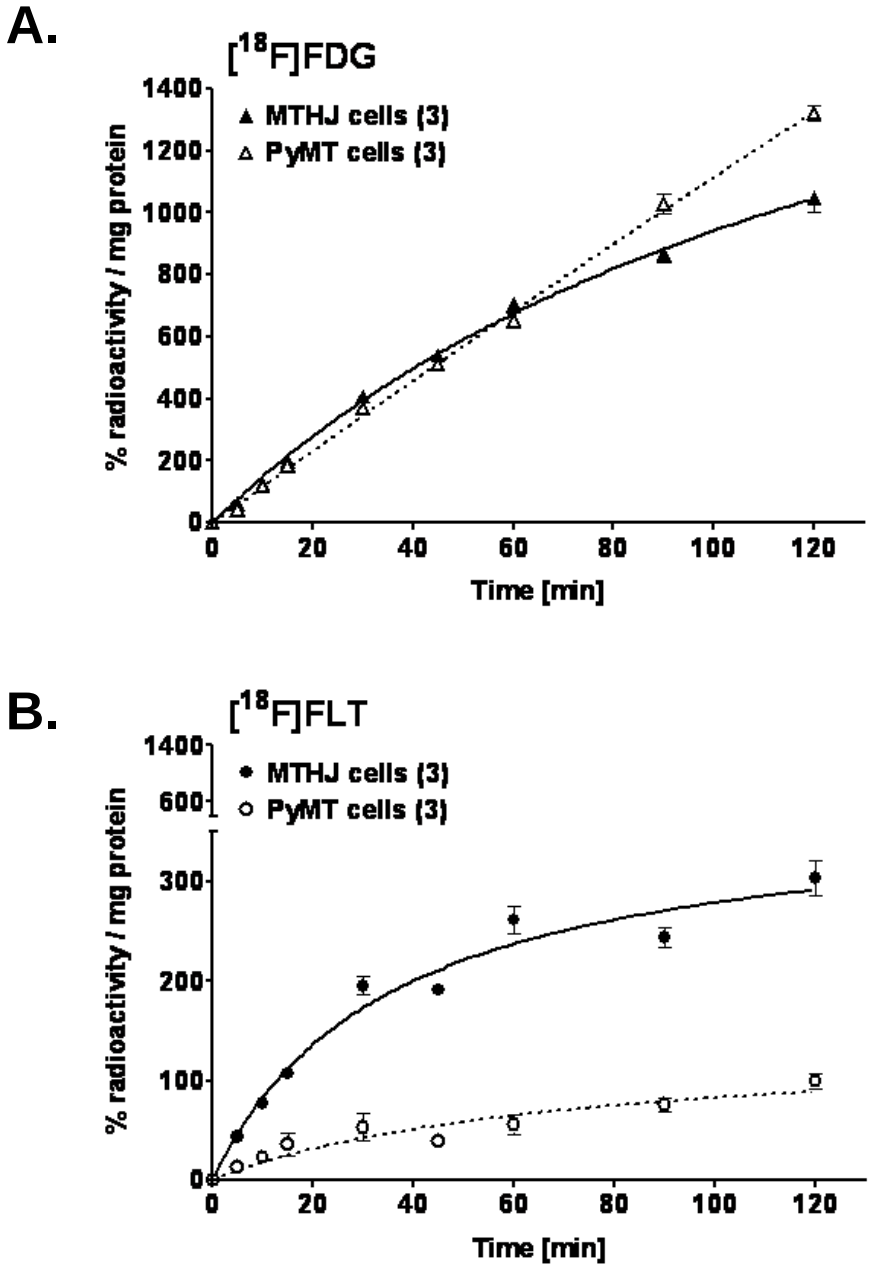

Figure 3.2. MTHJ cells accumulate slightly less [^{18}F]FDG (A) and significantly more [^{18}F]FLT (B) than PyMT cells *in vitro*.

In vitro cell uptake of [^{18}F]FDG (A) and [^{18}F]FLT (B) in cultured MTHJ cells and primary PyMT cells. Data are shown as mean % radioactivity / mg protein ± S.E.M. from triplicate samples in 3 separate experiments.

3.3.3. Tumors from MTHJ and Primary PyMT Cells Show Similar [^{18}F]FDG and [^{18}F]FLT Uptake in vivo

After analysis of radiotracer uptake *in vitro*, [^{18}F]FDG and [^{18}F]FLT uptake was studied in subcutaneously grown tumors from MTHJ and primary PyMT cells *in vivo*. Dynamic small animal PET experiments showed increasing uptake of [^{18}F]FDG in MTHJ tumors over a 60 min time period (Figure 3.3). As demonstrated in representative PET images, tumors started to become visible after 1 min p.i. of [^{18}F]FDG. After 60 min p.i., both tumors (one on the shoulder and one on the lower flank) were clearly visible. Both tumors could be delineated from surrounding tissue. SUV analysis of [^{18}F]FDG uptake in both tumors at 60 min p.i. revealed a SUV of 2.8 ± 0.4 (n = 6 tumors from three animals). Figure 3.4 shows representative small animal PET images of [^{18}F]FLT uptake in MTHJ tumors in the same animal that was used the following day for the [^{18}F]FDG experiment. [^{18}F]FLT was taken up into both tumors, and the tumor became visible at 5 min p.i.. SUV reached a value of 1.1 ± 0.1 (n = 6) at 60 min p.i.. Similar to MTHJ tumor-bearing mice, dynamic small animal PET studies were performed using [^{18}F]FDG and [^{18}F]FLT in mice bearing tumors from primary PyMT cells. Figure 3.5 illustrates small animal PET images after 60 min p.i. of [^{18}F]FLT and 24 h later with [^{18}F]FDG, respectively. SUVs of 2.5 ± 0.1 (n = 8) and 0.9 ± 0.05 (n = 8) were determined for [^{18}F]FDG and [^{18}F]FLT at 60 min p.i. for these PyMT tumors.

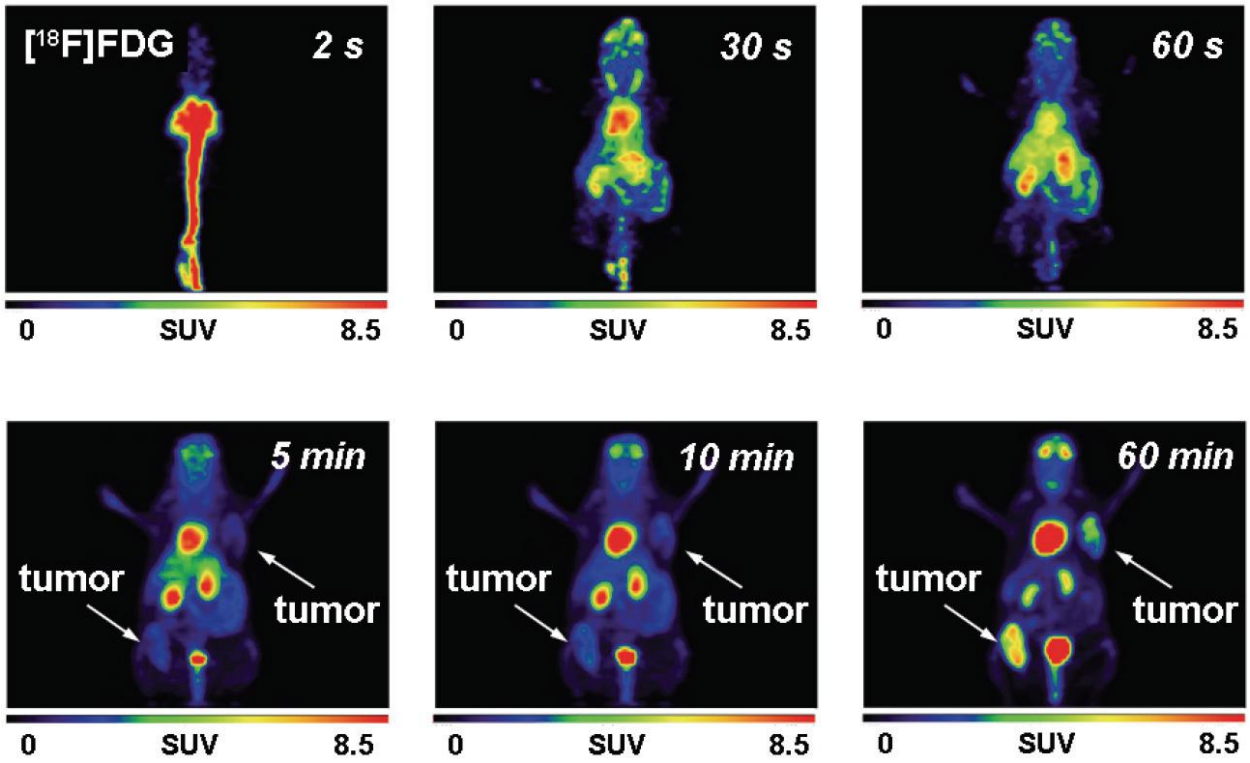

Figure 3.3. [^{18}F]FDG accumulates *in vivo* in MTHJ tumors over 60 minutes.

Representative dynamic small animal PET images (up to 60 min) of [^{18}F]FDG (7.2 MBq injected dose) in a FVB mouse bearing two MTHJ tumors. Images are presented as maximum intensity projections.

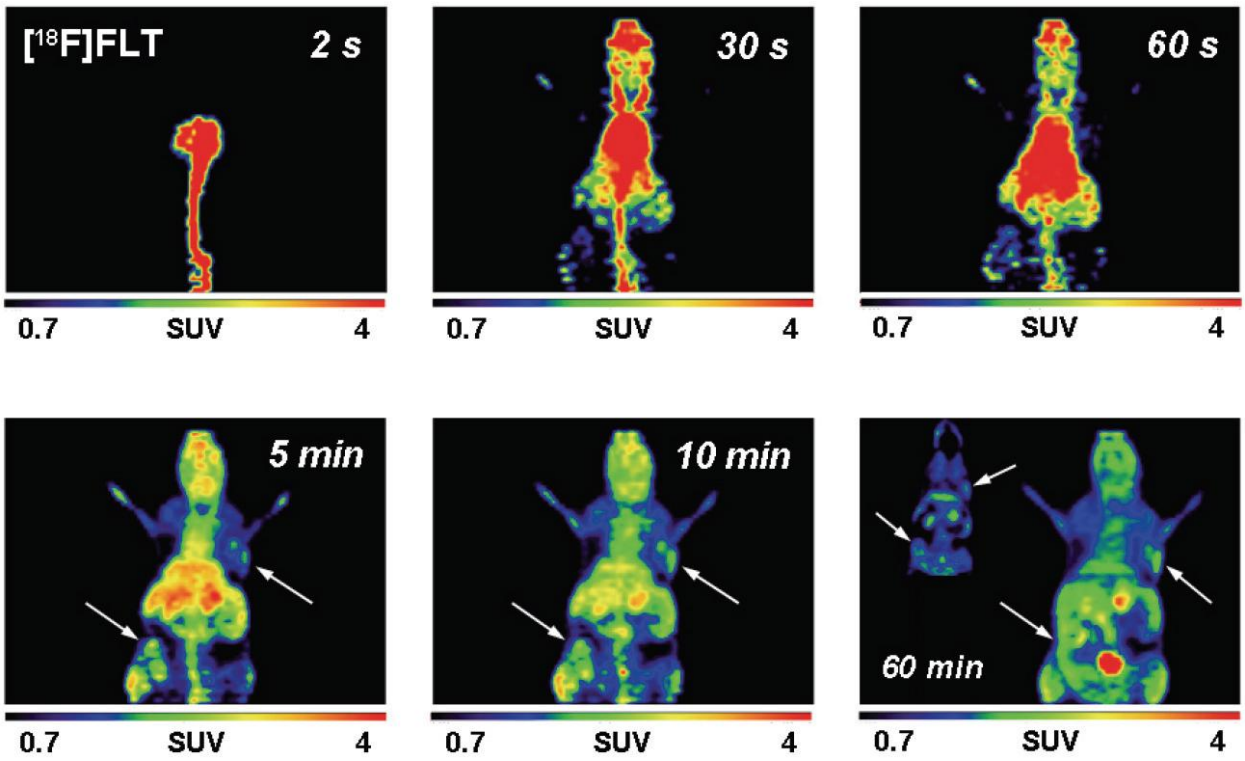

Figure 3.4. [^{18}F]FLT accumulates *in vivo* in MTHJ tumors over 60 minutes.

Representative dynamic small animal PET images (up to 60 min) of [^{18}F]FLT (4.5 MBq injected dose) in the same FVB mouse as shown in Figure 3.3 bearing two MTHJ tumors. [^{18}F]FLT was measured 24 hours prior to the [^{18}F]FDG scan. Images are presented as maximum intensity projections. The inset in the 60 min image displays of a coronal section through the tumor on the left lower flank to allow for better visualization.

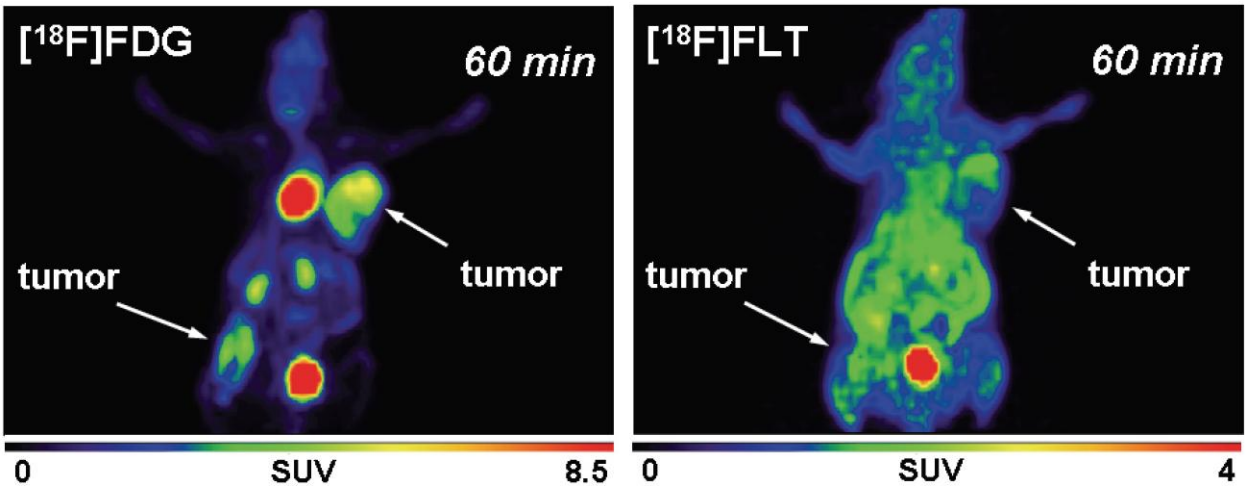

Figure 3.5. [^{18}F]FDG and [^{18}F]FLT both accumulate *in vivo* in PyMT tumors over 60 minutes.

Representative PET images at 60 min post injection of [^{18}F]FDG (6 MBq injected dose) and [^{18}F]FLT (5 MBq injected dose) in the same FVB mouse bearing two tumors from primary PyMT cells. [^{18}F]FDG was measured 24 hours after the [^{18}F]FLT scan. Images are presented as maximum intensity projections.

Time-activity curves (TACs) were generated for the uptake of both radiotracers in bilateral tumors and in muscle as reference tissue from 3 different mice bearing the MTHJ model and 4 different mice bearing PyMT tumors from primary cells (Figure 3.6). While [^{18}F]FDG uptake in both tumor models increased continuously over time, uptake of [^{18}F]FLT reached a plateau after approximately 5 to 10 min p.i.. [^{18}F]FLT uptake remained constant over the remaining total scanning time of 60 min. Uptake of [^{18}F]FDG was similar in MTHJ and PyMT tumors from primary cells. In contrast, uptake of [^{18}F]FLT seemed to be slightly lower in tumors from primary cells vs. MTHJ tumors, which is in good agreement with the observed lower cell uptake of [^{18}F]FLT in primary cells *in vitro*. However, this difference did not reach significance ($p = 0.071$). [^{18}F]FDG uptake in muscle tissue cleared slowly over time, while [^{18}F]FLT showed no clearance within the timeframe of the study (Figure 3.6). Based on the uptake and clearance patterns of both radiotracers in tumor and muscle tissue, tumor-muscle ratios were calculated (Figure 3.6). In both tumor models tumor-muscle ratios increased continuously over time for [^{18}F]FDG, but remained nearly constant in the case of [^{18}F]FLT. The tumor-muscle ratios over time were comparable in tumors from MTHJ and primary PyMT cells for each radiotracer studied.

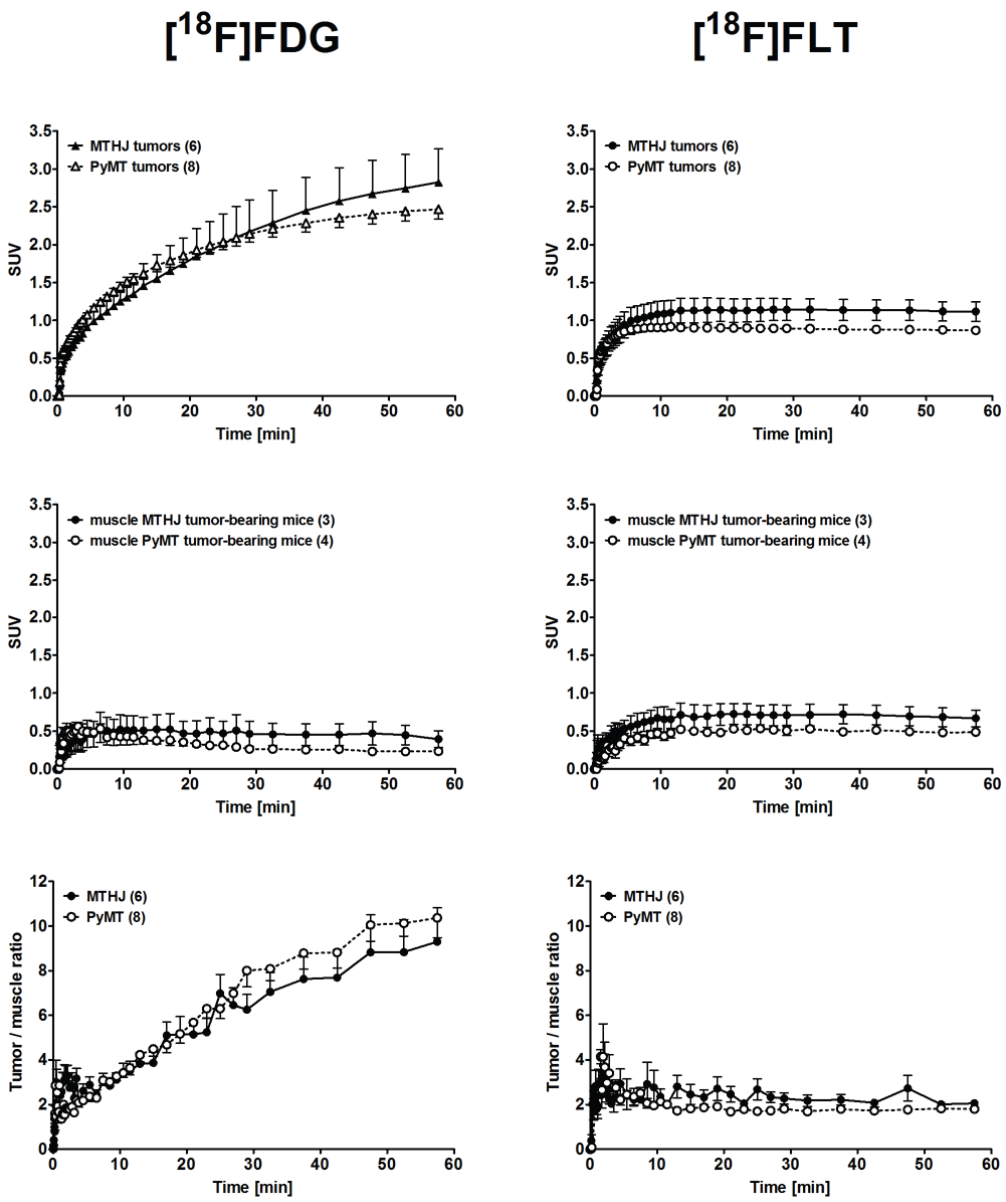

Figure 3.6. [^{18}F]FDG and [^{18}F]FLT accumulated in MTHJ and PyMT-derived tumors.

Radioactivity profile in MTHJ- and primary PyMT cell-derived tumor bearing FVB mice. Time activity curves are shown for the tumors (upper panels), muscle tissue (analyzed from the opposite shoulder region) of the same FVB mice (middle panels), and tumor/muscle ratios (lower panels) after single intravenous injections of [^{18}F]FDG (left) or [^{18}F]FLT (right). Data are shown as means ± S.E.M. from 6 MTHJ tumors in 3 tumor-bearing mice and for 8 primary PyMT cell-derived tumors in 4 tumor-bearing mice.

3.3.4. MTHJ Cells Show High [^{18}F]FHBG Accumulation **in vitro** *After Virus Infection*

To measure [^{18}F]FLT accumulation in MTHJ cells after infection with AdCMVTK and AdMPE$_2$TK, we generated dose response curves for each vector. Figure 3.7 shows that AdCMVTK induced an increase in tracer accumulation for [^{18}F]FLT at MOIs as low as 10 pfu/cell. AdMPE$_2$TK did not induce any [^{18}F]FLT accumulation at 10 pfu/cell (data not shown), and even MOIs as high as 250 pfu/cell were not able to induce an increase in [^{18}F]FLT accumulation significantly above that in uninfected cells (Figure 3.8).

In contrast, [^{18}F]FHBG does not accumulate in uninfected MTHJ cells. [^{18}F]FHBG accumulation, however, was induced by both AdCMVTK and AdMPE$_2$TK at MOIs of 50 and 250 pfu/cell, respectively (Figure 3.9). The fact that uninfected MTHJ cells show no [^{18}F]FHBG accumulation at all supports the substrate specificity of the [^{18}F]FHBG tracer for HSV-TK.

3.3.5. MTHJ Tumors Accumulate [^{18}F]FHBG **in vivo** *After AdCMVTK Injection*

To determine if Ad vector injection could increase radiotracer accumulation *in vivo*, dynamic small animal PET experiments were carried out using [^{18}F]FLT and [^{18}F]FHBG. Using the subcutaneous MTHJ tumor model, we compared two tumors in the same mouse: one tumor untreated; one tumor injected with either AdCMVTK or AdMPE$_2$TK two days prior to tracer injection. Over a 60 minute time frame we observed low tumor accumulation of [^{18}F]FLT in mice infected with AdCMVTK (Figure 3.10) and no detectable accumulation in tumors of mice treated with AdMPE$_2$TK (Figure 3.11). TACs confirmed these observations (Figure 3.12). 120 minute microPET scans revealed

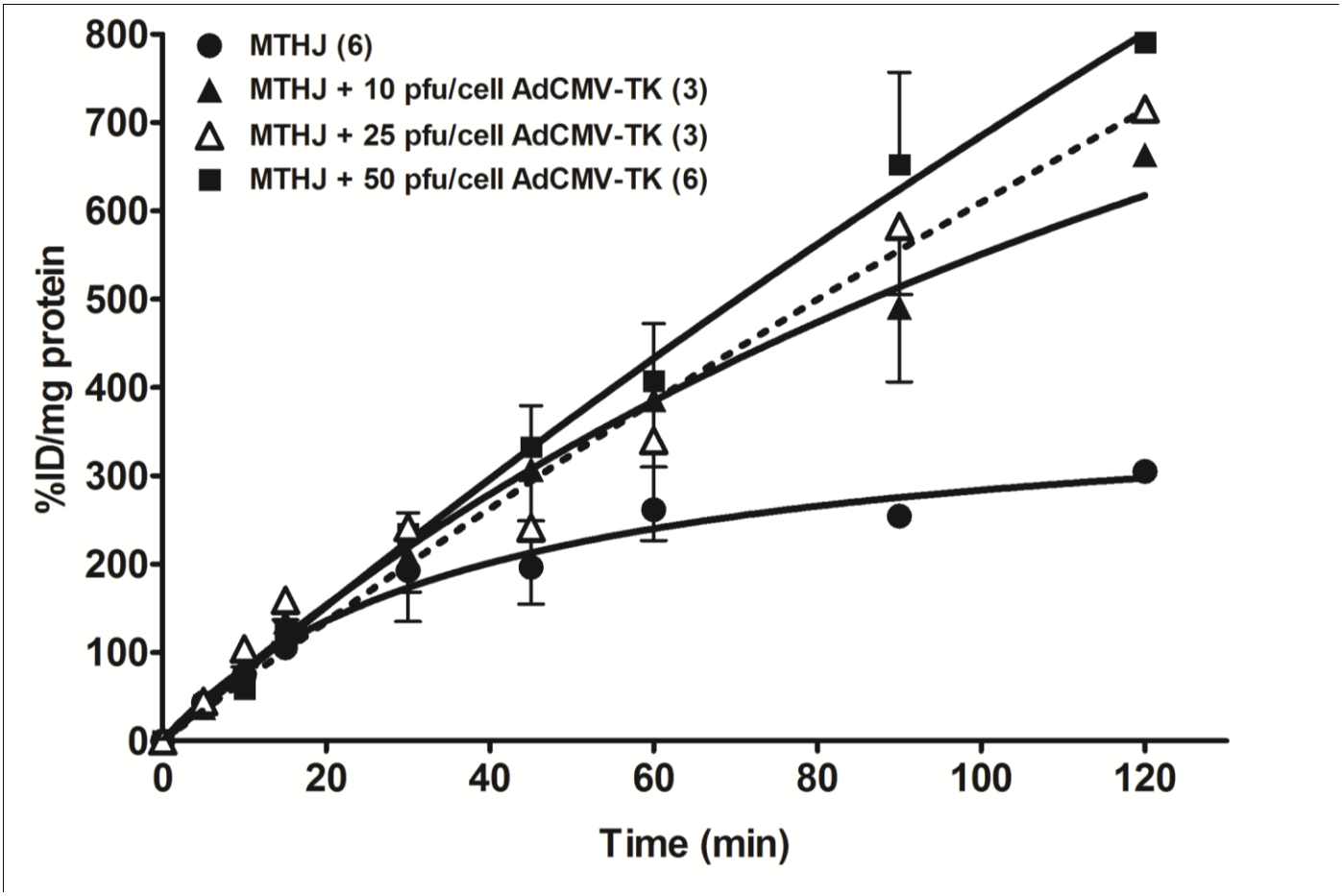

Figure 3.7. AdCMVTK infection induces increased [^{18}F]FLT accumulation in MTHJ cells *in vitro*.

MTHJ cells were untreated or infected with increasing concentrations of AdCMVTK then 2 days later [^{18}F]FLT uptake in the cultures was measured. The number of replicates for each sample is shown in brackets. % injected dose (ID)/mg protein is calculated as % of tracer accumulation per mg of total protein for the given sample lysate.

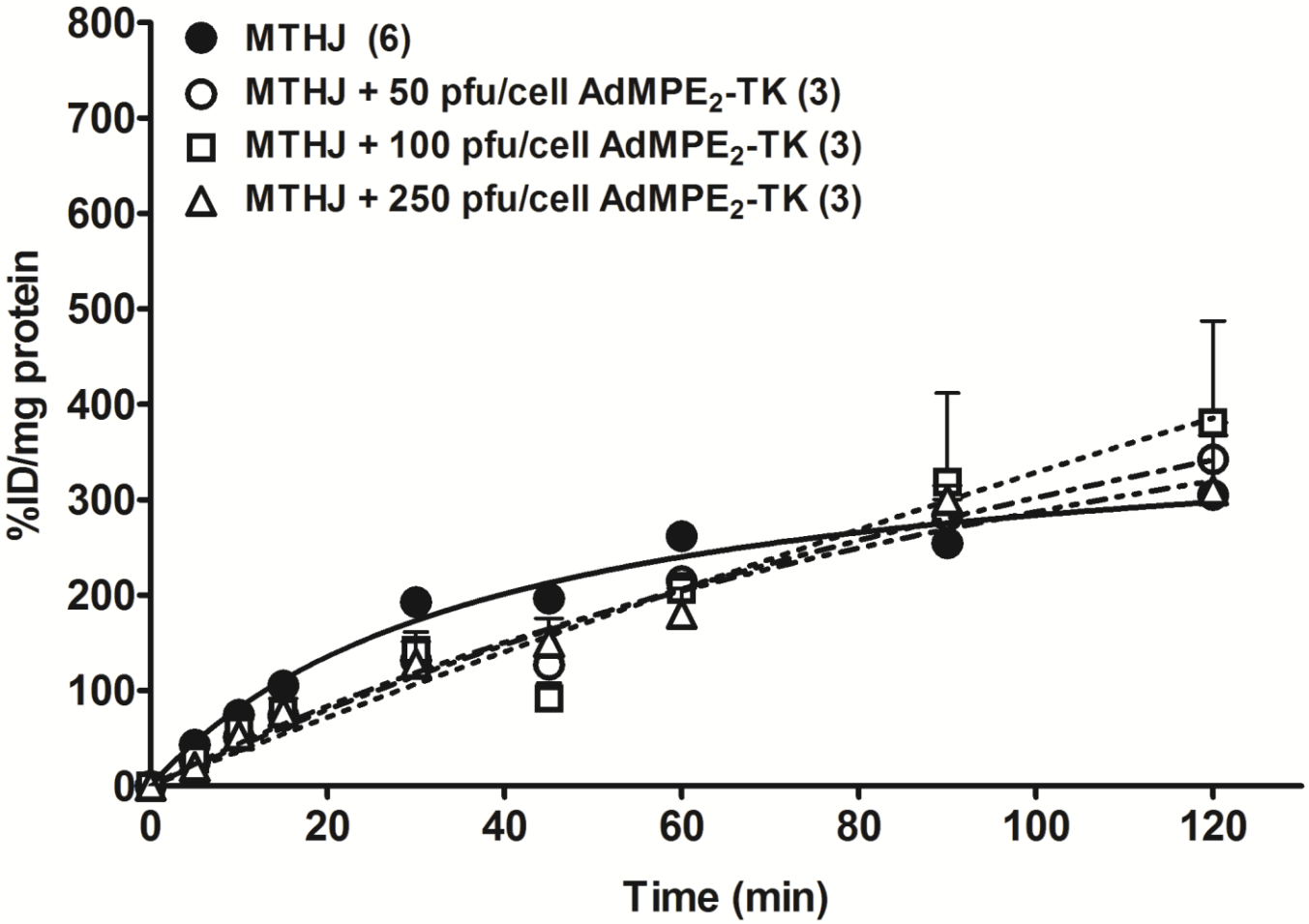

Figure 3.8. AdMPE$_2$TK infection does not induce increased [^{18}F]FLT accumulation in MTHJ cells *in vitro*.

MTHJ cells were untreated or infected with increasing concentrations of AdMPE$_2$TK then 2 days later [^{18}F]FLT uptake in the cultures was measured. The number of replicates for each sample is shown in brackets. % injected dose (ID)/mg protein is calculated as % of tracer accumulation per mg of total protein for the given sample lysate.

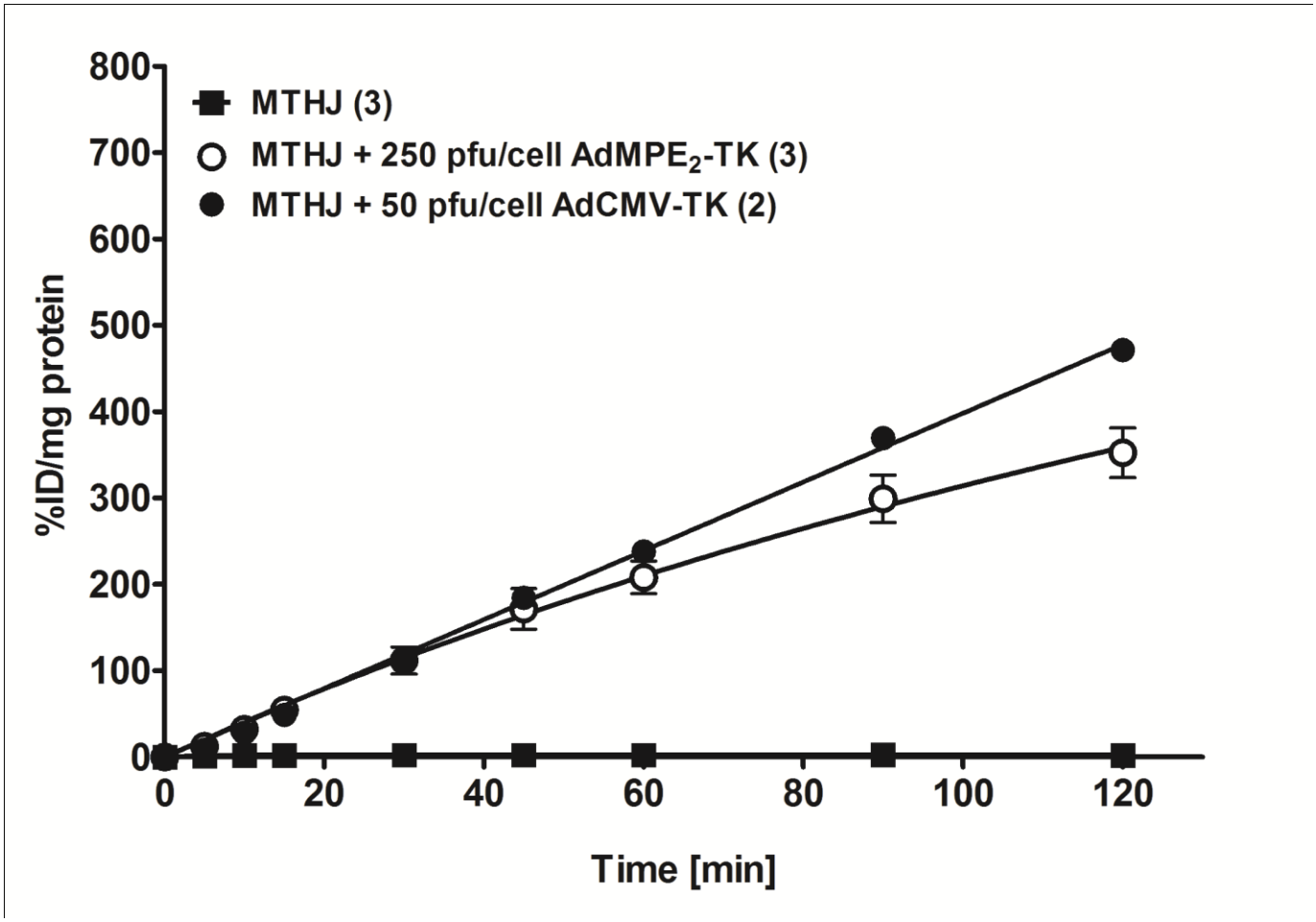

Figure 3.9. AdMPE$_2$TK and AdCMVTK infections induce increased [^{18}F]FHBG accumulation in MTHJ cells *in vitro*.

MTHJ cells were untreated or infected with 250 pfu AdMPE$_2$TK per cell or 50 pfu AdCMVTK per cell then 2 days later [^{18}F]FHBG uptake in the cultures was measured. The number of replicates for each sample is shown in brackets. % injected dose (ID)/mg protein is calculated as % of tracer accumulation per mg of total protein for the given sample lysate.

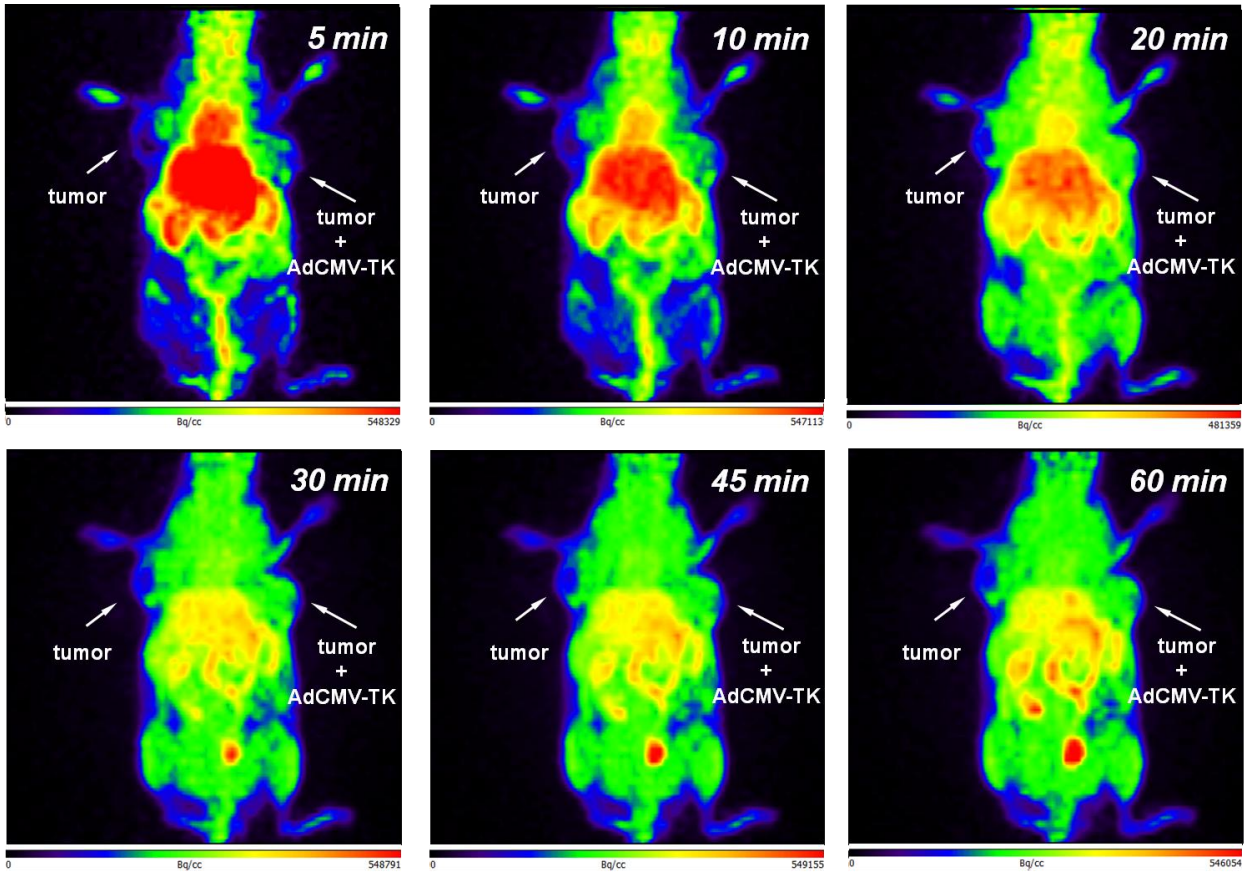

Figure 3.10. Intratumoral AdCMVTK injection induces a slight increase in [^{18}F]FLT accumulation in MTHJ tumors *in vivo* over 60 minutes.

One FVB mouse bearing two MTHJ tumors (one just below each shoulder) was used in this experiment. 4 x 10^8 pfu AdCMVTK was injected into the tumor below the right shoulder two days before imaging. Dynamic PET images were taken over a 60 minute timeframe starting immediately after intravenous injection of [^{18}F]FLT. Tracer uptake was measured by intensity (see intensity scale bars below each image).

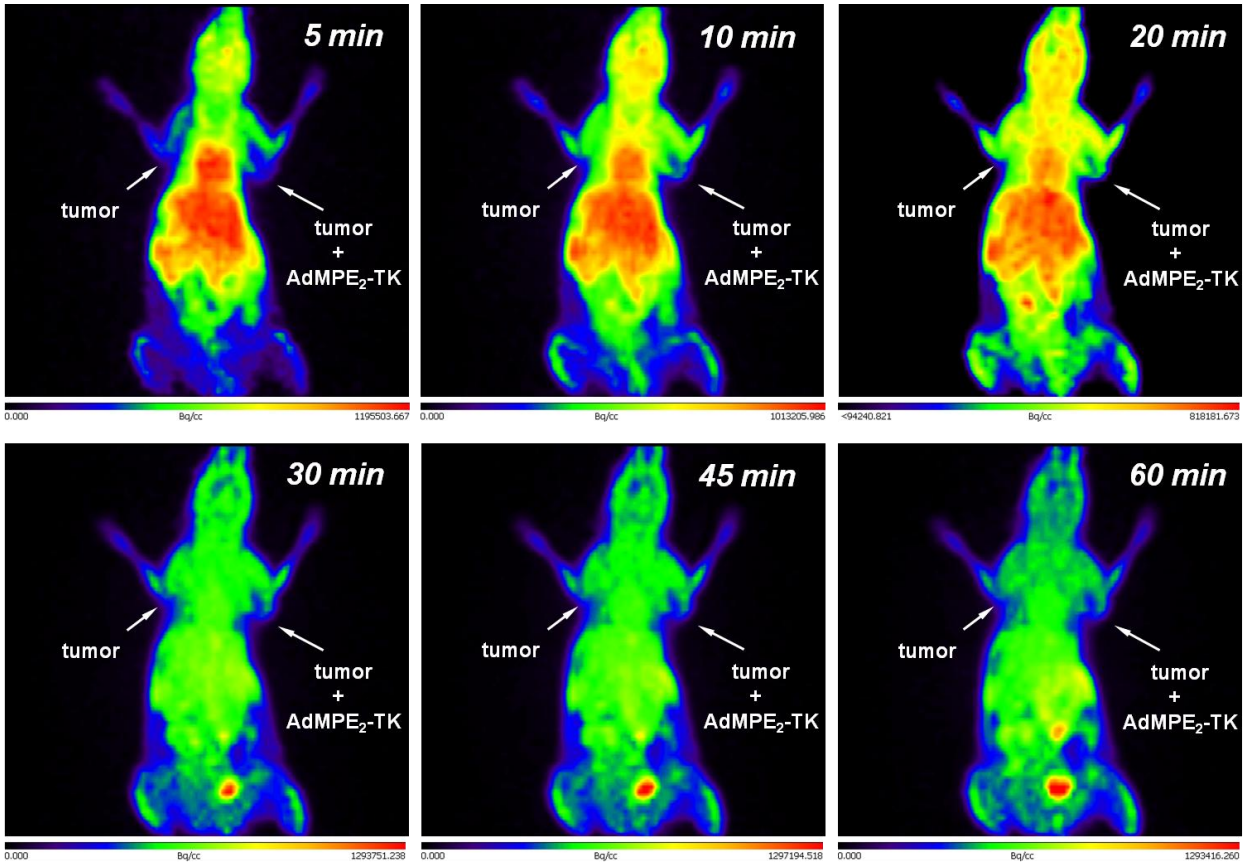

Figure 3.11. Intratumoral $AdMPE_2TK$ injection does not induce an increase in [^{18}F]FLT accumulation in MTHJ tumors *in vivo* over 60 minutes.

One FVB mouse bearing two MTHJ tumors (one just below each shoulder) was used in this experiment. 4 x 10^8 pfu AdCMVTK was injected into the tumor below the right shoulder two days before imaging. Dynamic PET images were taken over a 60 minute timeframe starting immediately after intravenous injection of [^{18}F]FLT. Tracer uptake was measured by intensity (see intensity scale bars below each image).

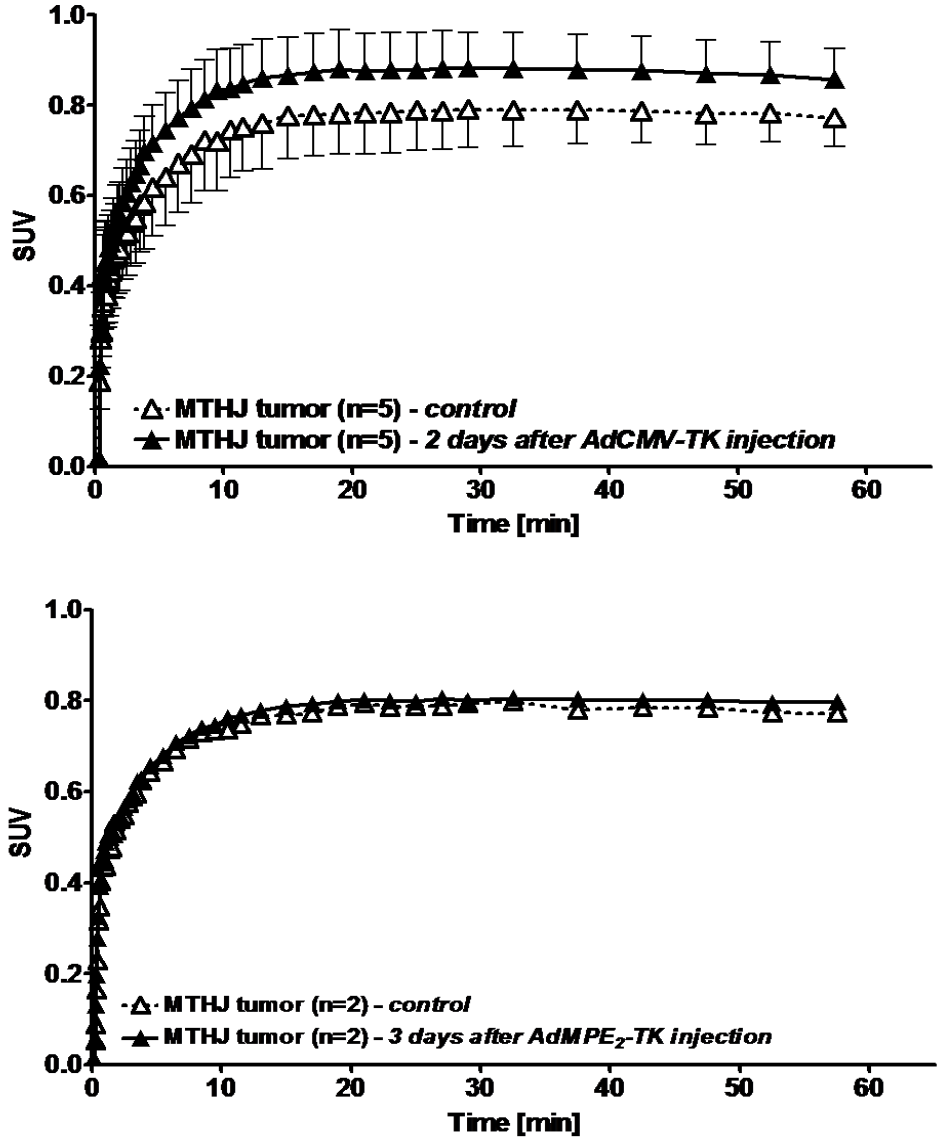

Figure 3.12. Increased [^{18}F]FLT accumulation in MTHJ tumors after injection with AdCMVTK but not AdMPE$_2$TK.

Time activity curves were generated from [^{18}F]FLT uptake in tumors of mice shown in Figures 4.4 and 4.5. Standard uptake value (SUV) is defined as the ratio of the concentration of the tracer in a region to the mean concentration in the body. (SUV = [tissue concentration (MBq/ml)]/[injected radioactivity (MBq)/body weight (g)]) (Paquet et al., 2004)

[^{18}F]FHBG accumulation in tumors injected with AdCMVTK (Figure 3.13), but not AdMPE_2TK injection (Figure 3.14). TACs are shown in Figure 3.15.

3.3.6. [^{18}F]FHBG Liver Accumulation in vivo *After Intratumoral AdCMVTK Injection*

TACs were generated comparing [^{18}F]FHBG uptake in livers, kidneys, and bladders (including urine) of mice before and 2 days after injection with AdCMVTK (Figure 3.16) or AdMPE_2TK (Figure 3.17). These results were similar to the results we observed with [^{18}F]FHBG accumulation in the virus-injected tumors: slight accumulation was observed only after injection of AdCMVTK. Interestingly, the [^{18}F]FHBG clearance from the liver and kidneys was slower than that from tumors in mice injected with AdCMVTK but not with AdMPE_2TK, even though identical amounts of virus were injected.

3.3.7. Biodistribution Studies Confirm [^{18}F]FHBG Liver Accumulation in vivo *After Intratumoral AdCMVTK Injection*

Biodistribution studies were carried out to confirm TACs generated from PET imaging. These experiments showed no statistical increase in [^{18}F]FHBG tumor accumulation after injection of AdCMVTK (Figure 3.18) or AdMPE_2TK (Figure 3.19), although we did observe a tendency for increased [^{18}F]FHBG tumor accumulation after injection with AdCMVTK. Livers of mice injected with AdCMVTK did accumulate [^{18}F]FHBG more than those injected with AdMPE_2TK or left untreated (Figure 3.20), reflecting the previous PET and TAC results.

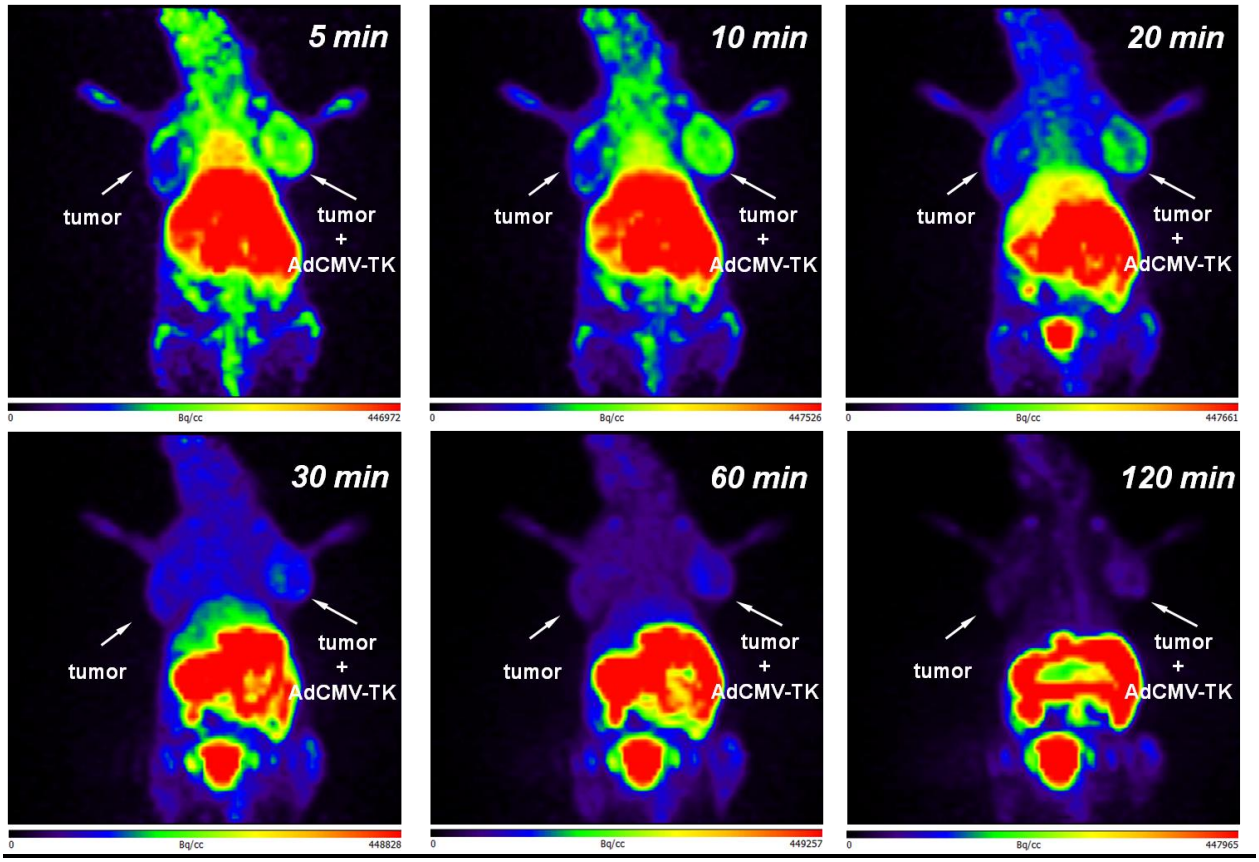

Figure 3.13. Intratumoral AdCMVTK injection induces increased [^{18}F]FHBG accumulation in MTHJ tumors *in vivo* over 120 minutes.

One FVB mouse bearing two MTHJ tumors (one just below each shoulder) was used in this experiment. 4 x 10^8 pfu AdCMVTK was injected into the tumor below the right shoulder two days before imaging. Dynamic PET images were taken over a 120 minute timeframe starting immediately after intravenous injection of [^{18}F]FHBG. Tracer uptake was measured by intensity (see intensity scale bars below each image).

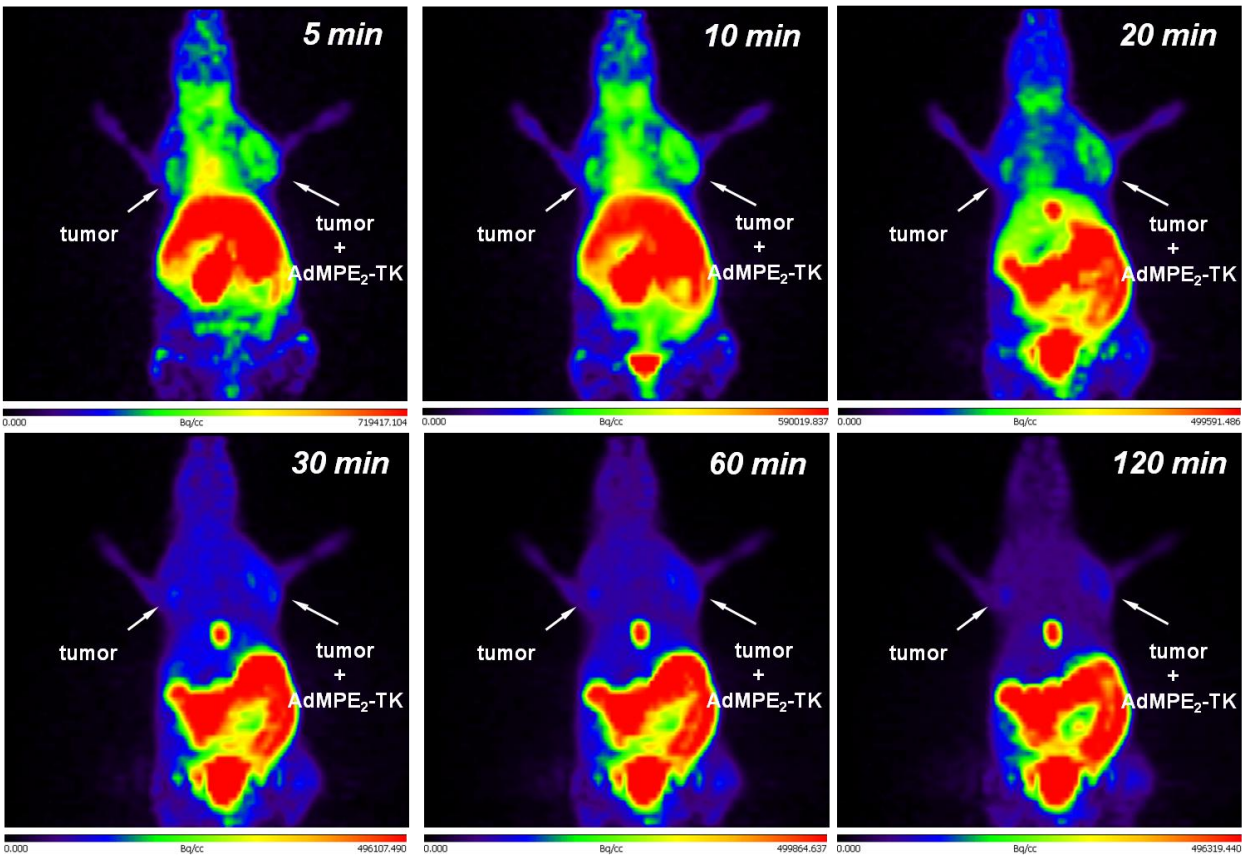

Figure 3.14. Intratumoral $AdMPE_2TK$ injection does not induce an increase in [^{18}F]FHBG accumulation in MTHJ tumors *in vivo* over 120 minutes.

One FVB mouse bearing two MTHJ tumors (one just below each shoulder) was used in this experiment. 4 x 10^8 pfu AdCMVTK was injected into the tumor below the right shoulder two days before imaging. Dynamic PET images were taken over a 120 minute timeframe starting immediately after intravenous injection of [^{18}F]FHBG. Tracer uptake was measured by intensity (see intensity scale bars below each image).

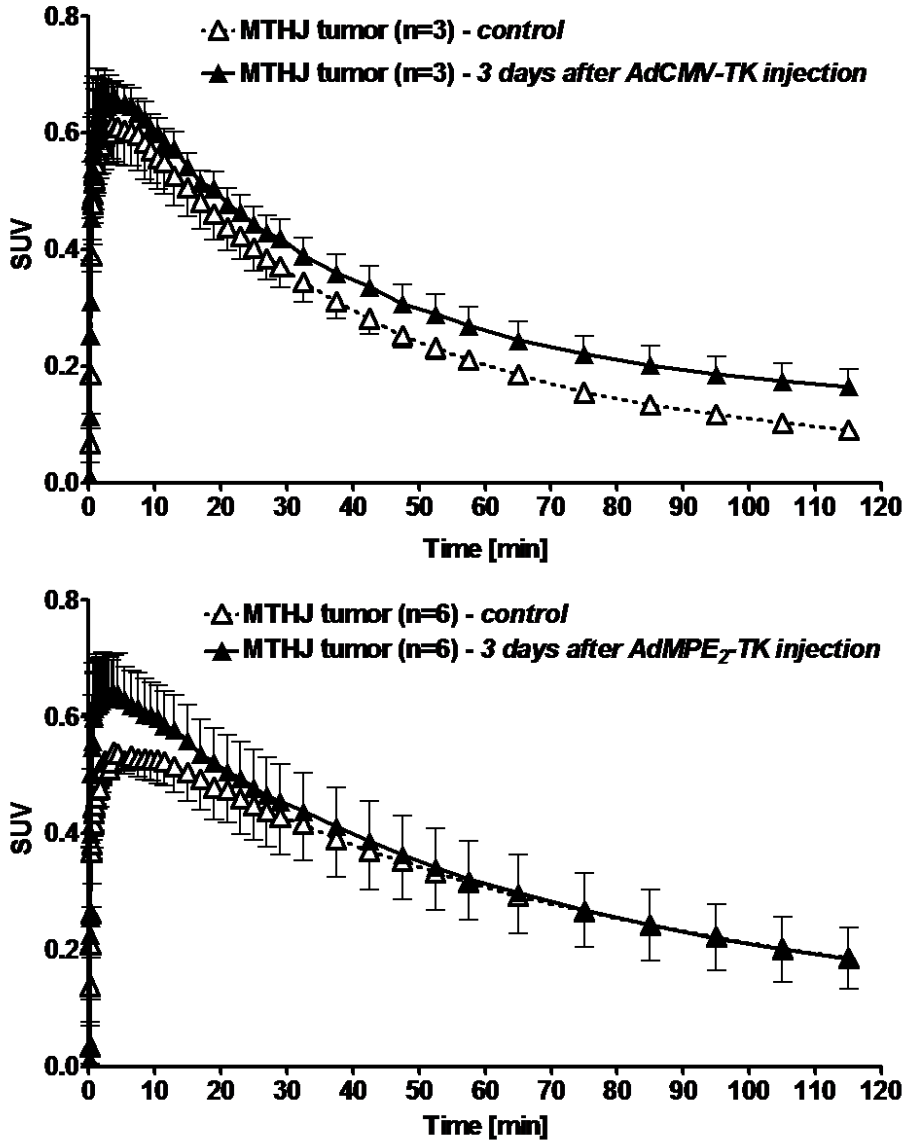

Figure 3.15. Increased [^{18}F]FHBG accumulation in MTHJ tumors after injection with AdCMVTK but not AdMPE$_2$TK.

Time activity curves were generated from [^{18}F]FHBG uptake in tumors of mice shown in Figures 4.7 (AdCMVTK) and 4.8 (AdMPE$_2$TK). Standard uptake value (SUV) is defined as the ratio of the concentration of the tracer in a region to the mean concentration in the body. (SUV = [tissue concentration (MBq/ml)]/[injected radioactivity (MBq)/body weight (g)]) (Paquet et al., 2004)

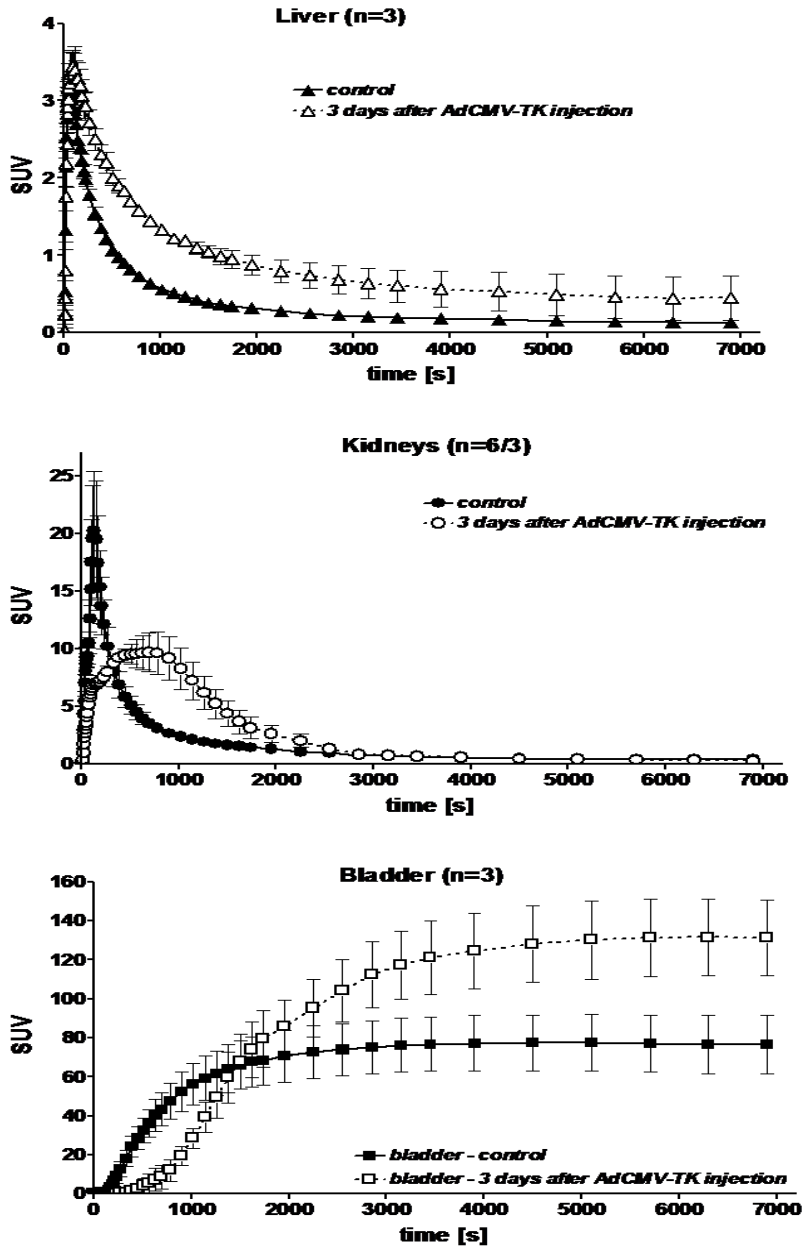

Figure 3.16. Increased [^{18}F]FHBG liver accumulation after intratumoral AdCMVTK injection.

Time activity curves were generated from [^{18}F]FHBG uptake in liver, kidneys, and bladders (including urine) of mice shown in Figure 4.7. Standard uptake value (SUV) is defined as the ratio of the concentration of the tracer in a region to the mean concentration in the body. (SUV = [tissue concentration (MBq/ml)]/[injected radioactivity (MBq)/body weight (g)]) (Paquet et al., 2004)

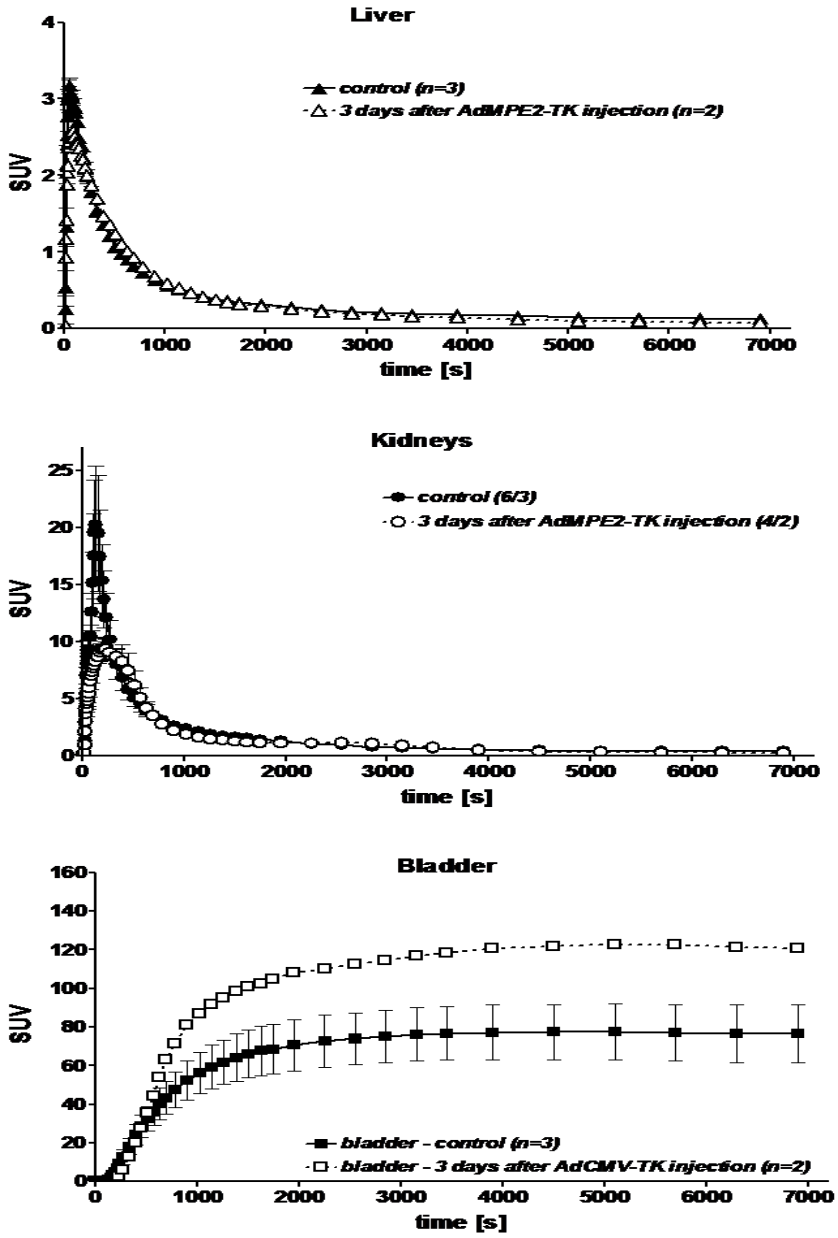

Figure 3.17. No increase in [^{18}F]FHBG liver accumulation after intratumoral AdMPE$_2$TK injection.

Time activity curves were generated from [^{18}F]FHBG uptake in liver, kidneys, and bladders (including urine) of mice shown in Figure 4.8. Standard uptake value (SUV) is defined as the ratio of the concentration of the tracer in a region to the mean concentration in the body. (SUV = [tissue concentration (MBq/ml)]/[injected radioactivity (MBq)/body weight (g)]) (Paquet et al., 2004)

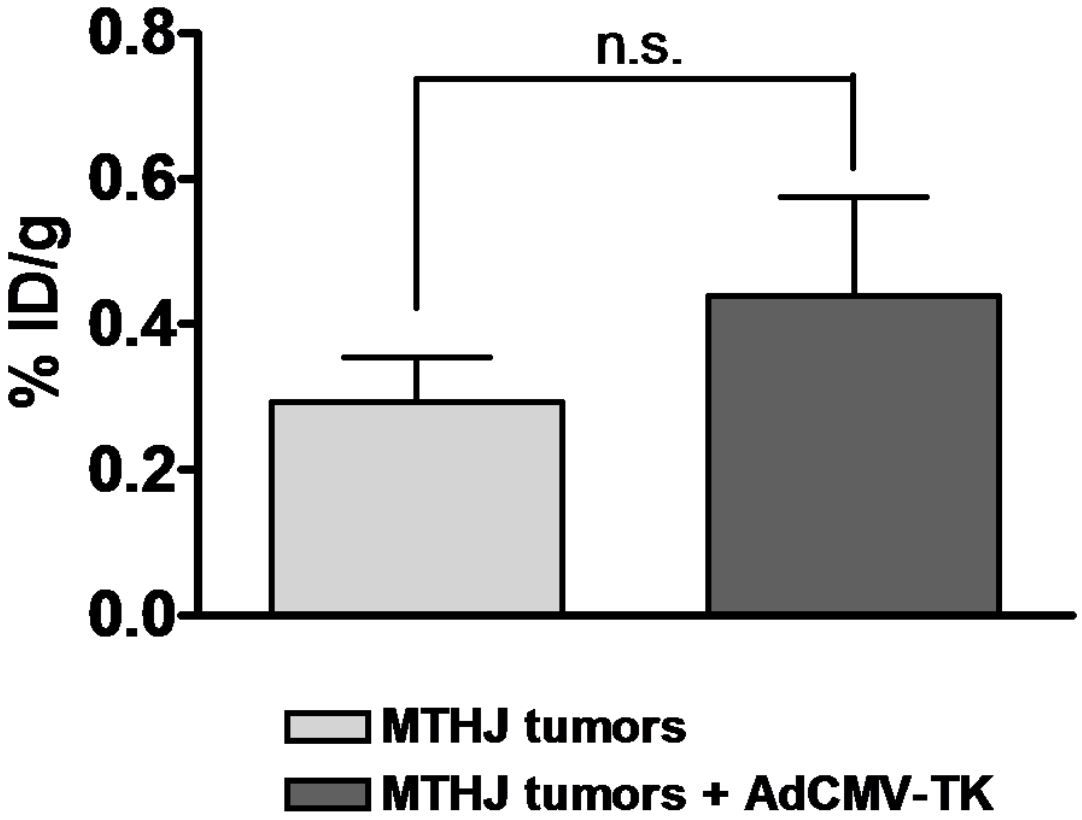

Figure 3.18. Biodistribution studies show AdCMVTK injection induces slight tendency for [^{18}F]FHBG accumulation in MTHJ tumors.

AdCMVTK-injected and control mice (5 mice per group) were euthanized 2h after [^{18}F]FHBG injection and total [^{18}F] activity in tumors were measured using a scintillation counter. %ID/mg protein represents % of total tracer accumulation per g of tumor. n.s. represents no statistically significant difference between the two groups.

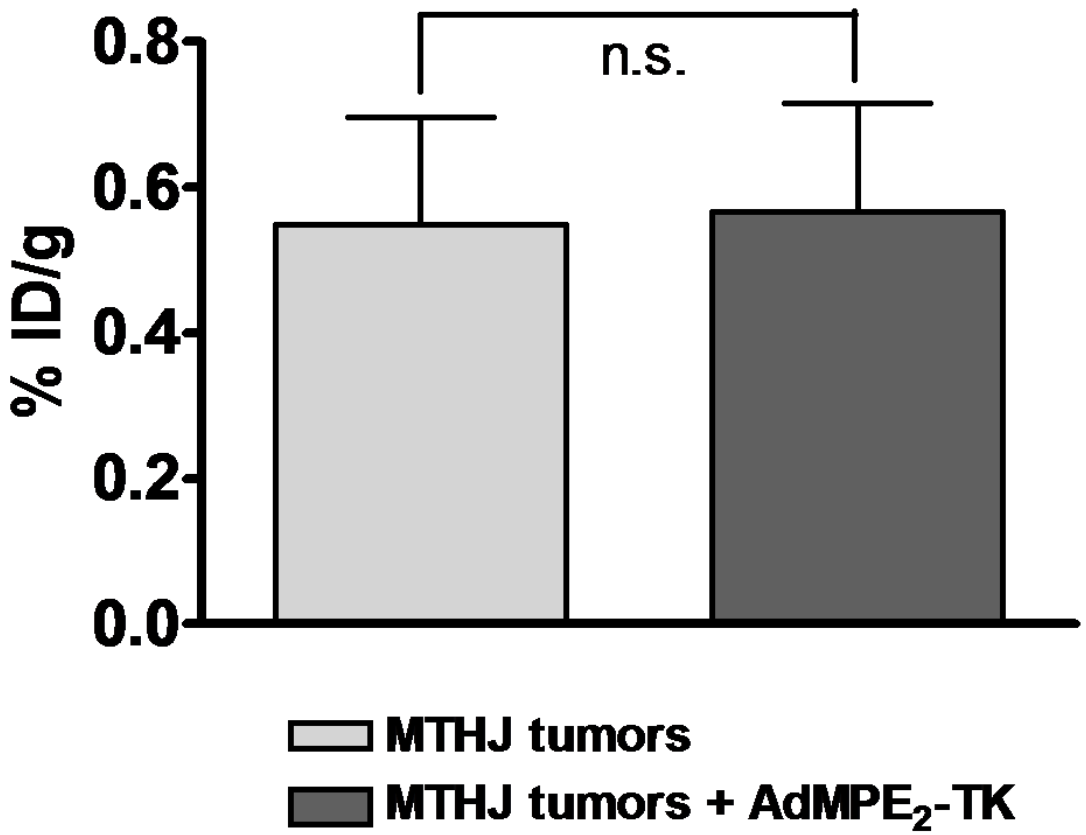

Figure 3.19. Biodistribution studies show AdMPE$_2$TK injection does not induce [^{18}F]FHBG accumulation in MTHJ tumors.

AdMPE$_2$TK-injected and control mice (8 mice per group) were euthanized 2h after [^{18}F]FHBG injection and total [^{18}F] activity in tumors were measured using a scintillation counter. %ID/mg protein represents % of total tracer accumulation per g of tumor. n.s. represents no statistically significant difference between the two groups.

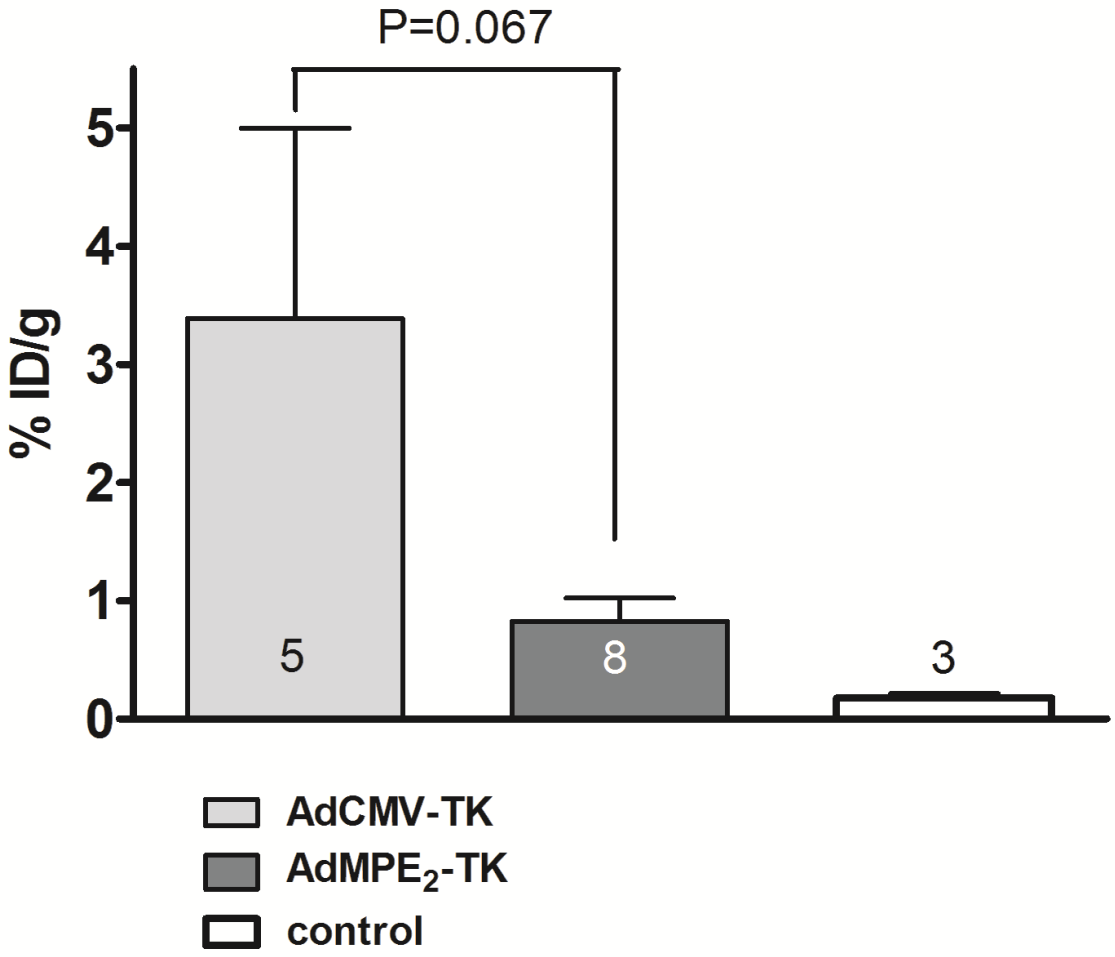

Figure 3.20. Biodistribution studies show intratumoral AdCMVTK injection induces increased [^{18}F]FHBG accumulation in liver.

AdCMVTK-injected, AdMPE$_2$TK-injected, and control mice were euthanized 2h after [^{18}F]FHBG injection and total [^{18}F] activity in livers were measured using a gamma counter. Sample sizes per group are shown on or above each bar. %ID/mg protein represents % of total tracer accumulation per g of tumor. Differences in [^{18}F]FHBG accumulation in livers from AdCMVTK-injected and AdMPE$_2$TK-injected mice were statistically significant at P=0.067.

3.4. DISCUSSION

One of the goals of the present study was to determine whether the tumor model established from cultured MTHJ cells would be functionally different from a model established from primary PyMT-derived mammary tumor cells. The study was designed to provide a reasonable platform to assess suitability of MTHJ as a pre-clinical breast cancer model using functional imaging with PET. An additional goal of this study was to investigate the potential of imaging a breast cancer-targeted adenoviral vector expressing HSV-TK ($AdMPE_2TK$). This was carried out by determining whether injection of the $AdMPE_2TK$ and the non-specific AdCMVTK vectors into murine mammary tumors would lead to an increase in HSV-TK expression in the tumor cells. This increase may be detectable utilizing PET with [^{18}F]FLT and [^{18}F]FHBG. By localizing HSV-TK to a mammary tumor using the breast cancer-specific MPE_2 promoter, we also aimed to exploit the high substrate specificity of the PET imaging agent [^{18}F]FHBG. This chapter describes the first attempt at *in vivo* imaging of gene expression from the MPE_2 promoter. $AdMPE_2TK$ was simultaneously studied for tumor regression capability (see Thesis Chapter 2) with the aspiration to generate a targeted vector with application in cancer therapy that can be tracked by PET imaging.

To assess the *in vivo* tumor models, we examined tumor growth, evaluated tracer uptake *in vitro* and studied the two types of PyMT-based mouse tumors *in vivo* with small animal PET imaging. The experimental data indicate that (i) MTHJ cells readily formed subcutaneous tumors at a high implantation rate with growth rates similar to that of the primary PyMT cells, (ii) *in vitro*, MTHJ and primary PyMT cells showed similar uptake of [^{18}F]FDG, whilst higher uptake was observed for [^{18}F]FLT in MTHJ cells

compared to primary cells, (iii) MTHJ- and primary PyMT-derived tumors showed comparable uptake of [^{18}F]FDG and [^{18}F]FLT, respectively, *in vivo*. This is indicative that there are no significant differences in metabolic and proliferation rates in both tumor models *in vivo*.

These results and the similarity of the PyMT transgenic mouse model to known biological signatures of human breast cancer (Lin et al., 2003) indicate that the immunocompetent murine MTHJ breast cancer mouse model should be very useful for the evaluation of novel anti-cancer therapies utilizing preclinical PET imaging.

Consistent with previous studies (Hummel, Safroneeva, and Mossman, 2005), cultured MTHJ cells were able to form palpable tumors in FVB mice. Growth of these cells *in vivo* was generally comparable to that of primary PyMT-derived cells, although the former was somewhat slower when high concentrations of cell inocula are compared. Since growth of MTHJ cells can easily be scaled up, MTHJ cells are less heterogeneous than primary tumor explants, and they do not require a continuous supply of animals as donors of tumor tissue, we propose that the MTHJ cell line is a valuable resource to study novel therapeutic interventions directed against breast cancer in an immunocompetent mouse model. Furthermore, slower growing tumors are preferable to allow analysis of the time course of treatment efficacy by means of PET imaging.

MTHJ cells showed three times higher uptake of [^{18}F]FLT compared to primary PyMT cells *in vitro* which is indicative of a higher proliferation rate in the cultivated MTHJ cells. In both cell lines glucose metabolism was highly active as evidenced by the observed

high [^{18}F]FDG uptake. However, after ≥ 80 min incubation time small differences were detectable between MTHJ and primary PyMT cells suggesting a slightly higher metabolic rate of glucose in primary PyMT cells. Comparable high cellular [^{18}F]FDG uptake levels as found during this study were observed for mouse EMT-6 mammary cells *in vitro* (Wuest et al., 2011). However, human BrCa cell lines such as MCF-7 showed lower [^{18}F]FDG uptake presumably reflecting lower metabolic rates of glucose in these tumors (Oswald et al., 2007).

Dynamic small animal PET imaging studies revealed high [^{18}F]FDG uptake in MTHJ tumors without reaching a plateau within 60 min p.i. Primary PyMT cell-derived tumors also showed a comparable [^{18}F]FDG uptake pattern *in vivo* which confirms the results from the *in vitro* studies. In comparison to the murine EMT-6 mammary tumor model, tumors from MTHJ cells as well as primary PyMT cells reached very high SUV levels of almost 3 for [^{18}F]FDG after 60 min p.i. (Shah et al., 2009; Thakur et al., 2010). Small animal PET studies with EMT-6 tumors demonstrated standard uptake values for [^{18}F]FDG in the range of 0.9 to 2 after 60 min p.i. (Aft et al., 2003; Wuest et al., 2011). A recent comprehensive and systematic study that compared [^{18}F]FDG and [^{18}F]FLT uptake profiles of several human tumor xenograft models reported mean SUVs of 0.3 – 1.59 for [^{18}F]FDG after 65 min p.i. (Keen et al., 2011). All mice were fasted for 4-8 h prior to injection of [^{18}F]FDG. With mean SUVs of 2.5 – 2.8, these PyMT models seems to have a much higher glucose metabolic rate and therefore may represent valuable pre-clinical mammary tumor models for the analysis of therapeutic interventions.

Uptake of [^{18}F]FLT was somewhat different in tumors from MTHJ and primary PyMT cells, although data analysis showed this difference did not reach a significant level. As primary PyMT cells showed a lower [^{18}F]FLT uptake level than MTHJ cells, the PyMT tumors would seem to have a slightly lower proliferation rate *in vivo*. This finding was not reflected by the growth curves which showed both tumor types displayed similar *in vivo* growth rates. Interestingly, SUVs of 0.9 – 1.1 for [^{18}F]FLT in both types of tumors are in the same range (0.2 – 1.4) as determined in several other studies (Cao et al., 2008; Keen et al., 2011; Rowland et al., 2006).

In summary, tumors derived from cultured MTHJ and primary PyMT cells showed a comparable radiotracer uptake profile for [^{18}F]FDG and [^{18}F]FLT which is indicative of comparable metabolic and proliferation rates in both tumors. The MTHJ tumor model represents a good and reliable pre-clinical mouse mammary tumor model for the analysis of the efficacy of therapeutic interventions. A systematic functional baseline characterization *in vivo* of a given tumor model is an important prerequisite for the design of a pre-clinical anti-cancer therapy study (Keen et al., 2011).

A further advantage of the MTHJ model is the complete immunocompetence of the mice. Most preclinical testing of novel anti-cancer therapeutics for breast cancer treatment is carried out in nude or SCID mice bearing human breast cancer xenografts (Kim, O'Hare, and Stein, 2004; Myoui et al., 2003; Noblitt et al., 2004; Wang, Norris, and Mansky, 2002). Nude mice, however, are immunodeficient and thus are not as comparable to the BrCa patient, whose immune system may enhance or repress the efficacy of therapy. In particular, the immune system may play a major role in the efficacy of oncolytic viruses and viral gene therapy vectors (Noblitt et al., 2005). Other

mouse cell lines, such as MT1A2 cells, have been studied as immunocompetent murine models for breast cancer. However, no PET imaging was used for characterization of the MT1A2 cell line. Furthermore, in our hands spontaneous regression of MT1A2 tumors occurred at a sufficiently high frequency to confound efficacy studies. Tumors of other immunocompetent murine models, such as those derived from 4T1 cells, demonstrate a very high growth rate. Therefore, both MT1A2 and 4T1 models seem to be less attractive than MTHJ for longitudinal mouse BrCa studies.

In conclusion, the immunocompetent murine MTHJ breast tumor model, which has high biological relevance to human breast cancer, displays functional similarities to the primary PyMT tumor model based on glucose metabolism and proliferation pattern. Further studies are needed to investigate other qualities of this tumor model (such as metastatic potential and receptor status) which may have implications for specific BrCa therapies. However, the observed high SUV levels for [^{18}F]FDG (SUV ~3) and reasonable SUVs for [^{18}F]FLT (SUV ~1) underscore the potential of this pre-clinical mouse model for the analysis and monitoring of novel therapeutic strategies by means of PET.

In vitro studies showed [^{18}F]FHBG uptake and accumulation in MTHJ cells infected with AdMPE_2TK at a high dose (Figure 3.9). While it was necessary to use a higher concentration of AdMPE_2TK than AdCMVTK to observe [^{18}F]FHBG accumulation, this was expected since the mCMV promoter is known to promote high transgene activity and accumulation should be dependent on HSV-TK expression. In fact, previous *in vitro* studies comparing mCMV and MPE_2 promoter-controlled expression of luciferase have shown approximately 10-fold higher expression levels from the CMV promoter in

MT1A2 cells (Shi, Graham, and Hitt, 2006). The MT1A2 cell line is similar to the MTHJ cell lines used in this study as they were both derived from mammary adenocarcinomas isolated from a transgenic mouse carrying the polyoma virus middle T transgene (Addison et al., 1995).

To date, no other groups have investigated PET tracer uptake in MTHJ cells after viral gene therapy. Here we have shown the potential of the MTHJ cell line for use in pre-clinical analysis and monitoring of therapeutics by PET (DeSilva et al., 2012). This set of experiments describes the first study to quantitatively measure [^{18}F]FLT and [^{18}F]FHBG uptake after AdMPE$_2$TK infection of MTHJ cells.

While *in vitro* results showed that AdMPE$_2$TK could increase [^{18}F]FHBG accumulation in MTHJ cells, *in vivo* analysis revealed that the amount of HSV-TK present in the tumor cells was not sufficient to lead to a higher [^{18}F]FHBG accumulation in the MTHJ tumor model. Both PET and biodistribution experiments showed AdMPE$_2$TK injection into established MTHJ tumors induced low to no increase in radiotracer accumulation 2 hours post-injection of tracer. Even the AdCMVTK vector induced only a minor increase of [^{18}F]FHBG accumulation in the *in vivo* tumor. This is contrary to other studies that have shown an Ad vector expressing HSV-TK under the control of the CMV promoter (Gambhir et al., 1999; Gambhir et al., 1998), although these studies involved radiolabeled GCV instead of [^{18}F]FHBG. One instance of an AdCMVTK vector inducing an increase in [^{18}F]FHBG accumulation is from Penuelas' group (Penuelas et al., 2005) where 4 of 7 patients show specific [^{18}F]FHBG accumulation within human tumor nodules that were injected with ≥ 10^{12} viral particles (≥ 7.7 x 10^9 pfu) of AdCMVTK. It is possible that our dose of 4 x 10^8 pfu AdCMVTK was too low to induce significant

[^{18}F]FHBG accumulation in immunocompetent mice. We chose to limit our viral dose to 4 x 10^8 pfu AdCMVTK per mouse since previous experiments in our lab have shown that FVB mice injected with this dose exhibited liver damage (confirmed through blood liver enzyme testing and immunohistochemistry). Since we expected the CMV promoter to induce approximately 10-fold higher expression than the MPE_2 promoter, it is not necessarily surprising that we were unable to observe [^{18}F]FHBG accumulation after AdMPE_2TK injection.

We were able to observe a mild increase in [^{18}F]FHBG liver accumulation after AdCMVTK injection as opposed to AdMPE_2TK injection. This finding, in combination with previous AdCMVTK data reflecting HSV-TK liver expression and subsequent toxicity, adds support to the rationale for using tumor targeted promoters in Ad gene therapy.

The safety of normal cells is of critical importance for any type of therapeutic cancer therapy, and more work must be done on using the MPE_2 promoter to increase HSV-TK expression in tumor cells. If this can be accomplished, a modified MPE_2TK vector holds promise as a non-toxic cancer gene therapy vector with the capacity for simultaneous visualization of HSV-TK expression through the use of [^{18}F]FHBG PET imaging. The BrCa-specific nature of the MPE_2 promoter in combination with PET's ability to image molecular changes within a cell could potentially be developed to provide an indication of treatment response in patients receiving breast cancer treatment. It is probable that this promoter may need to be combined with other targeting methods and/or gene expression enhancements to induce a greater increase in radiotracer accumulation for sufficient imaging. Work in our lab is currently in progress to investigate other options.

3.5. ACKNOWLEDGEMENTS

The authors would like to thank John Wilson, David Clendening, Jayden Sader and Blake Lazurko from the Edmonton PET Center for providing ^{18}F produced on a biomedical cyclotron, Jeff McPherson and Angela Westover for production of [^{18}F]FDG and Ali Akbari for the synthesis of [^{18}F]FLT. In addition we thank Kate Agopsowicz for assistance with *in vitro* work, and Gail Hipperson and Dan McGinn from the Vivarium of the Cross Cancer Institute for assisting in animal handling. This work was supported by grants from the Alberta Cancer Foundation (ACF) and the Canadian Breast Cancer Foundation (CBCF).

3.6. REFERENCES

Addison, C. L., Braciak, T., Ralston, R., Muller, W. J., Gauldie, J., and Graham, F. L. (1995). Intratumoral injection of an adenovirus expressing interleukin 2 induces regression and immunity in a murine breast cancer model. *Proc Natl Acad Sci U S A* **92**(18)**,** 8522-6.

Aft, R. L., Lewis, J. S., Zhang, F., Kim, J., and Welch, M. J. (2003). Enhancing targeted radiotherapy by copper(II)diacetyl- bis(N4-methylthiosemicarbazone) using 2-deoxy-D-glucose. *Cancer Res* **63**(17)**,** 5496-504.

Alauddin, M. M., and Conti, P. S. (1998). Synthesis and preliminary evaluation of 9-(4-[18F]-fluoro-3-hydroxymethylbutyl)guanine ([18F]FHBG): a new potential imaging agent for viral infection and gene therapy using PET. *Nucl Med Biol* **25**(3)**,** 175-80.

Alauddin, M. M., Shahinian, A., Gordon, E. M., Bading, J. R., and Conti, P. S. (2001). Preclinical evaluation of the penciclovir analog 9-(4-[(18)F]fluoro-3-hydroxymethylbutyl)guanine for in vivo measurement of suicide gene expression with PET. *J Nucl Med* **42**(11)**,** 1682-90.

Buck, A. K., Schirrmeister, H., Mattfeldt, T., and Reske, S. N. (2004). Biological characterisation of breast cancer by means of PET. *Eur J Nucl Med Mol Imaging* **31 Suppl 1,** S80-7.

Cao, Q., Li, Z. B., Chen, K., Wu, Z., He, L., Neamati, N., and Chen, X. (2008). Evaluation of biodistribution and anti-tumor effect of a dimeric RGD peptide-paclitaxel conjugate in mice with breast cancer. *Eur J Nucl Med Mol Imaging* **35**(8)**,** 1489-98.

Cochet, A., Generali, D., Fox, S. B., Ferrozzi, F., and Hicks, R. J. (2011). Positron emission tomography and neoadjuvant therapy of breast cancer. *J Natl Cancer Inst Monogr* **2011**(43)**,** 111-5.

Czernin, J., Benz, M. R., and Allen-Auerbach, M. S. Breast cancer. *Methods Mol Biol* **727,** 141-70.

Dawson, L. A., and Sharpe, M. B. (2006). Image-guided radiotherapy: rationale, benefits, and limitations. *Lancet Oncol* **7**(10)**,** 848-58.

Dehdashti, F., Mortimer, J. E., Trinkaus, K., Naughton, M. J., Ellis, M., Katzenellenbogen, J. A., Welch, M. J., and Siegel, B. A. (2009). PET-based estradiol challenge as a predictive biomarker of response to endocrine therapy in women with estrogen-receptor-positive breast cancer. *Breast Cancer Res Treat* **113**(3)**,** 509-17.

DeSilva, A., Wuest, M., Wang, M., Hummel, J., Mossman, K., Wuest, F., and Hitt, M. (2012). Comparative functional evaluation of immunocompetent mouse breast cancer models established from PyMT-tumors using small animal PET with [18F]FDG and [18F]FLT. *Am J Nucl Med Mol Imaging* **2**(1)**,** 88-98.

Escalona, S., Blasco, J. A., Reza, M. M., Andradas, E., and Gomez, N. A systematic review of FDG-PET in breast cancer. *Med Oncol* **27**(1)**,** 114-29.

Fleming, I. N., Gilbert, F. J., Miles, K. A., and Cameron, D. Opportunities for PET to deliver clinical benefit in cancer: breast cancer as a paradigm. *Cancer Imaging* **10,** 144-52.

Flier, J. S., Mueckler, M. M., Usher, P., and Lodish, H. F. (1987). Elevated levels of glucose transport and transporter messenger RNA are induced by ras or src oncogenes. *Science* **235**(4795)**,** 1492-5.

Gambhir, S. S., Barrio, J. R., Phelps, M. E., Iyer, M., Namavari, M., Satyamurthy, N., Wu, L., Green, L. A., Bauer, E., MacLaren, D. C., Nguyen, K., Berk, A. J., Cherry, S. R., and Herschman, H. R. (1999). Imaging adenoviral-directed reporter gene expression in living animals with positron emission tomography. *Proc Natl Acad Sci U S A* **96**(5)**,** 2333-8.

Gambhir, S. S., Barrio, J. R., Wu, L., Iyer, M., Namavari, M., Satyamurthy, N., Bauer, E., Parrish, C., MacLaren, D. C., Borghei, A. R., Green, L. A., Sharfstein, S., Berk, A. J., Cherry, S. R., Phelps, M. E., and Herschman, H. R. (1998). Imaging of adenoviral-directed herpes simplex virus type 1 thymidine kinase reporter gene expression in mice with radiolabeled ganciclovir. *J Nucl Med* **39**(11)**,** 2003-11.

Guy, C. T., Cardiff, R. D., and Muller, W. J. (1992). Induction of mammary tumors by expression of polyomavirus middle T oncogene: a transgenic mouse model for metastatic disease. *Mol Cell Biol* **12**(3)**,** 954-61.

Hamacher, K., Coenen, H. H., and Stocklin, G. (1986). Efficient stereospecific synthesis of no-carrier-added 2-[18F]-fluoro-2-deoxy-D-glucose using aminopolyether supported nucleophilic substitution. *J Nucl Med* **27**(2)**,** 235-8.

Hummel, J. L., Safroneeva, E., and Mossman, K. L. (2005). The role of ICP0-Null HSV-1 and interferon signaling defects in the effective treatment of breast adenocarcinoma. *Mol Ther* **12**(6)**,** 1101-10.

Keen, H., Pichler, B., Kukuk, D., Duchamp, O., Raguin, O., Shannon, A., Whalley, N., Jacobs, V., Bales, J., Gingles, N., Ricketts, S. A., and Wedge, S. R. (2011). An Evaluation of 2-deoxy-2-[(18)F]Fluoro-D-Glucose and 3'-deoxy-3'-[(18)F]-Fluorothymidine Uptake in Human Tumor Xenograft Models. *Mol Imaging Biol*.

Kim, J. B., O'Hare, M. J., and Stein, R. (2004). Models of breast cancer: is merging human and animal models the future? *Breast Cancer Res* **6**(1)**,** 22-30.

Kovesdi, I., Brough, D. E., Bruder, J. T., and Wickham, T. J. (1997). Adenoviral vectors for gene transfer. *Curr Opin Biotechnol* **8**(5)**,** 583-9.

Kurdziel, K. A., Kalen, J. D., Hirsch, J. I., Wilson, J. D., Agarwal, R., Barrett, D., Bear, H. D., and McCumiskey, J. F. (2007). Imaging multidrug resistance with 4-[18F]fluoropaclitaxel. *Nucl Med Biol* **34**(7)**,** 823-31.

Larson, S. M., Tjuvajev, J., and Blasberg, R. (1997). Triumph over mischance: a role for nuclear medicine in gene therapy. *J Nucl Med* **38**(8)**,** 1230-3.

Lee, J. H., Rosen, E. L., and Mankoff, D. A. (2009a). The role of radiotracer imaging in the diagnosis and management of patients with breast cancer: part 1--overview, detection, and staging. *J Nucl Med* **50**(4)**,** 569-81.

Lee, J. H., Rosen, E. L., and Mankoff, D. A. (2009b). The role of radiotracer imaging in the diagnosis and management of patients with breast cancer: part 2--response to therapy, other indications, and future directions. *J Nucl Med* **50**(5)**,** 738-48.

Lin, E. Y., Jones, J. G., Li, P., Zhu, L., Whitney, K. D., Muller, W. J., and Pollard, J. W. (2003). Progression to malignancy in the polyoma middle T oncoprotein mouse breast cancer model provides a reliable model for human diseases. *Am J Pathol* **163**(5)**,** 2113-26.

Macheda, M. L., Rogers, S., and Best, J. D. (2005). Molecular and cellular regulation of glucose transporter (GLUT) proteins in cancer. *J Cell Physiol* **202**(3)**,** 654-62.

Machulla, H. J., Blocher, A., Kuntzch, M., Piert, M., Wei, R., Grierson, J.R. (2000). Simplified labeling approach for synthesizing 39-deoxy-39-[18F]fluorothymidine ([18F]FLT). *J Radioanal Nucl Chem* **243,** 843-46.

Mankoff, D. A. (2008). Molecular imaging as a tool for translating breast cancer science. *Breast Cancer Res* **10 Suppl 1,** S3.

Murakami, R., Kumita, S. I., Yoshida, T., Ishihara, K., Kiriyama, T., Hakozaki, K., Yanagihara, K., Iida, S., and Tsuchiya, S. I. (2011). FDG-PET/CT in the diagnosis of recurrent breast cancer. *Acta Radiol*.

Myoui, A., Nishimura, R., Williams, P. J., Hiraga, T., Tamura, D., Michigami, T., Mundy, G. R., and Yoneda, T. (2003). C-SRC tyrosine kinase activity is associated with tumor colonization in bone and lung in an animal model of human breast cancer metastasis. *Cancer Res* **63**(16)**,** 5028-33.

Nichol, C., and Kim, E. E. (2001). Molecular imaging and gene therapy. *J Nucl Med* **42**(9)**,** 1368-74.

Noblitt, L. W., Bangari, D. S., Shukla, S., Knapp, D. W., Mohammed, S., Kinch, M. S., and Mittal, S. K. (2004). Decreased tumorigenic potential of EphA2-overexpressing breast cancer cells following treatment with adenoviral vectors that express EphrinA1. *Cancer Gene Ther* **11**(11)**,** 757-66.

Noblitt, L. W., Bangari, D. S., Shukla, S., Mohammed, S., and Mittal, S. K. (2005). Immunocompetent mouse model of breast cancer for preclinical testing of EphA2-targeted therapy. *Cancer Gene Ther* **12**(1)**,** 46-53.

Oswald, J., Treite, F., Haase, C., Kampfrath, T., Mading, P., Schwenzer, B., Bergmann, R., and Pietzsch, J. (2007). Experimental hypoxia is a potent stimulus for radiotracer uptake in vitro: comparison of different tumor cells and primary endothelial cells. *Cancer Lett* **254**(1)**,** 102-10.

Paquet, N., Albert, A., Foidart, J., and Hustinx, R. (2004). Within-patient variability of (18)F-FDG: standardized uptake values in normal tissues. *J Nucl Med* **45**(5)**,** 784-8.

Penuelas, I., Boan, J., Marti-Climent, J. M., Sangro, B., Mazzolini, G., Prieto, J., and Richter, J. A. (2004). Positron emission tomography and gene therapy: basic concepts and experimental approaches for in vivo gene expression imaging. *Mol Imaging Biol* **6**(4)**,** 225-38.

Penuelas, I., Mazzolini, G., Boan, J. F., Sangro, B., Marti-Climent, J., Ruiz, M., Ruiz, J., Satyamurthy, N., Qian, C., Barrio, J. R., Phelps, M. E., Richter, J. A., Gambhir, S. S., and Prieto, J. (2005). Positron emission tomography imaging of adenoviral-mediated transgene expression in liver cancer patients. *Gastroenterology* **128**(7)**,** 1787-95.

Pio, B. S., Park, C. K., Pietras, R., Hsueh, W. A., Satyamurthy, N., Pegram, M. D., Czernin, J., Phelps, M. E., and Silverman, D. H. (2006). Usefulness of 3'-[F-18]fluoro-3'-deoxythymidine with positron emission tomography in predicting breast cancer response to therapy. *Mol Imaging Biol* **8**(1)**,** 36-42.

Qiu, T. H., Chandramouli, G. V., Hunter, K. W., Alkharouf, N. W., Green, J. E., and Liu, E. T. (2004). Global expression profiling identifies signatures of tumor virulence in MMTV-PyMT-transgenic mice: correlation to human disease. *Cancer Res* **64**(17)**,** 5973-81.

Rasey, J. S., Grierson, J. R., Wiens, L. W., Kolb, P. D., and Schwartz, J. L. (2002). Validation of FLT uptake as a measure of thymidine kinase-1 activity in A549 carcinoma cells. *J Nucl Med* **43**(9)**,** 1210-7.

Reske, S. N., and Deisenhofer, S. (2006). Is 3'-deoxy-3'-(18)F-fluorothymidine a better marker for tumour response than (18)F-fluorodeoxyglucose? *Eur J Nucl Med Mol Imaging* **33 Suppl 1,** 38-43.

Rowland, D. J., Tu, Z., Xu, J., Ponde, D., Mach, R. H., and Welch, M. J. (2006). Synthesis and in vivo evaluation of 2 high-affinity 76Br-labeled sigma2-receptor ligands. *J Nucl Med* **47**(6)**,** 1041-8.

Schelling, M., Avril, N., Nahrig, J., Kuhn, W., Romer, W., Sattler, D., Werner, M., Dose, J., Janicke, F., Graeff, H., and Schwaiger, M. (2000). Positron emission tomography using [(18)F]Fluorodeoxyglucose for monitoring primary chemotherapy in breast cancer. *J Clin Oncol* **18**(8)**,** 1689-95.

Shah, C., Miller, T. W., Wyatt, S. K., McKinley, E. T., Olivares, M. G., Sanchez, V., Nolting, D. D., Buck, J. R., Zhao, P., Ansari, M. S., Baldwin, R. M., Gore, J. C., Schiff, R., Arteaga, C. L., and Manning, H. C. (2009). Imaging biomarkers predict response to anti-HER2 (ErbB2) therapy in preclinical models of breast cancer. *Clin Cancer Res* **15**(14)**,** 4712-21.

Shi, C. X., Graham, F. L., and Hitt, M. M. (2006). A convenient plasmid system for construction of helper-dependent adenoviral vectors and its application for analysis of the breast-cancer-specific mammaglobin promoter. *J Gene Med* **8**(4)**,** 442-51.

Sundararajan, L., Linden, H. M., Link, J. M., Krohn, K. A., and Mankoff, D. A. (2007). 18F-Fluoroestradiol. *Semin Nucl Med* **37**(6)**,** 470-6.

Tafreshi, N. K., Kumar, V., Morse, D. L., and Gatenby, R. A. (2010). Molecular and functional imaging of breast cancer. *Cancer Control* **17**(3)**,** 143-55.

Thakur, M. L., Devadhas, D., Zhang, K., Pestell, R. G., Wang, C., McCue, P., and Wickstrom, E. (2010). Imaging spontaneous MMTVneu transgenic murine mammary tumors: targeting metabolic activity versus genetic products. *J Nucl Med* **51**(1)**,** 106-11.

Tomayko, M. M., and Reynolds, C. P. (1989). Determination of subcutaneous tumor size in athymic (nude) mice. *Cancer Chemother Pharmacol* **24**(3)**,** 148-54.

Wang, H., Norris, K. M., and Mansky, L. M. (2002). Analysis of bovine leukemia virus gag membrane targeting and late domain function. *J Virol* **76**(16)**,** 8485-93.

Wang, S., Yuan, Y., Liao, L., Kuang, S. Q., Tien, J. C., O'Malley, B. W., and Xu, J. (2009). Disruption of the SRC-1 gene in mice suppresses breast cancer metastasis without affecting primary tumor formation. *Proc Natl Acad Sci U S A* **106**(1)**,** 151-6.

Wilson, J. S., Avila-Rodriguez, M. A., Johnson, R. R., Zyuzin, A., and McQuarrie, S. A. (2008). Niobium sputtered Havar foils for the high-power production of reactive [18F]fluoride by proton irradiation of [18O]H2O targets. *Appl Radiat Isot* **66**(5)**,** 565-70.

Wuest, M., Trayner, B. J., Grant, T. N., Jans, H. S., Mercer, J. R., Murray, D., West, F. G., McEwan, A. J., Wuest, F., and Cheeseman, C. I. (2011). Radiopharmacological evaluation of 6-deoxy-6-[18F]fluoro-D-fructose as a radiotracer for PET imaging of GLUT5 in breast cancer. *Nucl Med Biol* **38**(4)**,** 461-75.

CHAPTER 4:

Discussion

4.1. DISCUSSION

4.1.1. Targeted Gene Therapy: Importance for Breast Cancer

According to the Canadian Cancer Society and Statistics Canada, an average of 20 Canadians will be diagnosed with cancer and 8 will die from cancer every hour (CancerStats, 2011). Breast cancer is the most frequently diagnosed cancer in women (28% of all female cancer cases) and is the second leading cause of cancer-related mortality (14% of all female cancer cases) in Canada (CancerStats, 2011). While current breast cancer therapies such as standard radiotherapy have decreased the overall mortality rate and the risk of local recurrence, side effects in survivors can include radiation pneumonitis, rib fractures, secondary radiation-induced cancers, and cardiac toxicities (Darby et al., 2005). Chemotherapeutic drugs, such as anthracyclines, taxanes, and trastuzumab, are also known to induce cardiac toxicity including chronic heart failure (Bird and Swain, 2008; Ewer and Lippman, 2005; Valdivieso et al., 2012). While research is being done to limit these observed side effects, alternative treatments may aid in this objective. Targeted breast cancer gene therapy has potential to further improve breast cancer mortality rate while decreasing toxicity to non-cancer cells.

The research presented here outlines a cancer gene therapy approach utilizing an adenoviral vector to target the expression of an exogenous gene specifically in breast cancer cells. The presence of this gene product exclusively in cancer cells can induce therapeutic cell killing after prodrug administration or radiolabeled tracer accumulation for positron emission tomography (PET). Our work involves the use of the breast cancer-selective modified mammaglobin promoter (MPE_2) to drive the expression of the herpes simplex virus thymidine kinase (HSV-TK) gene. HSV-TK-expressing cells are

sensitive to treatment with ganciclovir (GCV) while non-expressing cells are not. HSV-TK-expressing cells are also able to accumulate 9-(4-[^{18}F]fluoro-3-hydroxymethylbutyl)-guanine ([^{18}F]FHBG), which allows for visualization of vector biodistribution *in vivo*.

4.1.2. Adenoviral Gene Therapy: Importance of Targeting

Our goal was to develop one adenoviral vector that could target the therapeutic effect of HSV-TK (with ganciclovir) to breast cancer cells and also allow for visualization of the therapeutic effect (with [^{18}F] labeled tracers). The importance of vector targeting in adenoviral gene therapy cannot be understated. One of the reasons adenoviral vectors were originally chosen as gene delivery vehicles was due to their wide tropism and ability to infect both quiescent and proliferating cells (Dormond, Perrier, and Kamen, 2009; Li et al., 1993; Quantin et al., 1992). This natural infectivity leads to expression of viral genes in a variety of cell types. In order to express gene aimed at killing cancer cells without damaging normal cells, this wide ranging expression must be restricted. The ability of scientists to restrict therapeutic gene expression impacts the efficacy of any gene therapy since expression in non-tumor cells can lead to unwanted patient toxicity.

We have shown breast cancer selectivity of the MPE_2 promoter to target HSV-TK expression to breast cancer cell lines *in vitro* and *in vivo*. However, we were not able to induce regression in MTHJ tumors. Since others have shown that GCV treatment can cause tumor regression with ≥ 10% of cells within a tumor expressing HSV-TK (Sandmair et al., 2000), it is possible that our vector administration simply did not induce HSV-TK expression in 10% tumor cells. Another possibility is that this model system may not permit the same level of bystander effect as previously studied breast cancer

models. MTHJ cells may contain lower numbers of gap junctions as other breast cancer models, especially considering that epithelial cells do not usually contain many gap junctions (Woodward et al., 1998). This could reduce the effectiveness of the bystander effect since gap junctions are believed to play a major role. It would be interesting to analyse MTHJ cells for their levels of gap junctions/connexins to determine if this may play a role in its effectiveness for HSV-TK/GCV gene therapy.

Separate from the tumor regression studies, we were able to show drastically reduced liver toxicity after AdMPE_2TK/GCV treatment compared to the same dose of untargeted AdCMVTK vector with GCV. The ubiquitously expressing cytomegalovirus promoter can induce high levels of expression and thus has been used in the past to drive expression of HSV-TK for both tumor regression (Chen et al., 1995) and PET imaging (Johnson et al., 2009). Due to its ubiquitous activity, however, its use is commonly associated with severe liver toxicity (Brand et al., 1997; Chen et al., 1995; O'Malley et al., 1995; van der Eb et al., 1998). These findings are consistent with our *in vivo* results in the MTHJ murine tumor model. On the contrary, use of the MPE_2 promoter did not induce any measurable HSV-TK expression in mouse livers.

4.1.3. Establishing the MTHJ model: Importance for Preclinical Testing

Here, using the unique MTHJ murine mammary tumor model, we establish the suitability of cultured MTHJ cells to readily form *in vivo* subcutaneous tumors at a high implantation rate that can take up and accumulate the standard positron emission tomography (PET) tracers [^{18}F]fluorodeoxyglucose ([^{18}F]FDG) and 3'-[^{18}F]fluoro-3'-deoxythymidine ([^{18}F]FLT). By characterizing this immunocompetent model, we have outlined its biological significance to human breast cancer and its usefulness, in

combination with PET imaging, for evaluation of novel preclinical cancer therapies (DeSilva et al., 2012). Another advantage of our model is that it is immunocompetent and thus more comparable to breast cancer patients. While many cancer therapeutics are being tested preclinically in nude or SCID mice bearing human breast cancer xenografts (Kim, O'Hare, and Stein, 2004; Myoui et al., 2003; Noblitt et al., 2004; Wang, Norris, and Mansky, 2002), these models cannot reveal the effect of a functional immune system. An immune reaction could significantly affect any cancer therapeutic, but it is especially important to consider when the therapeutic is known for its immune stimulation. Adenovirus vectors induce an inflammatory response (Bangari and Mittal, 2006; Bessis, GarciaCozar, and Boissier, 2004; Muruve, 2004) which can lead to either a reduction or enhancement in efficacy. One limitation of using Ad5 vectors is the fact that a majority of humans harbor anti-Ad5 immunity due to natural infection (Mast et al., 2010), which leads to vector neutralization and clearance from the body before any transgenes can be expressed (McCoy et al., 2007; Papp, Babiuk, and Baca-Estrada, 1999). The immune system can also have an effect on readministration of Ad5 vectors, as hepatocarcinoma patients receiving doses of AdCMVTK and imaged with [^{18}F]FHBG-PET did not reveal HSV-TK expression after the first dose (Penuelas et al., 2005b). A likely explanation was neutralization of the vector by the humoral immune response, as suggested by the author's experience that immunized animals show significantly reduced transduction (Penuelas et al., 2005b).

Some adenoviral vectors have been used to provoke the immune system to aid in tumor clearance, either as cancer vaccines (Hartman et al., 2010) and or to enhance the anti-tumor effect of Ad therapy (Koski et al., 2010). Rapid clearance of Ad may even be

beneficial to cancer gene therapy as it can produce desirable anti-cancer effects within a short period and protect the healthy cells from long-term exposure to toxic products (Sharma et al., 2009). In order to properly determine what role the immune system may play, it is important that a novel therapeutic be preclinically tested in an immunocompetent model such as the MTHJ model described here. We have shown in this thesis that the MTHJ model is a useful tool for testing Ad therapeutic vectors both *in vitro* and *in vivo*.

4.1.4. Characterizing the MTHJ Model: Importance for PET Imaging

Molecular imaging is a useful method for non-invasively studying gene expression *in vivo* (Penuelas et al., 2005a) and can be a powerful tool for measuring Ad vector therapeutic response. PET allows repeated quantitative measurements of transgene expression within live organisms. It can be used reliably to define transduction efficiency of a gene delivery vector and the duration and distribution of transgene expression throughout the body. This information is critical for understanding the overall gene therapy process as well as its clinical application (Sangro et al., 2002; Yu et al., 2000).

Here we report the first study investigating the uptake of PET tracers by MTHJ cells, both *in vitro* and *in vivo*. By measuring the uptake of standard PET tracers [^{18}F]FDG and [^{18}F]FLT, we were able to determine a baseline accumulation level which provides an indication of tumor metabolic and proliferation rate, respectively. Expression of HSV-TK from Ad vectors allows for PET imaging of vector biodistribution with labeled HSV-TK substrates. By characterizing the uptake of HSV-TK substrates [^{18}F]FLT and [^{18}F]FHBG in MTHJ cells before and after adenovirus administration, we were able to

show that this mouse model would provide a suitable background for investigation of novel PET imaging agents that can visualize therapeutic effect.

Our PET tracer accumulation studies also provided another means to measure HSV-TK expression from our Ad vectors. The AdMPE_2TK vector was able to induce a significant increase in [^{18}F]FHBG accumulation *in vitro* but not *in vivo*. Interestingly, even the AdCMVTK vector was not able to induce a significant increase in [^{18}F]FHBG accumulation *in vivo* in MTHJ tumors. Since expression from the AdMPE_2TK vector was expected to be roughly 10-fold less than expression from the AdCMVTK vector (Shi et al., 2004), it is perhaps not surprising that we were not able to visualize [^{18}F]FHBG accumulation.

The fact that our imaging experiments correlated with our tumor regression and toxicity studies further corroborates our finding that the MTHJ murine tumor model would be useful for preclinical visualization of transgene expression. This is consistent with other studies that found *in vivo* [^{18}F]FHBG-PET closely correlated with transgene expression as determined by mRNA abundance and protein levels at low levels of transgene expression (Gambhir et al., 1999).

While an MPE_2-controlled Ad vector still holds promise for breast cancer-specific HSV-TK expression, especially based on *in vitro* data, it is clear that more modifications must be made before an Ad vector utilizing the MPE_2 promoter can be used for human breast cancer gene therapy.

4.1.5. Future Directions

There are other targeting modalities currently being investigated that could aid in HSV-TK expression from an Ad vector. One example is transductional modifications to the Ad capsid that target the vector to the surface of cancer cells. By taking advantage of cellular receptors that are present primarily or exclusively on the surface of breast cancer cells, many studies are focused on generating transductionally targeted Ad vectors. Complementary to this line of research, many also believe that detargeting Ad vectors (especially Ad5 serotype vectors) may be just as important as retargeting (Khare et al., 2011). When delivered intravenously directly into the bloodstream, the bulk of adenoviral vectors are sequestered in the liver by Kupffer cells (Green et al., 2004; Schiedner et al., 2003; Zinn et al., 1998). Detargeting Ad vectors, potentially in combination with retargeting to specific cell types (Prill et al., 2011), may lead to Kupffer cell evasion and allow for injection of a larger vector dose with less toxicity. Transductional targeting may also refer to the use of chemical modifications to the capsid. Polyethylene glycol (PEG) polymers can be covalently attached to the surface of a virion to prolong its persistence in the blood and circumvent immune responses (Croyle et al., 2002; Mok et al., 2005; O'Riordan et al., 1999; Ogawara et al., 2004). Since PEGylation also reduces infection efficiency, functional molecules can also be added to the PEG polymers to enhance target-specific infectivity (Lanciotti et al., 2003; Ogawara et al., 2004; Xiong et al., 2006).

Another type of Ad vector targeting involves taking advantage of the difference in eukaryotic initiation factor (eIF) 4E levels between cancer cells and non-cancer cells (Kerekatte et al., 1995; Ramaswamy et al., 2003). The upregulation of eIF4E in cancer

cells allows for the protein translation of transcripts with complex secondary structures in their 5' untranslated regions (UTR) (Kevil et al., 1996; Sonenberg and Gingras, 1998). It has been shown that by generating a suicide gene (such as HSV-TK) with a complex 5' UTR, it is possible to limit translation of HSV-TK specifically to breast cancer cells (Mathis et al., 2006; Stoff-Khalili et al., 2008). This is referred to as translational targeting.

The 3' UTR of a transgene may also be modified to target transgene expression to cancer cells. By introducing target sites for a specific microRNA into a transgene, transgene expression can be suppressed up to 100-fold in cells in non-cancer that express the particular miRNA. Several microRNAs have been identified that are highly expressed in normal tissue (see review by Brown and Naldini, 2009 which includes other applications for microRNA in viral gene therapy). This type of targeting represents another method for increasing viral dose without increasing toxicity from the therapeutic gene and have been exploited to limit expression in normal tissues.

One commonly studied modality for increasing transgene expression involves the use of oncolytic Ad vectors that are modified to only replicate in tumor cells. One form of conditionally replicating Ad (CRAd) vectors can selectively replicate by using tumor specific promoters to control the expression of the adenoviral E1A region (Ji et al., 2009; Savontaus et al., 2002; Yang et al., 2011a; Yang et al., 2011b). By replicating within the tumor, Ad vectors can amplify their tumor cell killing effect.

It is more than likely that the most effective gene therapy strategies will use a combination of approaches to selectively kill cancer cells. For example, oncolytic cancer gene therapy has been shown to be insufficient as a stand-alone treatment in

many advanced tumors (Bourke et al., 2011), but surgical resections combined with oncolytic Ad administration have yielded a high efficacy (Pandha et al., 2009). Recent reports demonstrate that oncolytic adenoviruses can be 'armed' with HSV-TK such that treatment with ganciclovir enhances tumor cell killing from the replicating virus (Abate-Daga et al., 2011; Ji et al., 2009; Wildner, Blaese, and Morris, 1999b). An interesting future study would be the efficacy of a CRAd vector that uses the MPE_2 promoter to drive the expression of E1A and/or HSV-TK. The combination of preferential replication in breast cancer cells and HSV-TK/GCV killing (along with the bystander effect) could significantly enhance tumor regression and lead to an Ad vector with high therapeutic effect.

AdHSV-TK gene therapy is quite well suited as an adjuvant therapy. HSV-TK expression has been shown to enhance therapeutic effect when used in conjunction with radiation or chemotherapy (Vlachaki et al., 2001; Wildner, Blaese, and Morris, 1999a). HSV-TK could even be replaced by the HSV-sr39TK mutant, commonly used due to its higher thymidine phosphorylation efficiency (compared to HSV-TK) (Black, Kokoris, and Sabo, 2001). In fact, the HSV-sr39TK mutant was found to enhance the accumulation of many PET tracers such as [^{18}F] labelled ganciclovir, [^{18}F] labelled penciclovir, and [^{18}F]FHBG (Alauddin and Conti, 1998; Alauddin et al., 2001; Black, Kokoris, and Sabo, 2001; Gambhir et al., 2000a; Gambhir et al., 2000b; Min, Iyer, and Gambhir, 2003). The expression of the mutant HSV-sr39TK transgene in combination with [^{18}F]FHBG has been shown to be a very sensitive combination when used with adenoviral vector delivery (Min, Iyer, and Gambhir, 2003).

4.1.6. Conclusion

This thesis outlines the development and preclinical evaluation of the AdMPE_2TK for targeted breast cancer gene therapy. AdMPE_2TK combines the breast cancer specificity of the MPE_2 modified mammaglobin promoter with the HSV-TK transgene, which can be used for cell killing in combination with the prodrug ganciclovir or for PET imaging in combination with [^{18}F] radiotracers. Here we report the first time this breast cancer-specific vector was tested concurrently for its utility as a therapeutic and for its capacity to be imaged by PET. In addition we characterized a novel immunocompetent murine model for breast cancer which can be used for preclinical evaluation of other cancer therapeutics or imaging agents. Our results also highlight differences between *in vitro* assays and *in vivo* model systems. This research outlines the potential of the MPE_2 promoter and illustrates its application in breast cancer gene therapy.

4.2. REFERENCES

Abate-Daga, D., Andreu, N., Camacho-Sanchez, J., Alemany, R., Herance, R., Millan, O., and Fillat, C. (2011). Oncolytic adenoviruses armed with thymidine kinase can be traced by PET imaging and show potent antitumoural effects by ganciclovir dosing. *PLoS One* **6**(10)**,** e26142.

Alauddin, M. M., and Conti, P. S. (1998). Synthesis and preliminary evaluation of 9-(4-[18F]-fluoro-3-hydroxymethylbutyl)guanine ([18F]FHBG): a new potential imaging agent for viral infection and gene therapy using PET. *Nucl Med Biol* **25**(3)**,** 175-80.

Alauddin, M. M., Shahinian, A., Gordon, E. M., Bading, J. R., and Conti, P. S. (2001). Preclinical evaluation of the penciclovir analog 9-(4-[(18)F]fluoro-3-hydroxymethylbutyl)guanine for in vivo measurement of suicide gene expression with PET. *J Nucl Med* **42**(11)**,** 1682-90.

Bangari, D. S., and Mittal, S. K. (2006). Current strategies and future directions for eluding adenoviral vector immunity. *Curr Gene Ther* **6**(2)**,** 215-26.

Bessis, N., GarciaCozar, F. J., and Boissier, M. C. (2004). Immune responses to gene therapy vectors: influence on vector function and effector mechanisms. *Gene Ther* **11 Suppl 1,** S10-7.

Bird, B. R., and Swain, S. M. (2008). Cardiac toxicity in breast cancer survivors: review of potential cardiac problems. *Clin Cancer Res* **14**(1)**,** 14-24.

Black, M. E., Kokoris, M. S., and Sabo, P. (2001). Herpes simplex virus-1 thymidine kinase mutants created by semi-random sequence mutagenesis improve prodrug-mediated tumor cell killing. *Cancer Res* **61**(7)**,** 3022-6.

Bourke, M. G., Salwa, S., Harrington, K. J., Kucharczyk, M. J., Forde, P. F., de Kruijf, M., Soden, D., Tangney, M., Collins, J. K., and O'Sullivan, G. C. (2011). The emerging role of viruses in the treatment of solid tumours. *Cancer Treat Rev* **37**(8)**,** 618-32.

Brand, K., Arnold, W., Bartels, T., Lieber, A., Kay, M. A., Strauss, M., and Dorken, B. (1997). Liver-associated toxicity of the HSV-tk/GCV approach and adenoviral vectors. *Cancer Gene Ther* **4**(1)**,** 9-16.

Brown, B. D., and Naldini, L. (2009). Exploiting and antagonizing microRNA regulation for therapeutic and experimental applications. *Nat Rev Genet* **10**(8)**,** 578-85.

Canadian Cancer Society (2011). Canadian Cancer Statistics 2011. CancerStats. 2011.

Chen, S. H., Chen, X. H., Wang, Y., Kosai, K., Finegold, M. J., Rich, S. S., and Woo, S. L. (1995). Combination gene therapy for liver metastasis of colon carcinoma in vivo. *Proc Natl Acad Sci U S A* **92**(7)**,** 2577-81.

Croyle, M. A., Chirmule, N., Zhang, Y., and Wilson, J. M. (2002). PEGylation of E1-deleted adenovirus vectors allows significant gene expression on readministration to liver. *Hum Gene Ther* **13**(15)**,** 1887-900.

Darby, S. C., McGale, P., Taylor, C. W., and Peto, R. (2005). Long-term mortality from heart disease and lung cancer after radiotherapy for early breast cancer: prospective cohort study of about 300,000 women in US SEER cancer registries. *Lancet Oncol* **6**(8)**,** 557-65.

DeSilva, A., Wuest, M., Wang, M., Hummel, J., Mossman, K., Wuest, F., and Hitt, M. (2012). Comparative functional evaluation of immunocompetent mouse breast cancer models established from PyMT-tumors using small animal PET with [18F]FDG and [18F]FLT. *Am J Nucl Med Mol Imaging* **2**(1)**,** 88-98.

Dormond, E., Perrier, M., and Kamen, A. (2009). From the first to the third generation adenoviral vector: what parameters are governing the production yield? *Biotechnol Adv* **27**(2)**,** 133-44.

Ewer, M. S., and Lippman, S. M. (2005). Type II chemotherapy-related cardiac dysfunction: time to recognize a new entity. *J Clin Oncol* **23**(13)**,** 2900-2.

Gambhir, S. S., Barrio, J. R., Phelps, M. E., Iyer, M., Namavari, M., Satyamurthy, N., Wu, L., Green, L. A., Bauer, E., MacLaren, D. C., Nguyen, K., Berk, A. J., Cherry, S. R., and Herschman, H. R. (1999). Imaging adenoviral-directed reporter gene expression in living animals with positron emission tomography. *Proc Natl Acad Sci U S A* **96**(5)**,** 2333-8.

Gambhir, S. S., Bauer, E., Black, M. E., Liang, Q., Kokoris, M. S., Barrio, J. R., Iyer, M., Namavari, M., Phelps, M. E., and Herschman, H. R. (2000a). A mutant herpes simplex virus type 1 thymidine kinase reporter gene shows improved sensitivity for imaging reporter gene expression with positron emission tomography. *Proc Natl Acad Sci U S A* **97**(6)**,** 2785-90.

Gambhir, S. S., Herschman, H. R., Cherry, S. R., Barrio, J. R., Satyamurthy, N., Toyokuni, T., Phelps, M. E., Larson, S. M., Balatoni, J., Finn, R., Sadelain, M., Tjuvajev, J., and Blasberg, R. (2000b). Imaging transgene expression with radionuclide imaging technologies. *Neoplasia* **2**(1-2)**,** 118-38.

Green, N. K., Herbert, C. W., Hale, S. J., Hale, A. B., Mautner, V., Harkins, R., Hermiston, T., Ulbrich, K., Fisher, K. D., and Seymour, L. W. (2004). Extended plasma circulation time and decreased toxicity of polymer-coated adenovirus. *Gene Ther* **11**(16)**,** 1256-63.

Hartman, Z. C., Wei, J., Osada, T., Glass, O., Lei, G., Yang, X. Y., Peplinski, S., Kim, D. W., Xia, W., Spector, N., Marks, J., Barry, W., Hobeika, A., Devi, G., Amalfitano, A., Morse, M. A., Lyerly, H. K., and Clay, T. M. (2010). An adenoviral vaccine encoding full-length inactivated human Her2 exhibits potent immunogenicty and enhanced therapeutic efficacy without oncogenicity. *Clin Cancer Res* **16**(5)**,** 1466-77.

Ji, X., Zhang, J., Cheng, L., Wei, F., Li, H., Liu, X., Chen, X., Li, C., Wang, Y., and Huang, Q. (2009). Oncolytic adenovirus delivering herpes simplex virus thymidine kinase suicide gene reduces the growth of human retinoblastoma in an in vivo mouse model. *Exp Eye Res* **89**(2)**,** 193-9.

Johnson, M., Karanikolas, B. D., Priceman, S. J., Powell, R., Black, M. E., Wu, H. M., Czernin, J., Huang, S. C., and Wu, L. (2009). Titration of variant HSV1-tk gene expression to determine the sensitivity of 18F-FHBG PET imaging in a prostate tumor. *J Nucl Med* **50**(5)**,** 757-64.

Kerekatte, V., Smiley, K., Hu, B., Smith, A., Gelder, F., and De Benedetti, A. (1995). The proto-oncogene/translation factor eIF4E: a survey of its expression in breast carcinomas. *Int J Cancer* **64**(1)**,** 27-31.

Kevil, C. G., De Benedetti, A., Payne, D. K., Coe, L. L., Laroux, F. S., and Alexander, J. S. (1996). Translational regulation of vascular permeability factor by eukaryotic initiation factor 4E: implications for tumor angiogenesis. *Int J Cancer* **65**(6)**,** 785-90.

Khare, R., Chen, C. Y., Weaver, E. A., and Barry, M. A. (2011). Advances and future challenges in adenoviral vector pharmacology and targeting. *Curr Gene Ther* **11**(4)**,** 241-58.

Kim, J. B., O'Hare, M. J., and Stein, R. (2004). Models of breast cancer: is merging human and animal models the future? *Breast Cancer Res* **6**(1)**,** 22-30.

Koski, A., Kangasniemi, L., Escutenaire, S., Pesonen, S., Cerullo, V., Diaconu, I., Nokisalmi, P., Raki, M., Rajecki, M., Guse, K., Ranki, T., Oksanen, M., Holm, S. L., Haavisto, E.,

Karioja-Kallio, A., Laasonen, L., Partanen, K., Ugolini, M., Helminen, A., Karli, E., Hannuksela, P., Joensuu, T., Kanerva, A., and Hemminki, A. (2010). Treatment of cancer patients with a serotype 5/3 chimeric oncolytic adenovirus expressing GMCSF. *Mol Ther* **18**(10)**,** 1874-84.

Lanciotti, J., Song, A., Doukas, J., Sosnowski, B., Pierce, G., Gregory, R., Wadsworth, S., and O'Riordan, C. (2003). Targeting adenoviral vectors using heterofunctional polyethylene glycol FGF2 conjugates. *Mol Ther* **8**(1)**,** 99-107.

Li, Q., Kay, M. A., Finegold, M., Stratford-Perricaudet, L. D., and Woo, S. L. (1993). Assessment of recombinant adenoviral vectors for hepatic gene therapy. *Hum Gene Ther* **4**(4)**,** 403-9.

Mast, T. C., Kierstead, L., Gupta, S. B., Nikas, A. A., Kallas, E. G., Novitsky, V., Mbewe, B., Pitisuttithum, P., Schechter, M., Vardas, E., Wolfe, N. D., Aste-Amezaga, M., Casimiro, D. R., Coplan, P., Straus, W. L., and Shiver, J. W. (2010). International epidemiology of human pre-existing adenovirus (Ad) type-5, type-6, type-26 and type-36 neutralizing antibodies: correlates of high Ad5 titers and implications for potential HIV vaccine trials. *Vaccine* **28**(4)**,** 950-7.

Mathis, J. M., Williams, B. J., Sibley, D. A., Carroll, J. L., Li, J., Odaka, Y., Barlow, S., Nathan, C. O., Li, B. D., and DeBenedetti, A. (2006). Cancer-specific targeting of an adenovirus-delivered herpes simplex virus thymidine kinase suicide gene using translational control. *J Gene Med* **8**(9)**,** 1105-20.

McCoy, K., Tatsis, N., Korioth-Schmitz, B., Lasaro, M. O., Hensley, S. E., Lin, S. W., Li, Y., Giles-Davis, W., Cun, A., Zhou, D., Xiang, Z., Letvin, N. L., and Ertl, H. C. (2007). Effect of preexisting immunity to adenovirus human serotype 5 antigens on the immune responses of nonhuman primates to vaccine regimens based on human- or chimpanzee-derived adenovirus vectors. *J Virol* **81**(12)**,** 6594-604.

Min, J. J., Iyer, M., and Gambhir, S. S. (2003). Comparison of [18F]FHBG and [14C]FIAU for imaging of HSV1-tk reporter gene expression: adenoviral infection vs stable transfection. *Eur J Nucl Med Mol Imaging* **30**(11)**,** 1547-60.

Mok, H., Palmer, D. J., Ng, P., and Barry, M. A. (2005). Evaluation of polyethylene glycol modification of first-generation and helper-dependent adenoviral vectors to reduce innate immune responses. *Mol Ther* **11**(1)**,** 66-79.

Muruve, D. A. (2004). The innate immune response to adenovirus vectors. *Hum Gene Ther* **15**(12)**,** 1157-66.

Myoui, A., Nishimura, R., Williams, P. J., Hiraga, T., Tamura, D., Michigami, T., Mundy, G. R., and Yoneda, T. (2003). C-SRC tyrosine kinase activity is associated with tumor colonization in bone and lung in an animal model of human breast cancer metastasis. *Cancer Res* **63**(16)**,** 5028-33.

Noblitt, L. W., Bangari, D. S., Shukla, S., Knapp, D. W., Mohammed, S., Kinch, M. S., and Mittal, S. K. (2004). Decreased tumorigenic potential of EphA2-overexpressing breast cancer cells following treatment with adenoviral vectors that express EphrinA1. *Cancer Gene Ther* **11**(11)**,** 757-66.

O'Malley, B. W., Jr., Chen, S. H., Schwartz, M. R., and Woo, S. L. (1995). Adenovirus-mediated gene therapy for human head and neck squamous cell cancer in a nude mouse model. *Cancer Res* **55**(5)**,** 1080-5.

O'Riordan, C. R., Lachapelle, A., Delgado, C., Parkes, V., Wadsworth, S. C., Smith, A. E., and Francis, G. E. (1999). PEGylation of adenovirus with retention of infectivity and

protection from neutralizing antibody in vitro and in vivo. *Hum Gene Ther* **10**(8)**,** 1349-58.

Ogawara, K., Rots, M. G., Kok, R. J., Moorlag, H. E., Van Loenen, A. M., Meijer, D. K., Haisma, H. J., and Molema, G. (2004). A novel strategy to modify adenovirus tropism and enhance transgene delivery to activated vascular endothelial cells in vitro and in vivo. *Hum Gene Ther* **15**(5)**,** 433-43.

Pandha, H., Melcher, A., Harrington, K., and Vile, R. (2009). Oncolytic viruses: time to compare, contrast, and combine? 5th international meeting on replicating oncolytic virus therapeutics. Banff, Alberta, Canada, 18-22 March 2009. *Mol Ther* **17**(6)**,** 934-5.

Papp, Z., Babiuk, L. A., and Baca-Estrada, M. E. (1999). The effect of pre-existing adenovirus-specific immunity on immune responses induced by recombinant adenovirus expressing glycoprotein D of bovine herpesvirus type 1. *Vaccine* **17**(7-8)**,** 933-43.

Penuelas, I., Haberkorn, U., Yaghoubi, S., and Gambhir, S. S. (2005a). Gene therapy imaging in patients for oncological applications. *Eur J Nucl Med Mol Imaging* **32 Suppl 2,** S384-403.

Penuelas, I., Mazzolini, G., Boan, J. F., Sangro, B., Marti-Climent, J., Ruiz, M., Ruiz, J., Satyamurthy, N., Qian, C., Barrio, J. R., Phelps, M. E., Richter, J. A., Gambhir, S. S., and Prieto, J. (2005b). Positron emission tomography imaging of adenoviral-mediated transgene expression in liver cancer patients. *Gastroenterology* **128**(7)**,** 1787-95.

Prill, J. M., Espenlaub, S., Samen, U., Engler, T., Schmidt, E., Vetrini, F., Rosewell, A., Grove, N., Palmer, D., Ng, P., Kochanek, S., and Kreppel, F. (2011). Modifications of adenovirus hexon allow for either hepatocyte detargeting or targeting with potential evasion from Kupffer cells. *Mol Ther* **19**(1)**,** 83-92.

Quantin, B., Perricaudet, L. D., Tajbakhsh, S., and Mandel, J. L. (1992). Adenovirus as an expression vector in muscle cells in vivo. *Proc Natl Acad Sci U S A* **89**(7)**,** 2581-4.

Ramaswamy, S., Ross, K. N., Lander, E. S., and Golub, T. R. (2003). A molecular signature of metastasis in primary solid tumors. *Nat Genet* **33**(1)**,** 49-54.

Sandmair, A. M., Turunen, M., Tyynela, K., Loimas, S., Vainio, P., Vanninen, R., Vapalahti, M., Bjerkvig, R., Janne, J., and Yla-Herttuala, S. (2000). Herpes simplex virus thymidine kinase gene therapy in experimental rat BT4C glioma model: effect of the percentage of thymidine kinase-positive glioma cells on treatment effect, survival time, and tissue reactions. *Cancer Gene Ther* **7**(3)**,** 413-21.

Sangro, B., Qian, C., Ruiz, J., and Prieto, J. (2002). Tracing transgene expression in cancer gene therapy: a requirement for rational progress in the field. *Mol Imaging Biol* **4**(1)**,** 27-33.

Savontaus, M. J., Sauter, B. V., Huang, T. G., and Woo, S. L. (2002). Transcriptional targeting of conditionally replicating adenovirus to dividing endothelial cells. *Gene Ther* **9**(14)**,** 972-9.

Schiedner, G., Hertel, S., Johnston, M., Dries, V., van Rooijen, N., and Kochanek, S. (2003). Selective depletion or blockade of Kupffer cells leads to enhanced and prolonged hepatic transgene expression using high-capacity adenoviral vectors. *Mol Ther* **7**(1)**,** 35-43.

Sharma, A., Tandon, M., Bangari, D. S., and Mittal, S. K. (2009). Adenoviral vector-based strategies for cancer therapy. *Curr Drug ther* **4**(2)**,** 117-138.

Shi, C. X., Long, M. A., Liu, L., Graham, F. L., Gauldie, J., and Hitt, M. M. (2004). The human SCGB2A2 (mammaglobin-1) promoter/enhancer in a helper-dependent adenovirus vector directs high levels of transgene expression in mammary carcinoma cells but not in normal nonmammary cells. *Mol Ther* **10**(4)**,** 758-67.

Sonenberg, N., and Gingras, A. C. (1998). The mRNA 5' cap-binding protein eIF4E and control of cell growth. *Curr Opin Cell Biol* **10**(2)**,** 268-75.

Stoff-Khalili, M. A., Rivera, A. A., Nedeljkovic-Kurepa, A., DeBenedetti, A., Li, X. L., Odaka, Y., Podduturi, J., Sibley, D. A., Siegal, G. P., Stoff, A., Young, S., Zhu, Z. B., Curiel, D. T., and Mathis, J. M. (2008). Cancer-specific targeting of a conditionally replicative adenovirus using mRNA translational control. *Breast Cancer Res Treat* **108**(1)**,** 43-55.

Valdivieso, M., Kujawa, A. M., Jones, T., and Baker, L. H. (2012). Cancer survivors in the United States: a review of the literature and a call to action. *Int J Med Sci* **9**(2)**,** 163-73.

van der Eb, M. M., Cramer, S. J., Vergouwe, Y., Schagen, F. H., van Krieken, J. H., van der Eb, A. J., Borel Rinkes, I. H., van de Velde, C. J., and Hoeben, R. C. (1998). Severe hepatic dysfunction after adenovirus-mediated transfer of the herpes simplex virus thymidine kinase gene and ganciclovir administration. *Gene Ther* **5**(4)**,** 451-8.

Vlachaki, M. T., Chhikara, M., Aguilar, L., Zhu, X., Chiu, K. J., Woo, S., Teh, B. S., Thompson, T. C., Butler, E. B., and Aguilar-Cordova, E. (2001). Enhanced therapeutic effect of multiple injections of HSV-TK + GCV gene therapy in combination with ionizing radiation in a mouse mammary tumor model. *Int J Radiat Oncol Biol Phys* **51**(4)**,** 1008-17.

Wang, H., Norris, K. M., and Mansky, L. M. (2002). Analysis of bovine leukemia virus gag membrane targeting and late domain function. *J Virol* **76**(16)**,** 8485-93.

Wildner, O., Blaese, R. M., and Morris, J. C. (1999a). Synergy between the herpes simplex virus tk/ganciclovir prodrug suicide system and the topoisomerase I inhibitor topotecan. *Hum Gene Ther* **10**(16)**,** 2679-87.

Wildner, O., Blaese, R. M., and Morris, J. C. (1999b). Therapy of colon cancer with oncolytic adenovirus is enhanced by the addition of herpes simplex virus-thymidine kinase. *Cancer Res* **59**(2)**,** 410-3.

Woodward, T. L., Sia, M. A., Blaschuk, O. W., Turner, J. D., and Laird, D. W. (1998). Deficient epithelial-fibroblast heterocellular gap junction communication can be overcome by co-culture with an intermediate cell type but not by E-cadherin transgene expression. *J Cell Sci* **111 (Pt 23),** 3529-39.

Xiong, Z., Cheng, Z., Zhang, X., Patel, M., Wu, J. C., Gambhir, S. S., and Chen, X. (2006). Imaging chemically modified adenovirus for targeting tumors expressing integrin alphavbeta3 in living mice with mutant herpes simplex virus type 1 thymidine kinase PET reporter gene. *J Nucl Med* **47**(1)**,** 130-9.

Yang, S. W., Chanda, D., Cody, J. J., Rivera, A. A., Waehler, R., Siegal, G. P., Douglas, J. T., and Ponnazhagan, S. (2011a). Conditionally replicating adenovirus expressing TIMP2 increases survival in a mouse model of disseminated ovarian cancer. *PLoS One* **6**(10)**,** e25131.

Yang, S. W., Cody, J. J., Rivera, A. A., Waehler, R., Wang, M., Kimball, K. J., Alvarez, R. A., Siegal, G. P., Douglas, J. T., and Ponnazhagan, S. (2011b). Conditionally replicating adenovirus expressing TIMP2 for ovarian cancer therapy. *Clin Cancer Res* **17**(3)**,** 538-49.

Yu, Y., Annala, A. J., Barrio, J. R., Toyokuni, T., Satyamurthy, N., Namavari, M., Cherry, S. R., Phelps, M. E., Herschman, H. R., and Gambhir, S. S. (2000). Quantification of target gene expression by imaging reporter gene expression in living animals. *Nat Med* **6**(8)**,** 933-7.

Zinn, K. R., Douglas, J. T., Smyth, C. A., Liu, H. G., Wu, Q., Krasnykh, V. N., Mountz, J. D., Curiel, D. T., and Mountz, J. M. (1998). Imaging and tissue biodistribution of 99mTc-labeled adenovirus knob (serotype 5). *Gene Ther* **5**(6)**,** 798-808.